Regulation of Cardiac Hypertrophy: The Nuclear Option

Diederik Wouter Dimitri Kuster

Regulation of cardiac hypertrophy: the nuclear option

Cover design: S.S.W. Kuster

Thesis Erasmus Medical Center, Rotterdam

ISBN: 978-94-6191-121-6
Printed by: Ipskamp Drukkers

Regulation of Cardiac Hypertrophy: The Nuclear Option

Regulatie van cardiale hypertrofie: de kern van de zaak

Proefschrift
ter verkrijging van de graad van doctor aan
de Erasmus Universiteit Rotterdam
op gezag van de rector magnificus

Prof.dr. H.G. Schmidt

en volgens besluit van het College voor Promoties

De openbare verdediging zal plaatsvinden op
woensdag 14 december 2011 om 15.30 uur

Door
Diederik Wouter Dimitri Kuster

Geboren te Haarlem

Promotiecommissie

Promotor:	Prof.dr. D.J.G.M. Duncker
Overige leden:	Prof.dr. A.H.J. Danser Prof.dr. S. Philipsen Dr. J. van der Velden
Co-promotor:	Dr. A.J.M. Verhoeven

The studies in this thesis have been performed at the Laboratories for Biochemistry and Experimental Cardiology, Erasmus MC Faculty, the Netherlands

Financial support by the Dutch Heart Foundation and J.E. Jurriaanse Stichting for the publication of this thesis is gratefully acknowledged.

The research described in this thesis wsa supported by a grant of the Dutch Heart Foundation (DHF-2005B234)

Content

Chapter 1

General introduction

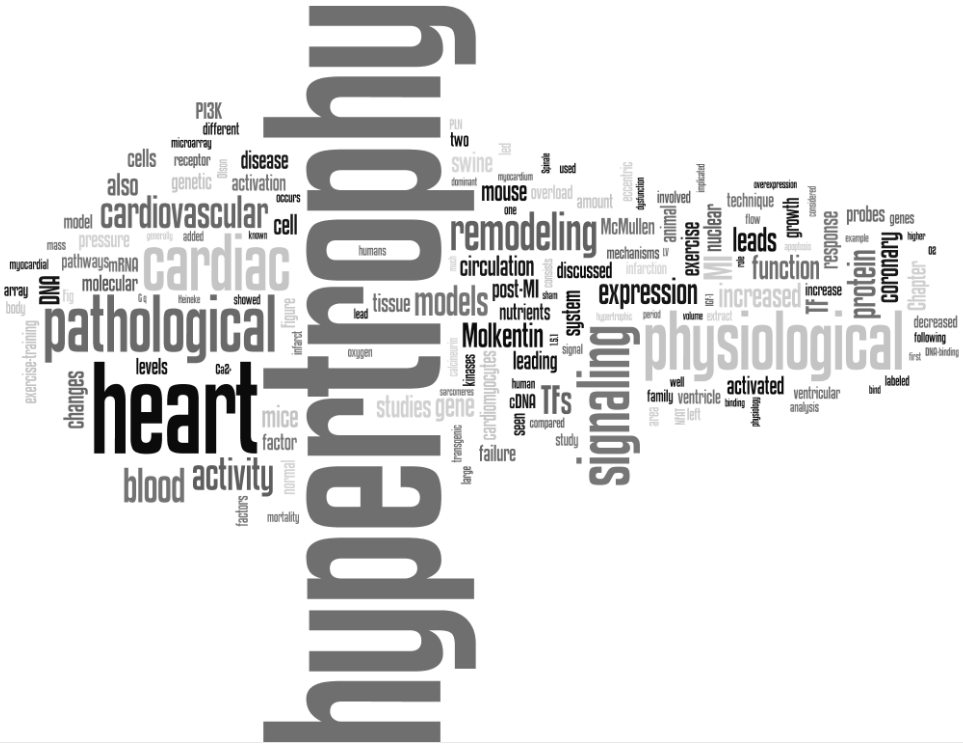

1. General Introduction

No other organ has inspired so many writers, poets and songwriters as the heart. It is the symbol of love and passion and was once believed to be the place where the soul resides. Even looking at it with the cold, unromantic eyes of science, one can appreciate the beauty of this remarkable organ and the circulation attached to it.

1.1 Circulation

All cells require O_2 and nutrients for normal function. In unicellular organisms the supply of O_2 and nutrients can be achieved by diffusion, which is the random movement of substances from higher to lower concentration. As most cells in multicellular organisms, such as humans, are not in direct contact with either the air or sources of nutrients, diffusion will not suffice. This is because diffusion is too slow to meet the cells' metabolic requirements. Therefore, a specialized system is needed to deliver O_2 and nutrients close to the cells of the body, i.e. the circulatory system. This system consists of a pump (the heart), a set of interconnected tubes (blood vessels) and a mixture of cells and fluid that fills the system (blood) (Widmaier *et al.*, 2011).

The heart pumps blood around the body continuously and beats on average 2.5 billion times during the lifetime of a human. The English physician William Harvey (1578-1657) was the first to describe the cardiovascular system as a closed circuit in his seminal work *De motu cordis* (Movement of the Heart) published in 1628. It has since been understood that the cardiovascular system consists of two serial circuits, the pulmonary and the systemic circulations, which both originate and terminate in the heart. The pulmonary circulation leads the deoxygenated

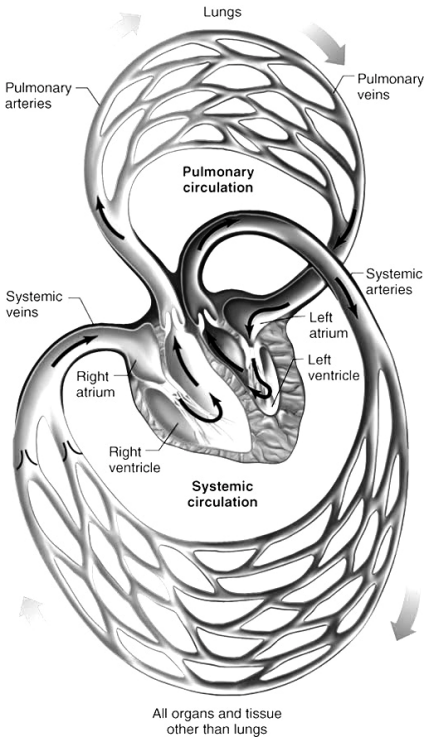

***Figure 1.1*. Two circulations of the cardiovascular system.** *In the pulmonary circulation deoxygenated blood (light grey), is passed through the lungs where oxygen is taken up and carbon dioxide is released. The oxygenated blood (dark grey) enters the systemic circulation where it provides the tissues of the body with oxygen and distributes nutrients. Adapted from (Widmaier et al., 2004).*

blood through the lungs where it becomes oxygenated and excess CO_2 is removed. It is then pumped into the systemic circulation, where it provides the tissues of the body and the heart itself with oxygen and nutrients (Fig 1.1).

1.2 The heart

The heart governs the movement of the blood through the two circulatory systems. It too consists of two parts, namely the right and the left side, both of which can be separated in atria and ventricles. In the atria the blood is collected when it returns from circulation, while the ventricles are responsible for the pumping of blood back into the circulation.
The right ventricle of the heart pumps blood into the low pressure pulmonary artery, while the left ventricle has to pump blood into the high pressure system of the aorta. Therefore the left ventricle has a much thicker, more muscular wall than the right ventricle.

To supply the heart itself with oxygen and nutrients, the coronary circulation is present. Because the heart pumps approximately once every second continuously throughout our lives, it uses a tremendous amount of energy and therefore needs a large amount of O_2 and nutrients. This is reflected in both the fact that 5% of total blood flow goes through the coronary circulation (the heart is about 0.5% of total body weight) and that 80% of the oxygen is extracted from blood during a single pass through this circulation, compared with 30-40% in skeletal muscle (Duncker & Bache, 2008). When the supply route to the heart gets obstructed, such as during a myocardial infarction (MI), this has grave consequences both for the heart and the rest of the body as will be discussed in the next section.

1.3 Myocardial infarction, cardiac remodeling and heart failure

Cardiovascular disease is one of the leading causes of mortality worldwide (Roger *et al.*, 2011). In the Netherlands cardiovascular disease is responsible for 30% of deaths and it is the leading cause of death for women (Vaartjes *et al.*, 2010). Nearly one third of cardiovascular disease-related mortality can be attributed to myocardial infarction (Vaartjes *et al.*, 2010). Myocardial infarction is caused by occlusion of a coronary artery resulting in ischemia of the downstream myocardial tissue.

MI will result in changes in ventricular architecture, both in the ischemic area and in the remote, non-infarcted area. Loss of viable myocardium leads to an abrupt drop in cardiac output and elicits a cascade of compensatory mechanisms, including neurohumoral activation, fluid retention and left ventricular (LV) remodeling, in an attempt to maintain normal pump function for perfusion of vital organs (Katz, 2008; Sutton & Sharpe, 2000). In the first hours after MI, myocyte necrosis, inflammation and edema are restricted to the ischemic area. This period is followed by scar formation in which fibroblast proliferation and

collagen deposition take place to replace the damaged tissue. Until the strengthening of the scarred region has completed, the infarcted region can thin and elongate without additional cell death, the so-called infarct expansion (Hutchins & Bulkley, 1978). Adding to the dilation of the ventricle is the eccentric hypertrophy occurring in the remote non-infarcted area of the heart (Erlebacher *et al.*, 1982; Pfeffer & Braunwald, 1990). This eccentric hypertrophy process continues even after complete healing of the infarct area (Fletcher *et al.*, 1981; Pfeffer *et al.*, 1991).

The extent of ventricular remodeling depends on a host of factors, such as infarct size, infarct location, time of reperfusion and co-morbidities (Pfeffer & Braunwald, 1990; Warren *et al.*, 1988). In the remote area numerous changes occur (Gajarsa & Kloner, 2011; Sutton & Sharpe, 2000), leading to decreased function and progression towards heart failure (White *et al.*, 1987b). Increased intracellular fibrosis (de Waard *et al.*, 2007; Jugdutt, 2003) is observed leading to myocardial stiffening, and impaired filling. Continuous loss of cardiomyocytes through apoptosis is seen in the remodeled myocardium (Dorn, 2009; Narula *et al.*, 2006), contributing to a vicious cycle of cell loss, as further cell loss increases the workload on the remaining cardiomyocytes leading to more apoptosis. Inflammatory mediators infiltrate the remodeled myocardium contributing to cardiac dysfunction (Nian *et al.*, 2004). Contractile dysfunction is observed in the surviving cardiomyocytes, leading to depressed pump function (van der Velden *et al.*, 2004). Blood flow to the remodeled myocardium can become impeded when the coronary vasculature does not grow commensurate with the increase in LV mass and because extravascular compression of the coronary vasculature increases with increased LV filling pressures (Haitsma *et al.*, 2001). Perturbations in Ca^{2+}-handling proteins, such as decreased SERCA 2A expression and function also lead to decreased contractility of the heart (Bito *et al.*, 2008; de Waard *et al.*, 2007).

Survival after myocardial infarction has risen markedly over the last decades with the advent of treatment options aimed at restoring flow to the ischemic tissue such as percutaneous coronary intervention (PCI) and coronary artery bypass grafting (CABG). Follow-up therapy consists of anti-platelet and anti-coagulation treatment, administration of beta-blockers and angiotensin-converting enzyme (ACE) inhibitors, combined with lipid lowering medications and advice on lifestyle changes (Alpert, 2011; Hass & Smith Jr., 2010). Although PCI and CABG have reduced mortality immediately post-MI, they have led to an increase in the incidence of heart failure (Velagaleti *et al.*, 2008). This is illustrated by the fact that heart failure can be the ultimate result of MI, which occurs in 10-40% of cases (Weir *et al.*, 2006). Cardiac remodeling -consisting of hypertrophy and dilation- still occurs notwithstanding current treatment. Despite its apparent appropriateness in maintaining

cardiac output at least short-term, post-MI remodeling constitutes an independent risk factor for the development of heart failure (White *et al.*, 1987b).

1.4 Effect of exercise on the heart

The beneficial effects of exercise on cardiovascular health are well established. Regular exercise-training leads to increased workload of the heart and therefore to cardiac hypertrophy. Although an increased cardiac mass is generally associated with a higher chance to develop cardiovascular disease (Levy *et al.*, 1990; Vakili *et al.*, 2001), this form of cardiac hypertrophy is not considered to be detrimental, as it comes without adverse clinical symptoms. Cardiac growth is roughly divided into two categories based on clinical outcome, i.e. physiological hypertrophy and pathological hypertrophy. Physiological hypertrophy in humans is seen during pregnancy and post-natal growth and after exercise-training. A striking example of physiological hypertrophy can be found in snakes. The heart of the Burmese python can grow by 40%, within 48 hours after ingesting a large meal (Andersen *et al.*, 2005). One of the features of physiological hypertrophy, and one that sets it apart from pathological hypertrophy, is that it is considered to be reversible. This holds true in the case of the python as 28 days after the meal, the heart has returned to its original size.

Physiological hypertrophy occurring in the athlete's heart is not associated with cardiac fibrosis or cardiac dysfunction typically seen in pathological hypertrophy (Weeks & McMullen, 2011). Nor is top level exercise over an extended period associated with an increased risk of cardiovascular disease (Pelliccia *et al.*, 2010). LV hypertrophy caused by exercise-training reverses upon detraining (Fagard *et al.*, 1983; Maron *et al.*, 1993). Physical activity is dose-dependently related to lower cardiovascular disease risk (Wannamethee & Shaper, 2001). Large cohort studies showed an inverse relationship between physical activity and cardiovascular mortality (Gielen *et al.*, 2001; Hakim *et al.*, 1998; Kannel *et al.*, 1986; Manson *et al.*, 2002). Physical inactivity is associated with high cardiovascular and total mortality (Booth & Lees, 2007).

1.5 Cardiac hypertrophy

The heart grows in response to an increased workload. The growth of the heart is accomplished by growth of the existing cardiomyocytes, rather than through cell-division. Although the view that all cardiomyocytes are terminally differentiated cells and as such cannot proliferate has been challenged in recent years (Beltrami *et al.*, 2001; Bergmann *et al.*, 2009), there is consensus that this capacity is very limited and not sufficient for cardiac repair following MI. Cardiomyocytes can grow in two ways: (*i*) in concentric hypertrophy, sarcomeres are added in parallel leading to an increase in cell thickness, and (*ii*) in eccentric hypertrophy, sarcomeres are added in series resulting in elongated cells (see Fig 1.2).

Concentric hypertrophy generally occurs in response to pressure overload, as in hypertension, aortic stenosis or certain forms of strength exercise-training such as weight lifting (Pluim *et al.*, 2000). The ventricle wall thickens but chamber volume stays relatively constant. Eccentric hypertrophy on the other hand, occurs in response to volume overload. Wall thickness remains normal, but the chamber dimension increases (Opie *et al.*, 2006). Myocardial infarction generally leads to eccentric hypertrophy, as does endurance exercise - raining such as cycling and running (Pluim *et al.*, 2000).

Pathological and physiological hypertrophy not only differ with respect to clinical outcome and reversibility, but also with respect to the molecular signalling underlying the two forms of hypertrophy (Bernardo *et al.*, 2010; Frey & Olson, 2003; Hill & Olson, 2008; Kehat & Molkentin, 2010), as will be discussed in the next part.

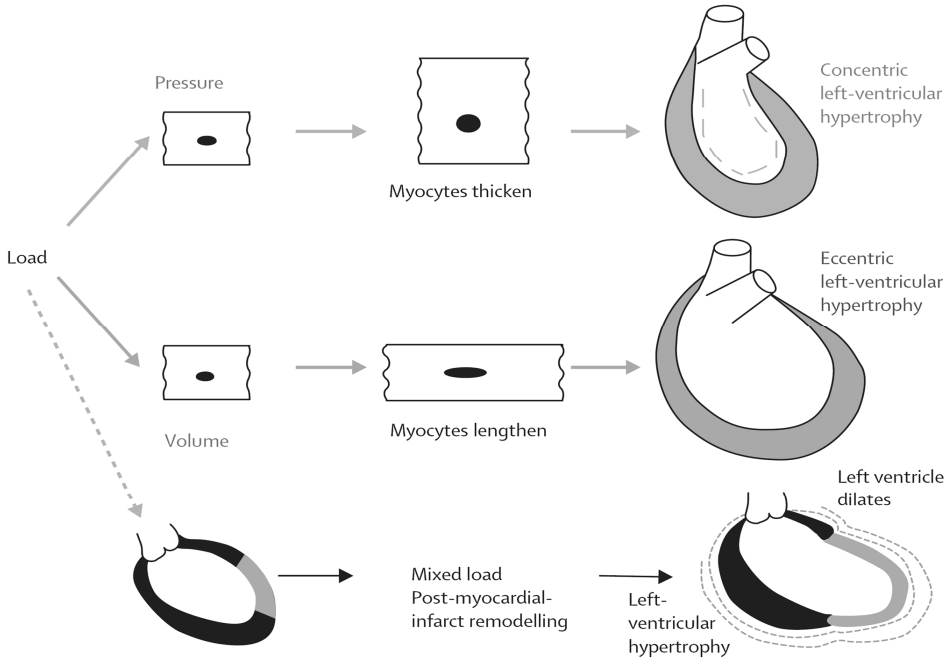

***Figure 1.2. Different forms of cardiac remodeling**. In response to pressure overload (e.g. hypertension), sarcomeres are added in series causing the cardiomyocyte to grow in width. This leads to a thicker walled heart with a normal ventricular diameter, i.e. concentric hypertrophy. In response to volume overload (e.g. valvular disorder), sarcomeres are added in parallel, which leads to a heart with normal wall thickness, but increased ventricular diameter, eccentric hypertrophy. In response to MI, hypertrophy of the viable tissue takes place, which is mainly eccentric in nature. In addition, expansion of the infarcted region may contribute to the dilatation of the left ventricle. Adapted from: (Opie et al., 2006).*

1.5.1 Molecular signaling in pathological hypertrophy

Cardiomyocyte hypertrophy signaling pathways are complex, as illustrated by the simplified scheme in Figure 1.3. Stress signals from various membrane receptors lead to the activation of downstream signaling cascades, among which cross-talk exists. The signaling cascade results in the activation or deactivation of, among others, various transcription factors. The changed activity of this set of transcription factors leads to the expression of genes that cause hypertrophy of the cell. Global gene expression studies show that distinct signaling pathways control the induction of pathological and physiological hypertrophy (Beisvag *et al.*, 2009; Galindo *et al.*, 2009; Kong *et al.*, 2005; Strom *et al.*, 2005).

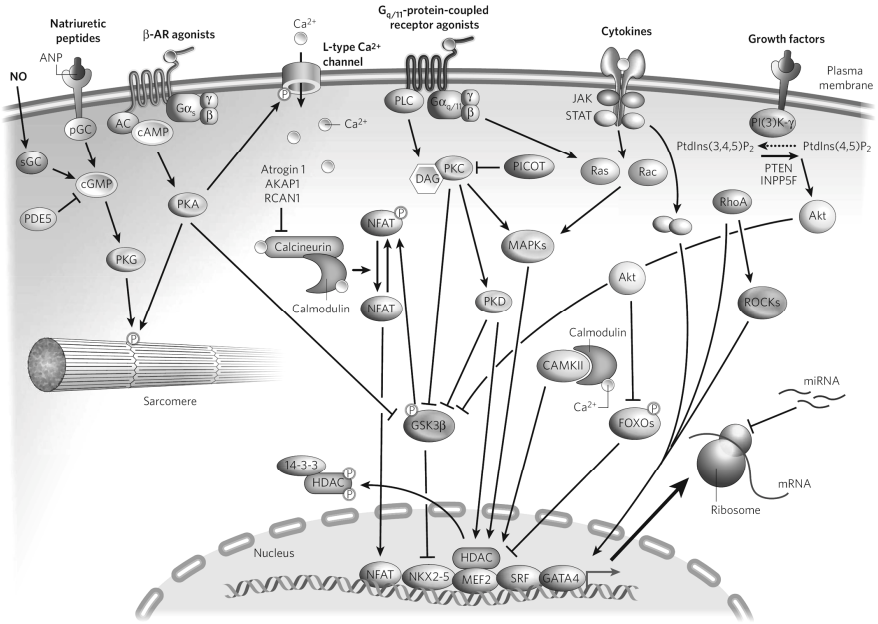

Figure 1.3: Signaling cascades mediating cardiac hypertrophy. *Stress signaling molecules bind to receptors in the cell membrane. Signals are transduced through a series of intracellular messengers to the nucleus, where they activate or deactivate transcription factors leading to the genetic reprogramming that cause hypertrophy. For clarity only a number of signaling cascades and interactions are depicted. Adapted from: (Mudd & Kass, 2008).*

In general it is thought that G-protein coupled receptor (GPCR) mediated signaling is involved in pathological hypertrophy, while growth receptor signaling initiates physiological cell growth (Frey & Olson, 2003; Heineke & Molkentin, 2006; Weeks & McMullen, 2011). Continuous infusion of an agonist for the G-coupled β-adrenergic (Stanton *et al.*, 1969) or angiotensin (Black *et al.*, 1995) receptors led to pathological

hypertrophy and endothelin administration to isolated cardiomyocytes also led to hypertrophy (Ito *et al.*, 1991). The angiotensin and endothelin receptor as well as the pro-hypertrophic α-adrenergic receptor are coupled to heterotrimeric G proteins of the $G_{\alpha q}$ subclass. This signaling molecule plays an essential role in pathological hypertrophy, as overexpression of $G_{\alpha q}$ led to hypertrophy with cardiac dysfunction (D'Angelo *et al.*, 1997), while in the cardiac specific $G_{\alpha q}$ KO mouse no cardiac hypertrophy was seen after pressure overload (Wettschureck *et al.*, 2001). One of the consequences of activation of $G_{\alpha q}$ is release of Ca^{2+} from the sarcoplasmic reticulum. The increase in Ca^{2+} leads to activation of the phosphatase calcineurin, which is a key regulator of pathological remodeling (De Windt *et al.*, 2001; Molkentin *et al.*, 1998). The pro-hypertrophic activity of calcineurin is mediated by the transcription factor (TF) nuclear factor of activated T-cells (NFAT), which is dephosphorylated and thereby activated (Molkentin *et al.*, 1998). The rise in Ca^{2+} also activates the Ca^{2+}/calmodulin dependent kinases (CaMK), which lead to hypertrophy through activation of the TF myocyte enhancer factor 2 (MEF2) (Passier *et al.*, 2000; Zhang & Brown, 2004).

Another family of signaling molecules involved in pathological hypertrophy are the mitogen-activated protein kinases (MAPKs) (Clerk *et al.*, 2007). They are also activated by, among others, GPCRs. MAPK signaling occurs by a sequential phosphorylation of different kinases, finally leading to the phosphorylation of p38-MAPKs, extracellular signal-regulated kinases (ERKs) and c-jun N-terminal kinases (JNKs). Studies in transgenic animal models indicate that ERKs might be positive regulators of hypertrophy, while p38 and JNK are considered negative regulators (Heineke & Molkentin, 2006), although controversy remains about the role of this family of kinases in pathological hypertrophy (Clerk *et al.*, 2007; Heineke & Molkentin, 2006; Kehat & Molkentin, 2010; Rose *et al.*, 2010).

This overview of signaling pathways discussed above is far from comprehensive, as a plethora of other signaling molecules have been implicated in pathological hypertrophy (Fig 1.3) (Clerk *et al.*, 2007; Frey & Olson, 2003; Heineke & Molkentin, 2006; Kehat & Molkentin, 2010; Mudd & Kass, 2008).

1.5.2 Molecular signaling in physiological hypertrophy

Physiological hypertrophy signaling has been less extensively studied than its pathological counterpart. Most of the studies have focused on the insulin-like growth factor 1 (IGF-1)/phosphatidylinositol 3'-kinase (PI3K) signaling axis (Fig 1.3) (Weeks & McMullen, 2011). Sampling of coronary sinus blood from professional football players showed increased levels of IGF-1, while angiotensin and endothelin levels were normal compared with healthy sedentary controls (Neri Serneri *et al.*, 2001). The same study showed a direct correlation between IGF-1 levels and left ventricular mass. Transgenic mice overexpressing the IGF1 receptor display an increase in heart mass with enhanced systolic function but without the

hallmark features of pathological hypertrophy, such as fibrosis and apoptosis (McMullen *et al.*, 2004). Binding of IGF-1 to its receptor leads to the activation of PI3K. PI3K signaling is both necessary and sufficient for physiological hypertrophy as has been established by two transgenic mouse models. The first mouse model expressed a constitutively active PI3K activity in the heart resulting in hypertrophy with normal cardiac function (Shioi *et al.*, 2000). The second mouse model expressed a dominant negative PI3K, which showed a decrease in heart mass at baseline (Shioi *et al.*, 2000). PI3K is important for physiological hypertrophy, but not for pathological hypertrophy, as the dominant negative PI3K mouse showed an attenuated increase to swim training induced cardiac hypertrophy, while pathological hypertrophy induced by pressure overload, was not affected (McMullen *et al.*, 2003).

The kinase Akt is downstream of PI3K and becomes activated upon phosphorylation. Phosphorylation of Akt is seen in animal models of physiological hypertrophy (Kemi *et al.*, 2008; McMullen *et al.*, 2004; McMullen *et al.*, 2003), but not pathological hypertrophy (Kemi *et al.*, 2008; McMullen *et al.*, 2003). Akt plays an important role in promoting protein synthesis (Faridi *et al.*, 2003), cell growth (Faridi *et al.*, 2003; Latronico *et al.*, 2004) and cell survival (Datta *et al.*, 1999; Fujio *et al.*, 2000) and in preventing apoptosis (Dhanasekaran *et al.*, 2008).

1.5.3 Transcription factors

The multitudes of signaling pathways that are activated in hypertrophy converge in the nucleus and lead to the activation of specific TFs. This in turn will lead to the expression of the genes responsible for the pathological or physiological phenotype. Similar to the signaling pathways, much more is known about TFs mediating pathological hypertrophy, than TFs involved in physiological hypertrophy. A number of them will be discussed below.

NFAT was already introduced in section 1.5.1. The NFAT family consists of 5 family members (NFAT1-5), of which NFAT1-4 are activated by calcineurin, while NFAT5 is activated in response to osmotic stress (Morancho *et al.*, 2008). The calcineurin sensitive NFAT isoforms are activated in pathological (Molkentin *et al.*, 1998; Wilkins *et al.*, 2004) but not in physiological hypertrophy (Wilkins *et al.*, 2004). Knocking out the NFATc2 isoform attenuates hypertrophy in mice following a pathological but not a physiological stimulus (Bourajjaj *et al.*, 2008). MEF2, also briefly mentioned above, is a regulator of hypertrophic gene expression (Czubryt & Olson, 2004). Transgenic cardiospecific overexpression of MEF2 in mice led to a dilated cardiomyopathy phenotype (Xu *et al.*, 2006). GATA4's role in hypertrophy signaling has been well described (Liang & Molkentin, 2002). GATA4 is known to interact with NFAT3 (Molkentin *et al.*, 1998) and overexpression of GATA4 leads to cardiac hypertrophy (Liang *et al.*, 2001). Unlike NFAT, GATA4 deletion leads to attenuation of both pathological and physiological hypertrophy (Oka *et al.*, 2006). Another TF implicated in hypertrophy signaling is serum response factor (SRF). SRF's transcriptional activity is higher

in neonatal cardiomyocytes treated with hypertrophic stimuli (Davis *et al.*, 2003). Furthermore, SRF overexpression in a transgenic mouse model led to hypertrophy and cardiomyopathy (Zhang *et al.*, 2001). Nuclear factor (NF)-κB is known to be activated after MI in murine models (Kawano *et al.*, 2006) and in failing human heart (Wong *et al.*, 1998). Activation of NF-κB is required for the development of cardiac hypertrophy following pressure overload in mice (Li *et al.*, 2004). Knocking out NF-κB leads to increased survival and prevents the progression towards heart failure in a mouse model of post-MI remodeling (Kawano *et al.*, 2006).

Using an elegant bioinformatical approach to look for TF binding sites in genes that were differentially expressed in human end-stage heart failure, Hannenhalli *et al.* identified the Forkhead Box (FOX) family of TFs to be involved in cardiac remodeling (Hannenhalli *et al.*, 2006). This is a large family of TFs, whose function in the heart is mostly anti-hypertrophic. The FOXO TFs are thought to suppress hypertrophy via inhibition of calcineurin signaling (Ni *et al.*, 2006), while FOXP1 binds to NFAT3 and blocks its activity (Bai & Kerppola, 2011). Identifying TFs involved in post-MI remodeling in swine will be discussed in Chapter 4.

Heat shock factor 1 (HSF-1) has been implicated in physiological hypertrophy as its activity was increased in the heart after exercise-training but not in pressure overload-induced hypertrophy (Sakamoto *et al.*, 2006). Furthermore, when mice with decreased HSF-1 activity were exercise trained, they developed hypertrophy with decreased systolic function reminiscent of pathological hypertrophy (Sakamoto *et al.*, 2006). Another TF implicated in physiological hypertrophy is CCAAT/enhancer binding protein β (C/EBPβ), which is downregulated in response to exercise (Bostrom *et al.*, 2010). A C/EBPβ$^{+/-}$ mouse with reduced C/EBPβ protein level mimicked physiological hypertrophy at baseline and was protected against pathological hypertrophy (Bostrom *et al.*, 2010). Transcription factors mediating physiological hypertrophy in exercise-trained swine will be discussed in Chapter 5.

1.6 Methods for studying cardiac remodeling and transcriptional regulation

The astounding amount of knowledge about the molecular mechanisms of hypertrophy and post-MI remodeling could only be achieved through the use of animal models. Especially for mechanistic insights into the complex signaling pathways and the interplay between cardiomyocytes and other cardiac cells such as fibroblasts and endothelial cells studies in cell culture would not suffice.

1.6.1 Animal models of post-MI remodeling

The most often used animals in biomedical research are mice and rats. This is due to costs, ease of handling, short gestation period and rapid development to adulthood. Moreover, they can be used for genetic engineering, which has revolutionized studies in signaling pathways and much of the knowledge that was discussed in section 1.5.1 was obtained from studies in transgenic or gene knock out mice. However transgenic mice are not the catchall for molecular biology. To borrow a quote from Cook *et al.*'s provocative review: "What have genetic mice done for us?" (Cook *et al.*, 2009). Showing that a protein is involved in hypertrophy, by either knocking the gene out or by overexpressing it, does not necessarily mean that this protein is also important in the human disease. This is illustrated by a phospholamban (PLN) knock out mouse. PLN inhibits SERCA2a thereby reducing Ca^{2+} loading into the sarcoplasmic reticulum (SR) and thus contractility. As discussed before, SERCA 2a expression and activity is downregulated in heart failure. $PLN^{-/-}$ mice have increased SR Ca^{2+} loading and cardiac function, which is in stark contrast to people having a genetic mutation in the PLN gene, who despite having no detectable PLN protein expression, develop dilated cardiomyopathy (Haghighi *et al.*, 2003). Despite their attractiveness, there are obvious drawbacks in using mouse and rats for cardiovascular research, such as that the cardiovascular physiology and anatomy is quite different from humans. Rodents have much higher levels of heart rate and cardiac contractility (Kass *et al.*, 1998), have a different α/β-myosin heavy chain expression pattern (Swynghedauw, 1986) and different Ca^{2+}-cycling (Bers, 2002). Mice and rats are also sympathetically dominant, whereas humans are parasympathetically dominant (Lameris *et al.*, 2000).

Large animals, such as the pig, more closely approximate the human cardiovascular system and are therefore suitable to serve as translational models for studying post-MI remodeling (Dixon & Spinale, 2009; Yarbrough & Spinale, 2003). Pigs have a clear advantage over rodent models in resembling humans more closely in terms of heart rate and contractility (Kass *et al.*, 1998), and autonomic control thereof (Dixon & Spinale, 2009; Hasenfuss, 1998), as well as myofilament protein composition (Dixon & Spinale, 2009; Hasenfuss, 1998) and function (Hamdani *et al.*, 2008). Post-MI remodeling in swine has been extensively studied which allowed insight in various mechanisms, such as the mechanisms of infarct expansion (Mukherjee *et al.*, 2003), alterations in myofilament function (van der Velden *et al.*, 2004), changes in coronary blood flow regulation (Duncker *et al.*, 2008), molecular signaling (Chapter 2) and genetic reprogramming (Chapter 4). Notwithstanding its translational power, an inherent drawback of the pig as a model organism is that its genome has not been fully sequenced yet. Overcoming these experimental challenges will be rewarded by gaining insight into cardiac remodeling in a large animal model with better translational potential than murine models.

1.6.2 Animal models of physiological remodeling

To study the molecular and physiological mechanisms underlying physiological hypertrophy, various animal models and hypertrophy stimuli have been used (Wang *et al.*, 2010). The majority of studies are performed in mice and physiological hypertrophy is induced by treadmill running, voluntary wheel running or swim training. The amount of hypertrophy is generally limited, with the biggest effect seen with swim training (Wang *et al.*, 2010). Larger animal models have also been used to study physiological hypertrophy, most notably dogs and swine exercise trained on treadmills. An extended period of exercise-training in swine resulted in cardiac hypertrophy (Laughlin *et al.*, 1991; White *et al.*, 1987a), as well as increased coronary blood flow capacity, decreased heart rate (Laughlin *et al.*, 1991) and increased stroke volume (White *et al.*, 1987a). However, studies into the molecular changes underlying physiological hypertrophy in swine have mostly been lacking.

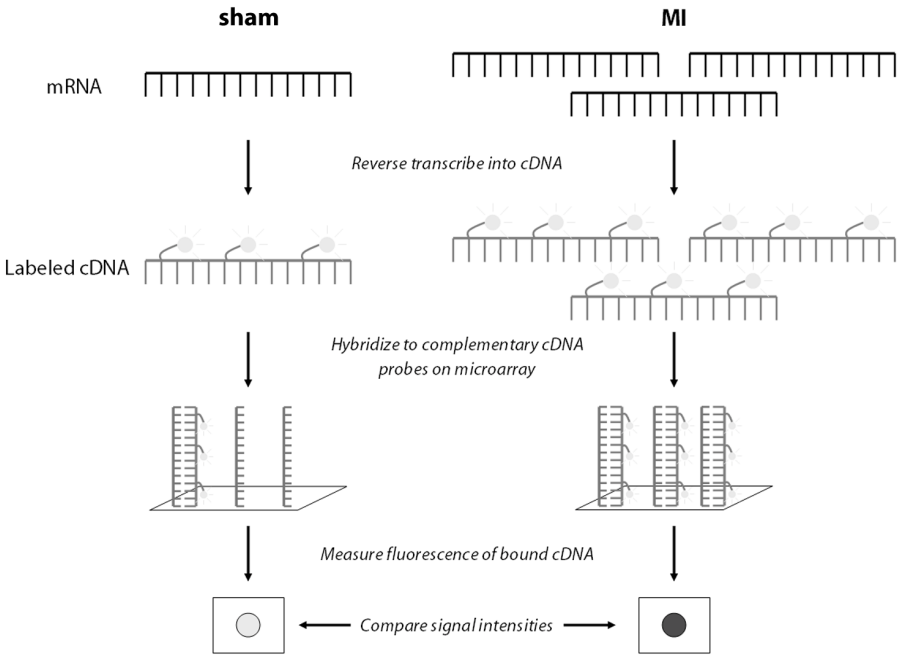

Figure 1.4: Overview of microarray experiment. *RNA is isolated from Sham and MI heart tissue. In this example, the mRNA of a single gene is shown and MI hearts contain three times more of this mRNA than sham tissue. mRNA is reverse transcribed into cDNA labeled with a fluorescent marker. The labeled cDNA is then hybridized to the complementary cDNA deposited on the microarray surface. The fluorescence signal intensities are measured and MI and sham signals are compared. In this example MI gives a stronger signal, as more labeled cDNA bound to the array. In a microarray experiment more than 20,000 different mRNAs can be measured simultaneously.*

1.6.2 Unbiased approaches

Reductionistic studies into the molecular mechanisms of cardiac hypertrophy (described in sections 1.5.1 & 1.5.2) have provided a wealth of information. However the use of genetic models in studies of cardiovascular disease soon illustrated the complexity of cardiovascular diseases, as many gene knockout animal models lacked a clear phenotype. The completion of the Human Genome Project and the advent of the "omics" technologies, have shifted attention towards more holistic approaches. These approaches are also termed unbiased, as the question is not: "what happens when I knock out 'my favorite gene' ?", but rather "what changes can be detected in a certain disease state?".

An example of such a technique is gene expression microarray analysis. With this technique the mRNA levels of all genes can be studied simultaneously and semi-quantitatively (Braam & Bluyssen, 2005). Gene expression microarrays are made by deposition of thousands of DNA probes (e.g. representing all known porcine genes) on a carrier surface. Total RNA is isolated and mRNA is then reverse transcribed into labeled cDNA. This cDNA is then hybridized to the DNA on the carrier surface, where the signal from the label can be detected. The amount of signal is dependent on the amount of cDNA that will bind and thus

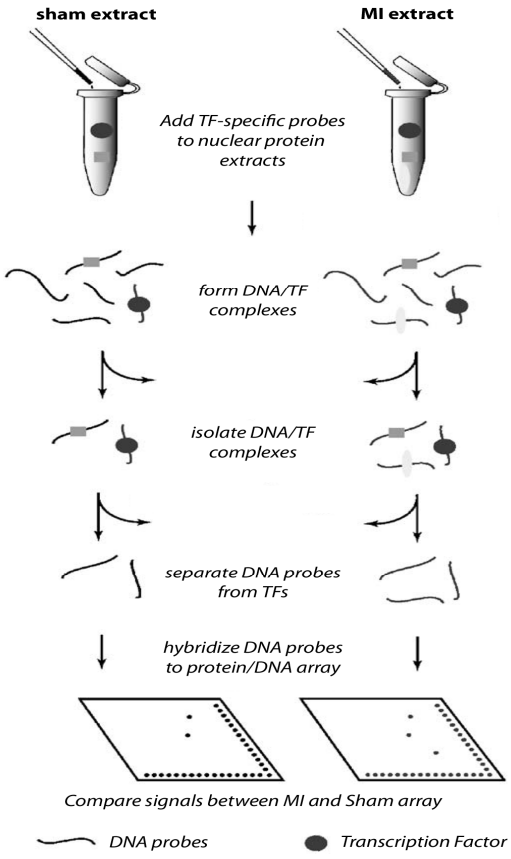

Figure 1.5: Protein/DNA array. *Nuclear protein is extracted from sham and MI hearts. A set of 345 biotin-labeled TF-specific DNA probes are added to each extract. During incubation, the TFs that are present in the nuclear extract will bind to their corresponding DNA-probe. All unbound DNA-probes are washed away. Next, the bound DNA probes are separated from the TFs and hybridized to the complementary DNA probe on the array. Signal is produced by incubation the biotin-labeled probes on the array with streptavidin-HRP followed by enhanced chemiluminesence. Signal intensities are compared between sham and MI arrays and difference in signal indicates a difference in TF DNA-binding activity. Figure adapted from: (Jiang et al., 2003).*

on the amount of the specific mRNA present in the sample (see Fig 1.4). With this technique the gene expression of thousands of genes can be measured in a single experiment (Braam & Bluyssen, 2005). Since Velculescu et al. first published this technique (Velculescu *et al.*, 1995), gene expression profiling has taken flight. Numerous studies have applied this technique to murine models to look at changes in gene expression in the heart following MI (Mirotsou *et al.*, 2006), or after exercise (Kong *et al.*, 2005). Microarray analysis of pathological and physiological hypertrophy in swine will be described in Chapters 4 & 5.

Not only mRNA levels but also levels of TFs can be examined in an unbiased fashion. With protein/DNA arrays one can assess the DNA-binding activity of numerous TFs at the same time (Jiang *et al.*, 2003). With this technique, a nuclear protein extract is incubated with a mixture of labeled TF-specific binding DNA probes (see Fig 1.5). Only DNA probes that bind to a TF in the nuclear protein extract are retained, while the non-binding probes are washed away. The remaining DNA probes are then detected and semi-quantitated by hybridization to an array of complementary DNA. Signal intensity at a specific spot is thus dependent on the DNA binding activity of the particular TF in the nuclear protein extract. This method is semi-quantitative, so that the DNA-binding activity of TFs can be compared across different disease states. This technique will be used in Chapters 4 & 5 to study TF DNA-binding activity in nuclear extracts from heart tissue (Chapter 3), following a pathological or physiological hypertrophic stimulus.

1.7 Aim and outline of this thesis

We hypothesize that the changes between pathological and physiological hypertrophy are the result of genetic reprogramming early after onset of the hypertrophic stimulus. The main aim of this thesis is to identify these changes in genetic programming in an unbiased and integrative fashion and in a physiologically relevant, large animal model.

In Chapter 2 we argue that systems biology and integrative physiology should not be considered separate entities, but that integration of the “omics” technology into integrative physiology is necessary to understand complex processes at multiple levels. In this thesis, we apply this integrative physiology approach to investigate post-MI remodeling and regulation of coronary blood during exercise in swine.

In order to study TF activity, nuclear protein extracts from cardiac tissue are required. In Chapter 3 we optimized a nuclear protein extraction method to efficiently and reproducibly obtain nuclear proteins from frozen heart tissue.

In Chapter 4 we combined microarray analysis with bioinformatical TF analysis and protein/DNA array analysis to study the TFs that control post-MI remodeling in swine.

In Chapter 5 we investigated the TFs that drive exercise-training induced hypertrophy in swine and made a comprehensive comparison between the molecular changes seen in pathological and physiological hypertrophy.

1.8 References

Alpert JS (2011). What you need to know if you have coronary artery disease. *Circulation* **124**, e176-e178.

Andersen JB, Rourke BC, Caiozzo VJ, Bennett AF, & Hicks JW (2005). Physiology: postprandial cardiac hypertrophy in pythons. *Nature* **434**, 37-38.

Bai S & Kerppola TK (2011). Opposing Roles of FoxP1 and Nfat3 in Transcriptional Control of Cardiomyocyte Hypertrophy. *Mol Cell Biol* **31**, 3068-3080.

Beisvag V, Kemi OJ, Arbo I, Loennechen JP, Wisloff U, Langaas M, Sandvik AK, & Ellingsen O (2009). Pathological and physiological hypertrophies are regulated by distinct gene programs. *Eur J Cardiovasc Prev Rehabil* **16**, 690-697.

Beltrami AP, Urbanek K, Kajstura J, Yan SM, Finato N, Bussani R, Nadal-Ginard B, Silvestri F, Leri A, Beltrami CA, & Anversa P (2001). Evidence that human cardiac myocytes divide after myocardial infarction. *N Engl J Med* **344**, 1750-1757.

Bergmann O, Bhardwaj RD, Bernard S, Zdunek S, Barnabe-Heider F, Walsh S, Zupicich J, Alkass K, Buchholz BA, Druid H, Jovinge S, & Frisen J (2009). Evidence for cardiomyocyte renewal in humans. *Science* **324**, 98-102.

Bernardo BC, Weeks KL, Pretorius L, & McMullen JR (2010). Molecular distinction between physiological and pathological cardiac hypertrophy: experimental findings and therapeutic strategies. *Pharmacol Ther* **128**, 191-227.

Bers DM (2002). Cardiac excitation-contraction coupling. *Nature* **415**, 198-205.

Bito V, Heinzel FR, Biesmans L, Antoons G, & Sipido KR (2008). Crosstalk between L-type Ca2+ channels and the sarcoplasmic reticulum: alterations during cardiac remodelling. *Cardiovasc Res* **77**, 315-324.

Black MJ, Bertram JF, Campbell JH, & Campbell GR (1995). Angiotensin II induces cardiovascular hypertrophy in perindopril-treated rats. *J Hypertens* **13**, 683-692.

Booth FW & Lees SJ (2007). Fundamental questions about genes, inactivity, and chronic diseases. *Physiol Genomics* **28**, 146-157.

Bostrom P, Mann N, Wu J, Quintero PA, Plovie ER, Panakova D, Gupta RK, Xiao C, MacRae CA, Rosenzweig A, & Spiegelman BM (2010). C/EBPbeta controls exercise-induced cardiac growth and protects against pathological cardiac remodeling. *Cell* **143**, 1072-1083.

Bourajjaj M, Armand AS, da Costa Martins PA, Weijts B, van der Nagel R., Heeneman S, Wehrens XH, & De Windt LJ (2008). NFATc2 is a necessary mediator of calcineurin-dependent cardiac hypertrophy and heart failure. *J Biol Chem* **283**, 22295-22303.

Braam B & Bluyssen H (2005). Expression profiling in cardiovascular disease using microarrays. In *Cardiovascular Research: New Technologies, Methods, and Applications*, eds. Pasterkamp G & de Kleijn DP, pp. 3-44. Springer, New York.

Clerk A, Cullingford TE, Fuller SJ, Giraldo A, Markou T, Pikkarainen S, & Sugden PH (2007). Signaling pathways mediating cardiac myocyte gene expression in physiological and stress responses. *J Cell Physiol* **212**, 311-322.

Cook SA, Clerk A, & Sugden PH (2009). Are transgenic mice the 'alkahest' to understanding myocardial hypertrophy and failure? *J Mol Cell Cardiol* **46**, 118-129.

Czubryt MP & Olson EN (2004). Balancing contractility and energy production: the role of myocyte enhancer factor 2 (MEF2) in cardiac hypertrophy. *Recent Prog Horm Res* **59**, 105-124.

D'Angelo DD, Sakata Y, Lorenz JN, Boivin GP, Walsh RA, Liggett SB, & Dorn GW (1997). Transgenic Galphaq overexpression induces cardiac contractile failure in mice. *Proc Natl Acad Sci U S A* **94**, 8121-8126.

Datta SR, Brunet A, & Greenberg ME (1999). Cellular survival: a play in three Akts. *Genes Dev* **13**, 2905-2927.

Davis FJ, Gupta M, Camoretti-Mercado B, Schwartz RJ, & Gupta MP (2003). Calcium/calmodulin-dependent protein kinase activates serum response factor transcription activity by its dissociation from histone deacetylase, HDAC4. Implications in cardiac muscle gene regulation during hypertrophy. *J Biol Chem* **278**, 20047-20058.

de Waard MC, van der Velden J, Bito V, Ozdemir S, Biesmans L, Boontje NM, Dekkers DH, Schoonderwoerd K, Schuurbiers HC, de Crom R, Stienen GJ, Sipido KR, Lamers JM, & Duncker DJ (2007). Early exercise training normalizes myofilament function and attenuates left ventricular pump dysfunction in mice with a large myocardial infarction. *Circ Res* **100**, 1079-1088.

De Windt LJ, Lim HW, Bueno OF, Liang Q, Delling U, Braz JC, Glascock BJ, Kimball TF, del Monte F., Hajjar RJ, & Molkentin JD (2001). Targeted inhibition of calcineurin attenuates cardiac hypertrophy in vivo. *Proc Natl Acad Sci U S A* **98**, 3322-3327.

Dhanasekaran A, Gruenloh SK, Buonaccorsi JN, Zhang R, Gross GJ, Falck JR, Patel PK, Jacobs ER, & Medhora M (2008). Multiple antiapoptotic targets of the PI3K/Akt survival pathway are activated by epoxyeicosatrienoic acids to protect cardiomyocytes from hypoxia/anoxia. *Am J Physiol Heart Circ Physiol* **294**, H724-H735.

Dixon JA & Spinale FG (2009). Large animal models of heart failure: a critical link in the translation of basic science to clinical practice. *Circ Heart Fail* **2**, 262-271.

Dorn GW (2009). Apoptotic and non-apoptotic programmed cardiomyocyte death in ventricular remodelling. *Cardiovasc Res* **81**, 465-473.

Duncker DJ & Bache RJ (2008). Regulation of coronary blood flow during exercise. *Physiol Rev* **88**, 1009-1086.

Duncker DJ, de Beer VJ, & Merkus D (2008). Alterations in vasomotor control of coronary resistance vessels in remodelled myocardium of swine with a recent myocardial infarction. *Med Biol Eng Comput* **46**, 485-497.

Erlebacher JA, Weiss JL, Eaton LW, Kallman C, Weisfeldt ML, & Bulkley BH (1982). Late effects of acute infarct dilation on heart size: a two dimensional echocardiographic study. *Am J Cardiol* **49**, 1120-1126.

Fagard R, Aubert A, Lysens R, Staessen J, Vanhees L, & Amery A (1983). Noninvasive assessment of seasonal variations in cardiac structure and function in cyclists. *Circulation* **67**, 896-901.

Faridi J, Fawcett J, Wang L, & Roth RA (2003). Akt promotes increased mammalian cell size by stimulating protein synthesis and inhibiting protein degradation. *Am J Physiol Endocrinol Metab* **285**, E964-E972.

Fletcher PJ, Pfeffer JM, Pfeffer MA, & Braunwald E (1981). Left ventricular diastolic pressure-volume relations in rats with healed myocardial infarction. Effects on systolic function. *Circ Res* **49**, 618-626.

Frey N & Olson EN (2003). Cardiac hypertrophy: the good, the bad, and the ugly. *Annu Rev Physiol* **65**, 45-79.

Fujio Y, Nguyen T, Wencker D, Kitsis RN, & Walsh K (2000). Akt promotes survival of cardiomyocytes in vitro and protects against ischemia-reperfusion injury in mouse heart. *Circulation* **101**, 660-667.

Gajarsa JJ & Kloner RA (2011). Left ventricular remodeling in the post-infarction heart: a review of cellular, molecular mechanisms, and therapeutic modalities. *Heart Fail Rev* **16**, 13-21.

Galindo CL, Skinner MA, Errami M, Olson LD, Watson DA, Li J, McCormick JF, McIver LJ, Kumar NM, Pham TQ, & Garner HR (2009). Transcriptional profile of isoproterenol-induced cardiomyopathy and comparison to exercise-induced cardiac hypertrophy and human cardiac failure. *BMC Physiol* **9**, 23.

Gielen S, Schuler G, & Hambrecht R (2001). Exercise training in coronary artery disease and coronary vasomotion. *Circulation* **103**, E1-E6.

Haghighi K, Kolokathis F, Pater L, Lynch RA, Asahi M, Gramolini AO, Fan GC, Tsiapras D, Hahn HS, Adamopoulos S, Liggett SB, Dorn GW, MacLennan DH, Kremastinos DT, & Kranias EG (2003). Human phospholamban null results in lethal dilated cardiomyopathy revealing a critical difference between mouse and human. *J Clin Invest* **111**, 869-876.

Haitsma DB, Bac D, Raja N, Boomsma F, Verdouw PD, & Duncker DJ (2001). Minimal impairment of myocardial blood flow responses to exercise in the remodeled left ventricle early after myocardial infarction, despite significant hemodynamic and neurohumoral alterations. *Cardiovasc Res* **52**, 417-428.

Hakim AA, Petrovitch H, Burchfiel CM, Ross GW, Rodriguez BL, White LR, Yano K, Curb JD, & Abbott RD (1998). Effects of walking on mortality among nonsmoking retired men. *N Engl J Med* **338**, 94-99.

Hamdani N, de Waard MC, Messer AE, Boontje NM, Kooij V, van Dijk SJ, Versteilen A, Lamberts R, Merkus D, Dos Remedios C, Duncker DJ, Borbely A, Papp Z, Paulus W, Stienen GJ, Marston SB, & van der Velden J (2008). Myofilament dysfunction in cardiac disease from mice to men. *J Muscle Res Cell Motil* **29**, 189-201.

Hannenhalli S, Putt ME, Gilmore JM, Wang J, Parmacek MS, Epstein JA, Morrisey EE, Margulies KB, & Cappola TP (2006). Transcriptional genomics associates FOX transcription factors with human heart failure. *Circulation* **114**, 1269-1276.

Hasenfuss G (1998). Animal models of human cardiovascular disease, heart failure and hypertrophy. *Cardiovasc Res* **39**, 60-76.

Hass EE & Smith Jr. SC (2010). Post-Hospital Phase of an Acute Coronary Syndrome. In *Cardiology*, eds. Crawford MH, DiMarco JP, & Paulus WJ, pp. 427-447. Mosby Elsevier, Philadelphia.

Heineke J & Molkentin JD (2006). Regulation of cardiac hypertrophy by intracellular signalling pathways. *Nat Rev Mol Cell Biol* **7**, 589-600.

Hill JA & Olson EN (2008). Cardiac plasticity. *N Engl J Med* **358**, 1370-1380.

Hutchins GM & Bulkley BH (1978). Infarct expansion versus extension: two different complications of acute myocardial infarction. *Am J Cardiol* **41**, 1127-1132.

Ito H, Hirata Y, Hiroe M, Tsujino M, Adachi S, Takamoto T, Nitta M, Taniguchi K, & Marumo F (1991). Endothelin-1 induces hypertrophy with enhanced expression of muscle-specific genes in cultured neonatal rat cardiomyocytes. *Circ Res* **69**, 209-215.

Jiang X, Norman M, & Li X (2003). Use of an array technology for profiling and comparing transcription factors activated by TNFalpha and PMA in HeLa cells. *Biochim Biophys Acta* **1642**, 1-8.

Jugdutt BI (2003). Ventricular remodeling after infarction and the extracellular collagen matrix: when is enough enough? *Circulation* **108**, 1395-1403.

Kannel WB, Belanger A, D'Agostino R, & Israel I (1986). Physical activity and physical demand on the job and risk of cardiovascular disease and death: the Framingham Study. *Am Heart J* **112**, 820-825.

Kass DA, Hare JM, & Georgakopoulos D (1998). Murine cardiac function: a cautionary tail. *Circ Res* **82**, 519-522.

Katz AM (2008). The "modern" view of heart failure: how did we get here? *Circ Heart Fail* **1**, 63-71.

Kawano S, Kubota T, Monden Y, Tsutsumi T, Inoue T, Kawamura N, Tsutsui H, & Sunagawa K (2006). Blockade of NF-kappaB improves cardiac function and survival after myocardial infarction. *Am J Physiol Heart Circ Physiol* **291**, H1337-H1344.

Kehat I & Molkentin JD (2010). Molecular pathways underlying cardiac remodeling during pathophysiological stimulation. *Circulation* **122**, 2727-2735.

Kemi OJ, Ceci M, Wisloff U, Grimaldi S, Gallo P, Smith GL, Condorelli G, & Ellingsen O (2008). Activation or inactivation of cardiac Akt/mTOR signaling diverges physiological from pathological hypertrophy. *J Cell Physiol* **214**, 316-321.

Kong SW, Bodyak N, Yue P, Liu Z, Brown J, Izumo S, & Kang PM (2005). Genetic expression profiles during physiological and pathological cardiac hypertrophy and heart failure in rats. *Physiol Genomics* **21**, 34-42.

Lameris TW, de Zeeuw S, Alberts G, Boomsma F, Duncker DJ, Verdouw PD, Veld AJ, & van Den Meiracker AH (2000). Time course and mechanism of myocardial catecholamine release during transient ischemia in vivo. *Circulation* **101**, 2645-2650.

Latronico MV, Costinean S, Lavitrano ML, Peschle C, & Condorelli G (2004). Regulation of cell size and contractile function by AKT in cardiomyocytes. *Ann N Y Acad Sci* **1015**, 250-260.

Laughlin MH, Hale CC, Novela L, Gute D, Hamilton N, & Ianuzzo CD (1991). Biochemical characterization of exercise-trained porcine myocardium. *J Appl Physiol* **71**, 229-235.

Levy D, Garrison RJ, Savage DD, Kannel WB, & Castelli WP (1990). Prognostic implications of echocardiographically determined left ventricular mass in the Framingham Heart Study. *N Engl J Med* **322**, 1561-1566.

Li Y, Ha T, Gao X, Kelley J, Williams DL, Browder IW, Kao RL, & Li C (2004). NF-kappaB activation is required for the development of cardiac hypertrophy in vivo. *Am J Physiol Heart Circ Physiol* **287**, H1712-H1720.

Liang Q, De Windt LJ, Witt SA, Kimball TR, Markham BE, & Molkentin JD (2001). The transcription factors GATA4 and GATA6 regulate cardiomyocyte hypertrophy in vitro and in vivo. *J Biol Chem* **276**, 30245-30253.

Liang Q & Molkentin JD (2002). Divergent signaling pathways converge on GATA4 to regulate cardiac hypertrophic gene expression. *J Mol Cell Cardiol* **34**, 611-616.

Manson JE, Greenland P, LaCroix AZ, Stefanick ML, Mouton CP, Oberman A, Perri MG, Sheps DS, Pettinger MB, & Siscovick DS (2002). Walking compared with vigorous exercise for the prevention of cardiovascular events in women. *N Engl J Med* **347**, 716-725.

Maron BJ, Pelliccia A, Spataro A, & Granata M (1993). Reduction in left ventricular wall thickness after deconditioning in highly trained Olympic athletes. *Br Heart J* **69**, 125-128.

McMullen JR, Shioi T, Huang WY, Zhang L, Tarnavski O, Bisping E, Schinke M, Kong S, Sherwood MC, Brown J, Riggi L, Kang PM, & Izumo S (2004). The insulin-like growth factor 1 receptor induces physiological heart growth via the phosphoinositide 3-kinase(p110alpha) pathway. *J Biol Chem* **279**, 4782-4793.

McMullen JR, Shioi T, Zhang L, Tarnavski O, Sherwood MC, Kang PM, & Izumo S (2003). Phosphoinositide 3-kinase(p110alpha) plays a critical role for the induction of

physiological, but not pathological, cardiac hypertrophy. *Proc Natl Acad Sci U S A* **100**, 12355-12360.

Mirotsou M, Dzau VJ, Pratt RE, & Weinberg EO (2006). Physiological genomics of cardiac disease: quantitative relationships between gene expression and left ventricular hypertrophy. *Physiol Genomics* **27**, 86-94.

Molkentin JD, Lu JR, Antos CL, Markham B, Richardson J, Robbins J, Grant SR, & Olson EN (1998). A calcineurin-dependent transcriptional pathway for cardiac hypertrophy. *Cell* **93**, 215-228.

Morancho B, Minguillon J, Molkentin JD, Lopez-Rodriguez C, & Aramburu J (2008). Analysis of the transcriptional activity of endogenous NFAT5 in primary cells using transgenic NFAT-luciferase reporter mice. *BMC Mol Biol* **9**, 13.

Mudd JO & Kass DA (2008). Tackling heart failure in the twenty-first century. *Nature* **451**, 919-928.

Mukherjee R, Brinsa TA, Dowdy KB, Scott AA, Baskin JM, Deschamps AM, Lowry AS, Escobar GP, Lucas DG, Yarbrough WM, Zile MR, & Spinale FG (2003). Myocardial infarct expansion and matrix metalloproteinase inhibition. *Circulation* **107**, 618-625.

Narula J, Haider N, Arbustini E, & Chandrashekhar Y (2006). Mechanisms of disease: apoptosis in heart failure--seeing hope in death. *Nat Clin Pract Cardiovasc Med* **3**, 681-688.

Neri Serneri GG, Boddi M, Modesti PA, Cecioni I, Coppo M, Padeletti L, Michelucci A, Colella A, & Galanti G (2001). Increased cardiac sympathetic activity and insulin-like growth factor-I formation are associated with physiological hypertrophy in athletes. *Circ Res* **89**, 977-982.

Ni YG, Berenji K, Wang N, Oh M, Sachan N, Dey A, Cheng J, Lu G, Morris DJ, Castrillon DH, Gerard RD, Rothermel BA, & Hill JA (2006). Foxo transcription factors blunt cardiac hypertrophy by inhibiting calcineurin signaling. *Circulation* **114**, 1159-1168.

Nian M, Lee P, Khaper N, & Liu P (2004). Inflammatory cytokines and postmyocardial infarction remodeling. *Circ Res* **94**, 1543-1553.

Oka T, Maillet M, Watt AJ, Schwartz RJ, Aronow BJ, Duncan SA, & Molkentin JD (2006). Cardiac-specific deletion of Gata4 reveals its requirement for hypertrophy, compensation, and myocyte viability. *Circ Res* **98**, 837-845.

Opie LH, Commerford PJ, Gersh BJ, & Pfeffer MA (2006). Controversies in ventricular remodelling. *Lancet* **367**, 356-367.

Passier R, Zeng H, Frey N, Naya FJ, Nicol RL, McKinsey TA, Overbeek P, Richardson JA, Grant SR, & Olson EN (2000). CaM kinase signaling induces cardiac hypertrophy and activates the MEF2 transcription factor in vivo. *J Clin Invest* **105**, 1395-1406.

Pelliccia A, Kinoshita N, Pisicchio C, Quattrini F, Dipaolo FM, Ciardo R, Di GB, Guerra E, De BE, Casasco M, Culasso F, & Maron BJ (2010). Long-term clinical consequences of intense, uninterrupted endurance training in olympic athletes. *J Am Coll Cardiol* **55**, 1619-1625.

Pfeffer JM, Pfeffer MA, Fletcher PJ, & Braunwald E (1991). Progressive ventricular remodeling in rat with myocardial infarction. *Am J Physiol* **260**, H1406-H1414.

Pfeffer MA & Braunwald E (1990). Ventricular remodeling after myocardial infarction. Experimental observations and clinical implications. *Circulation* **81**, 1161-1172.

Pluim BM, Zwinderman AH, van der Laarse A, & van der Wall EE (2000). The athlete's heart. A meta-analysis of cardiac structure and function. *Circulation* **101**, 336-344.

Roger VL, Go AS, Lloyd-Jones DM, Adams RJ, Berry JD, Brown TM, Carnethon MR, Dai S, de SG, Ford ES, Fox CS, Fullerton HJ, Gillespie C, Greenlund KJ, Hailpern SM, Heit JA, Ho PM, Howard VJ, Kissela BM, Kittner SJ, Lackland DT, Lichtman JH, Lisabeth LD, Makuc DM, Marcus GM, Marelli A, Matchar DB, McDermott MM, Meigs JB, Moy CS, Mozaffarian D, Mussolino ME, Nichol G, Paynter NP, Rosamond WD, Sorlie PD, Stafford RS, Turan TN, Turner MB, Wong ND, & Wylie-Rosett J (2011). Heart disease and stroke statistics--2011 update: a report from the American Heart Association. *Circulation* **123**, e18-e209.

Rose BA, Force T, & Wang Y (2010). Mitogen-activated protein kinase signaling in the heart: angels versus demons in a heart-breaking tale. *Physiol Rev* **90**, 1507-1546.

Sakamoto M, Minamino T, Toko H, Kayama Y, Zou Y, Sano M, Takaki E, Aoyagi T, Tojo K, Tajima N, Nakai A, Aburatani H, & Komuro I (2006). Upregulation of heat shock transcription factor 1 plays a critical role in adaptive cardiac hypertrophy. *Circ Res* **99**, 1411-1418.

Shioi T, Kang PM, Douglas PS, Hampe J, Yballe CM, Lawitts J, Cantley LC, & Izumo S (2000). The conserved phosphoinositide 3-kinase pathway determines heart size in mice. *EMBO J* **19**, 2537-2548.

Stanton HC, Brenner G, & Mayfield ED, Jr. (1969). Studies on isoproterenol-induced cardiomegaly in rats. *Am Heart J* **77**, 72-80.

Strom CC, Aplin M, Ploug T, Christoffersen TE, Langfort J, Viese M, Galbo H, Haunso S, & Sheikh SP (2005). Expression profiling reveals differences in metabolic gene expression between exercise-induced cardiac effects and maladaptive cardiac hypertrophy. *FEBS J* **272**, 2684-2695.

Sutton MG & Sharpe N (2000). Left ventricular remodeling after myocardial infarction: pathophysiology and therapy. *Circulation* **101**, 2981-2988.

Swynghedauw B (1986). Developmental and functional adaptation of contractile proteins in cardiac and skeletal muscles. *Physiol Rev* **66**, 710-771.

Vaartjes I, van Dis I, Visseren FLJ, & Bots ML (2010). Hart- en vaatziekten in Nederland. In *Hart- en vaatziekten in Nederland 2010. Cijfers over leefstijl- en risicofactoren, ziekte en sterfte*. pp. 7-28. Nederlandse Hartstichting, Den Haag.

Vakili BA, Okin PM, & Devereux RB (2001). Prognostic implications of left ventricular hypertrophy. *Am Heart J* **141**, 334-341.

van der Velden J, Merkus D, Klarenbeek BR, James AT, Boontje NM, Dekkers DH, Stienen GJ, Lamers JM, & Duncker DJ (2004). Alterations in myofilament function contribute to left ventricular dysfunction in pigs early after myocardial infarction. *Circ Res* **95**, e85-e95.

Velagaleti RS, Pencina MJ, Murabito JM, Wang TJ, Parikh NI, D'Agostino RB, Levy D, Kannel WB, & Vasan RS (2008). Long-term trends in the incidence of heart failure after myocardial infarction. *Circulation* **118**, 2057-2062.

Velculescu VE, Zhang L, Vogelstein B, & Kinzler KW (1995). Serial analysis of gene expression. *Science* **270**, 484-487.

Wang Y, Wisloff U, & Kemi OJ (2010). Animal models in the study of exercise-induced cardiac hypertrophy. *Physiol Res* **59**, 633-644.

Wannamethee SG & Shaper AG (2001). Physical activity in the prevention of cardiovascular disease: an epidemiological perspective. *Sports Med* **31**, 101-114.

Warren SE, Royal HD, Markis JE, Grossman W, & McKay RG (1988). Time course of left ventricular dilation after myocardial infarction: influence of infarct-related artery and success of coronary thrombolysis. *J Am Coll Cardiol* **11**, 12-19.

Weeks KL & McMullen JR (2011). The athlete's heart vs. the failing heart: can signaling explain the two distinct outcomes? *Physiology (Bethesda)* **26**, 97-105.

Weir RA, McMurray JJ, & Velazquez EJ (2006). Epidemiology of heart failure and left ventricular systolic dysfunction after acute myocardial infarction: prevalence, clinical characteristics, and prognostic importance. *Am J Cardiol* **97**, 13F-25F.

Wettschureck N, Rutten H, Zywietz A, Gehring D, Wilkie TM, Chen J, Chien KR, & Offermanns S (2001). Absence of pressure overload induced myocardial hypertrophy after conditional inactivation of Galphaq/Galpha11 in cardiomyocytes. *Nat Med* **7**, 1236-1240.

White FC, McKirnan MD, Breisch EA, Guth BD, Liu YM, & Bloor CM (1987a). Adaptation of the left ventricle to exercise-induced hypertrophy. *J Appl Physiol* **62**, 1097-1110.

White HD, Norris RM, Brown MA, Brandt PW, Whitlock RM, & Wild CJ (1987b). Left ventricular end-systolic volume as the major determinant of survival after recovery from myocardial infarction. *Circulation* **76**, 44-51.

Widmaier EP, Raff H, & Strang KT (2011). Cardiovascular Physiology. In *Vander's Human Physiology* pp. 353-433. McGraw-Hill, New York.

Widmaier EP, Raff H, & Strang KT (2004). Cardiovascular Physiology. In *Vander, Sherman & Luciano's Human Physiology* McGraw-Hill, New York.

Wilkins BJ, Dai YS, Bueno OF, Parsons SA, Xu J, Plank DM, Jones F, Kimball TR, & Molkentin JD (2004). Calcineurin/NFAT coupling participates in pathological, but not physiological, cardiac hypertrophy. *Circ Res* **94**, 110-118.

Wong SC, Fukuchi M, Melnyk P, Rodger I, & Giaid A (1998). Induction of cyclooxygenase-2 and activation of nuclear factor-kappaB in myocardium of patients with congestive heart failure. *Circulation* **98**, 100-103.

Xu J, Gong NL, Bodi I, Aronow BJ, Backx PH, & Molkentin JD (2006). Myocyte enhancer factors 2A and 2C induce dilated cardiomyopathy in transgenic mice. *J Biol Chem* **281**, 9152-9162.

Yarbrough WM & Spinale FG (2003). Large animal models of congestive heart failure: a critical step in translating basic observations into clinical applications. *J Nucl Cardiol* **10**, 77-86.

Zhang T & Brown JH (2004). Role of Ca2+/calmodulin-dependent protein kinase II in cardiac hypertrophy and heart failure. *Cardiovasc Res* **63**, 476-486.

Zhang X, Azhar G, Chai J, Sheridan P, Nagano K, Brown T, Yang J, Khrapko K, Borras AM, Lawitts J, Misra RP, & Wei JY (2001). Cardiomyopathy in transgenic mice with cardiac-specific overexpression of serum response factor. *Am J Physiol Heart Circ Physiol* **280**, H1782-H1792.

Chapter 2

‘Integrative Physiology 2.0’: integration of systems biology into physiology and its application to cardiovascular homeostasis

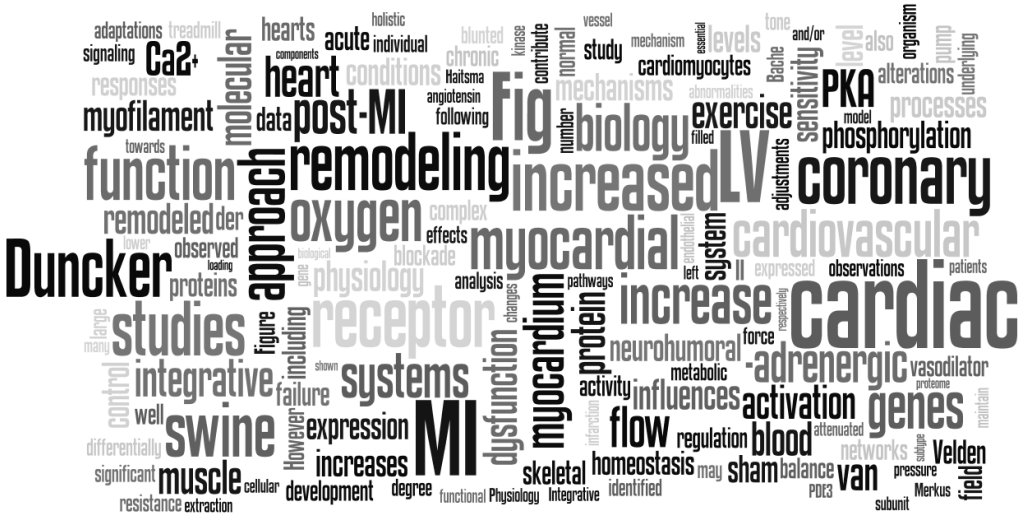

Diederik W. D. Kuster, Daphne Merkus, Jolanda van der Velden, Adrie J.M. Verhoeven & Dirk J. Duncker

J Physiol (2011) 589: 1037-1045

Abstract

Since the completion of the Human Genome Project and the advent of the large scaled unbiased '-omics' techniques, the field of systems biology has emerged. Systems biology aims to move away from the traditional reductionist molecular approach, which focused on understanding the role of single genes or proteins, towards a more holistic approach by studying networks and interactions between individual components of networks. From a conceptual standpoint, systems biology elicits a 'back to the future' experience for any integrative physiologist. However, many of the new techniques and modalities employed by systems biologists yield tremendous potential for integrative physiologists to expand their tool arsenal to (quantitatively) study complex biological processes, such as cardiac remodeling and heart failure, in a truly holistic fashion. We therefore advocate that systems biology should not become/stay a separate discipline with '-omics' as its playing field, but should be integrated into physiology to create 'Integrative Physiology 2.0'.

2.1 Introduction

Maintenance of homeostasis is essential for survival of an organism. The cardiovascular system has therefore developed a high degree of plasticity to maintain circulatory homeostasis in a wide variety of circumstances. Defense mechanisms include acute adjustments, e.g. the cardiovascular adaptations to a sudden increase in physical activity, as well as chronic adjustments, e.g. cardiac remodeling to a chronic elevation in hemodynamic loading conditions following myocardial injury, volume or pressure overload. These adjustments require highly integrated and orchestrated responses involving a large number of controlled variables. In view of the importance of adequate circulatory responses for the survival of an organism, these processes are characterized by a high level of redundancy involving complex signaling pathways that display significant interactions at multiple levels. Integrative physiology has been able to decipher many aspects of cardiovascular homeostasis, including the regulation of coronary blood flow (Duncker & Bache, 2008) as well as the short- and long-term regulation of blood pressure and cardiac function (Guyton, 1992, Hester, 2011). In other areas of cardiovascular homeostasis, including cardiac hypertrophy, integrative physiology has provided tremendous insight into this process at the organ and cellular level, but only very limited insight into its molecular basis (Fig. 2.1). The emergence of the field of molecular biology has enabled cardiovascular researchers to obtain deeper insight into this complex process (Mudd & Kass, 2008).

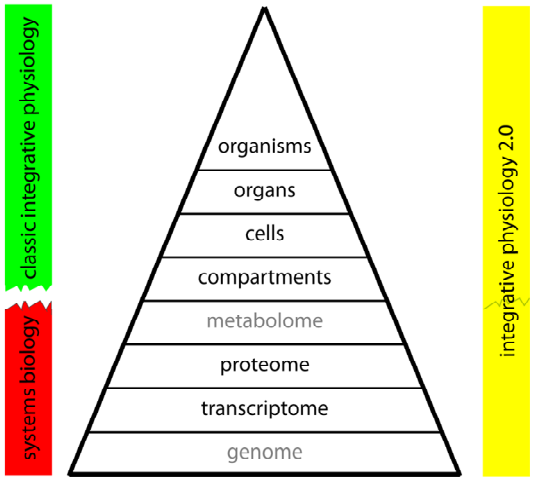

Figure 2.1. From systems biology and classical integrative physiology towards Integrative Physiology 2.0. *A process such as cardiac remodeling should be studied at different levels and the findings integrated. The bars on the left illustrate the dichotomy between classic integrative physiology and systems biology. The bar on the right illustrates the 'Integrative physiology 2.0' approach, which integrates the large scale unbiased '-omics' studies of systems biology with integrative physiology. Levels shown with a grey font have not been studied by our group, to date.*

Initial molecular studies in the cardiovascular field principally consisted of observational work, looking at gene and/or protein expression and changes therein in cardiovascular disease states (e.g. (Brand *et al.*, 1992; Katz, 1988)). These studies were followed by more mechanistic approaches to test the involvement of identified (novel)

genes and their products, mainly by virtue of knocking out and/or over-expressing a gene of interest (Frey & Olson, 2003; Heineke & Molkentin, 2006). This reductionist approach has significant value in monogenic diseases. However, the use of genetic models in studies of cardiovascular disease soon illustrated the complexity of cardiovascular diseases, as many gene knock-out animal models lacked a clear phenotype. These findings were initially interpreted to suggest that the gene was not important, while a more physiological interpretation is that other genes increased their activity and acted to compensate. These observations, in conjunction with the completion of the Human Genome Project and the advent of the '-omics' technologies, stimulated the emergence of the field of systems biology. As outlined elsewhere in this issue of *The Journal of Physiology*, systems biology aims to move beyond the traditional reductionist molecular approach (which focused on understanding the role of single genes or proteins), towards a more holistic approach by studying networks and interactions between individual components of networks. The strength of this integrative molecular approach is that, even when a perturbation in a molecular pathway does not result in clear phenotypic changes, the responsible compensatory adaptations will likely be mirrored in adaptations in the transcriptome, proteome and/or metabolome. Until now, systems biology has been mainly considered a research field in its own right. However, to date systems biology has been applied to relatively simple systems, including cultured cells and bacteria, but has not been applied to studies of homeostasis in complex organisms, including mammals, a field that has traditionally been the domain of integrative physiology (Fig. 2.1). We believe that integration of the complementary disciplines of systems biology and integrative physiology is essential to advance our understanding of complex biological processes.

In this article we will present studies on the adjustments of the myocardium to acute and chronic increases in loading conditions, in order to highlight the established strengths of classical integrative physiology and the promise of integrating systems biology and physiology. We begin to review our studies using classical *in vivo* physiology approaches to study regulation of cardiac function and coronary blood flow in response to acute exercise. We will then discuss how we have implemented biochemistry, molecular biology, and more recently bioinformatics to study biological processes in a more holistic rather than reductionistic fashion to understand complex processes such as cardiac remodeling and hypertrophy.

2.2 Plasticity of the cardiovascular system: acute responses to exercise

One of the most dramatic challenges for the cardiovascular system is represented by sudden heavy physical exercise, requiring both central and regional hemodynamic

adjustments in order to meet increases in metabolic needs of skeletal and cardiac muscle. A fivefold increase in cardiac output together with a redistribution of flow away from visceral organs and tissues is needed to accommodate sufficient increases in skeletal muscle and myocardial blood flow. The increases in muscle blood flow are facilitated by a small increase in aortic blood pressure but are opposed by the compressive forces generated by the contracting muscle, acting on the intramuscular vasculature. Consequently, the increases in flow are principally due to vasodilatation of the resistance vessels within the skeletal and cardiac muscle.

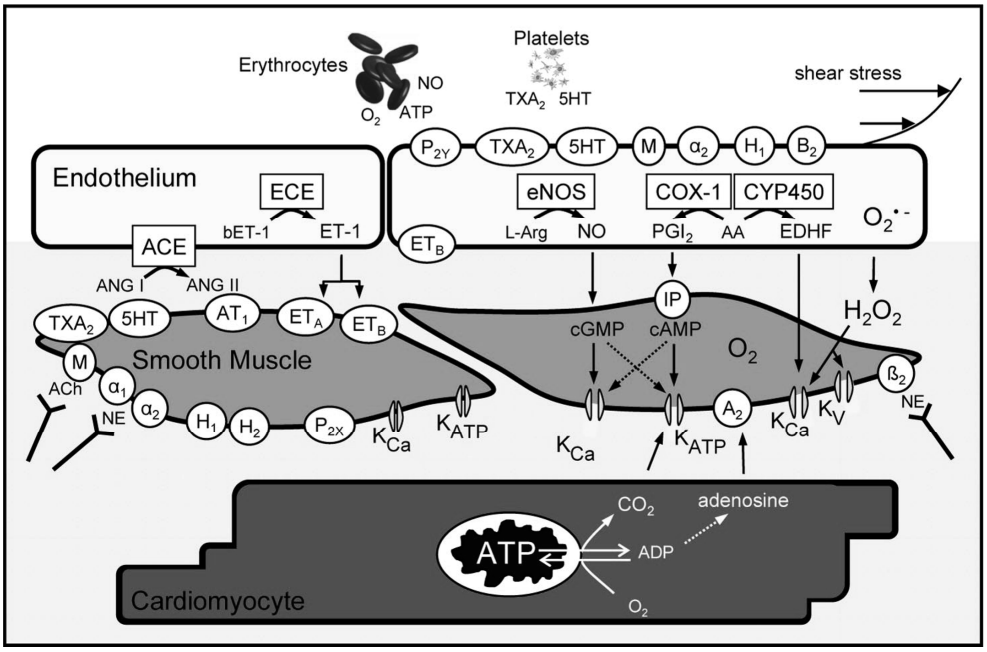

Figure 2.2. Schematic drawing of the various influences that determine coronary vasomotor tone and diameter. *Influences include autonomic nervous system activity, metabolic factors from cardiomyocytes and endothelial factors. The latter are modified by physical forces (shear stress), as well as erythrocyte and platelet-derived products acting on the endothelium. TxA2, thromboxane A2 (receptor); 5HT, serotonin or 5-hydroxytryptamine (receptor); P2X and P2Y, purinergic receptor subtypes 2X and 2Y thatmediate ATP-induced vasoconstriction and vasodilatation, respectively; ACh, acetylcholine; M, muscarinic receptor; H1 and H2, histamine receptors type 1 and 2; B2, bradykinin receptor subtype 2; ANG I and ANG II, angiotensin I and II; AT1, angiotensin II receptor subtype 1; ET, endothelin; ETA and ETB, endothelin receptor subtypes A and B; A2, adenosine receptor subtype 2; β2, β2-adrenergic receptor; α1 and α2, α-adrenergic receptors; NO, nitric oxide; eNOS, endothelial NO synthase; PGI2, prostacyclin; IP, prostacyclin receptor; COX-1, cyclooxygenase-1; EDHF, endothelium-derived hyperpolarizing factor; CYP450, cytochrome P450 2C9; KCa, calcium-sensitive K+ channel; KATP, ATP-sensitive K+ channel; KV, voltage-sensitive K+ channel; AA, arachidonic acid; L-Arg, L-arginine; O2–, superoxide. Receptors and enzymes are indicated by an oval and rectangle, respectively. From Duncker & Bache (2008), modified with permission from the American Physiological Society.*

A large number of vascular control mechanisms have been identified that can contribute to metabolic regulation of resistance vessel tone in the heart and skeletal muscle (Fig. 2.2), including blood-derived, endothelial, metabolic and sympathetic influences. However, unraveling of the exact mechanism that mediates the exercise-induced vasodilatation has proven to be difficult (Duncker & Bache, 2008; Duncker & Merkus, 2007; Laughlin *et al.*, 1996; Rowell, 2004; Tune *et al.*, 2004). Since maintenance of tissue perfusion is essential for adequate cardiac and skeletal muscle function and organismal survival, it is not surprising that regulation of tissue blood flow is characterized by a high number of redundant control mechanisms (Duncker & Bache, 2008; Rowell, 2004). A consequence of this non-linear redundancy design is that pharmacological blockade of a single vasodilator mechanism may have little or no effect (and may thus not reveal the actual contribution of that mechanism), as other vasodilator pathways will increase their activity and act to compensate. Only when multiple pathways are blocked will an effect become apparent, which is then greater than the sum of the effects of blocking the individual pathways. Indeed, studies in cardiac and skeletal muscle have demonstrated that simultaneous blockade of various vasodilator substances was required to attenuate the increase in skeletal muscle flow (Boushel, 2003; Murrant & Sarelius, 2002) or coronary blood flow (Duncker & Bache, 2008) during exercise. These observations demonstrate the importance of an integrative approach looking at the whole system and the interaction between the individual components.

2.3 Plasticity of the cardiovascular system: cardiac remodeling after myocardial infarction

The cardiovascular system is not only able to respond quickly to acute challenges, but also has the plasticity to respond to chronic changes in hemodynamic loading conditions, for example as occurs following an acute myocardial infarction (MI). Loss of a significant portion of myocardial tissue results in an immediate decrease in cardiac pump function, leading to neurohumoral activation that is aimed at restoring pump function. The neurohumoral activation results in a wide array of responses varying from the immediate (seconds–minutes) positive chronotropic, inotropic and lusitropic cardiac effects and sub-acute (hours–days) volume retention, to the chronic (days–months) cardiac remodeling, characterized by hypertrophy of the cardiac muscle (Katz, 2008). All these responses aim to maintain pump function of the injured heart. However, despite the apparent appropriateness of the hypertrophic remodeling response to maintain cardiac pump function early after MI (van Kats *et al.*, 2000), hypertrophic remodeling constitutes an independent risk factor for the long-term development of congestive heart failure (Levy *et*

al., 1990; Vakili *et al.*, 2001). The mechanism underlying progressive deterioration of left ventricular (LV) function towards overt heart failure remains incompletely understood, but may involve (i) continuous loss of cardiomyocytes through apoptosis (Narula *et al.*, 2006), (ii) a primary reduction in contractile function of the surviving myocardium (van der Velden *et al.*, 2004), (iii) alterations in extracellular matrix leading to progressive LV dilatation (Spinale, 2007), and/or (iv) myocardial blood flow abnormalities, resulting in impaired myocardial O_2 delivery to the non-infarcted region (van Veldhuisen *et al.*, 1998). Blood flow to the remodeled myocardium can become impeded as the coronary vasculature does not grow commensurate with the increase in LV mass and because extravascular compression of the coronary vasculature increases with increased LV filling pressures (Haitsma *et al.*, 2001). In addition, an increase in coronary resistance vessel tone, secondary to neurohumoral activation and endothelial dysfunction, could also contribute to the impaired myocardial oxygen supply.

Consequently, we explored in a series of studies the alterations in regulation of coronary resistance vessel tone in post-MI remodeled myocardium. For this purpose we employed a porcine model of MI produced by permanent ligation of the left circumflex coronary artery, which results in transmural infarction of 20–25% of the LV free wall, and studied swine at 2–3 weeks after induction of MI. Swine were not only studied at rest but also during graded treadmill exercise to further stress the remodeled

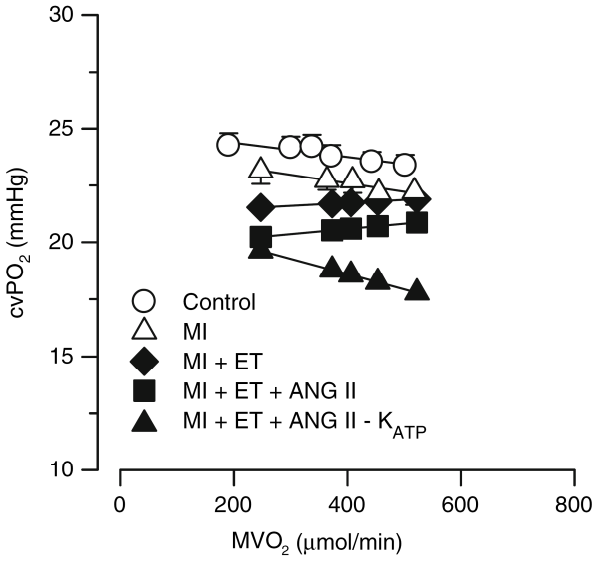

Figure 2.3. Myocardial oxygen balance in normal and MI swine. *Shown are the relations between myocardial oxygen consumption (MVO_2) and coronary venous oxygen tension ($cvPO_2$) in 30 normal swine (open circles) and 20 MI swine (open triangles) under control conditions. Data were obtained at rest and during increases in MVO_2 produced by graded treadmill exercise (1–5 km h^{-1} in normal swine and 1–4 km h^{-1} in MI swine). In addition, we have depicted the computed relations in MI swine if the ET (filled diamonds) and ANG II (filled squares) vasoconstrictor influences (which were both attenuated in MI swine) and the K_{ATP} (filled triangles) vasodilator influences (which were enhanced in MI swine) would have been identical to those in normal swine. The graph clearly illustrates that the adaptations in coronary vasomotor control act to blunt perturbations in oxygen balance in remodeled myocardium of swine with a recent MI. Modified from Duncker et al. (2008) with permission from Springer Science+Business Media.*

hearts and recruit the cardiac and coronary functional reserve capacity, to facilitate elucidation of compensatory mechanisms that become activated to maintain cardiovascular homeostasis. These studies indicate that myocardial oxygen balance is mildly perturbed in remodeled myocardium. Thus at a similar level of cardiac work and hence oxygen consumption, coronary blood flow and hence myocardial oxygen supply are lower in MI compared to normal swine, forcing the myocardium to increase its oxygen extraction leading to a lower coronary venous oxygen content (Fig. 2.3). That the relatively small degree of perturbation in the oxygen balance was associated with myocardial metabolic distress was also reflected in the increased vasodilator influence through opening of K_{ATP} channels, particularly during exercise (Merkus *et al.*, 2005b). Unexpectedly, we observed that despite increased circulating levels of noradrenalin, angiotensin II and endothelin-1, the coronary influences of *α*-adrenergic tone were not increased (Duncker *et al.*, 2005), while the coronary vasoconstrictor influences of endogenous endothelin (Merkus *et al.*, 2005a) and angiotensin II (Merkus *et al.*, 2006) were virtually abolished. Thus, early after myocardial infarction, small perturbations in myocardial oxygen balance were observed in remodeled myocardium. However, adaptations in coronary resistance vessel control,

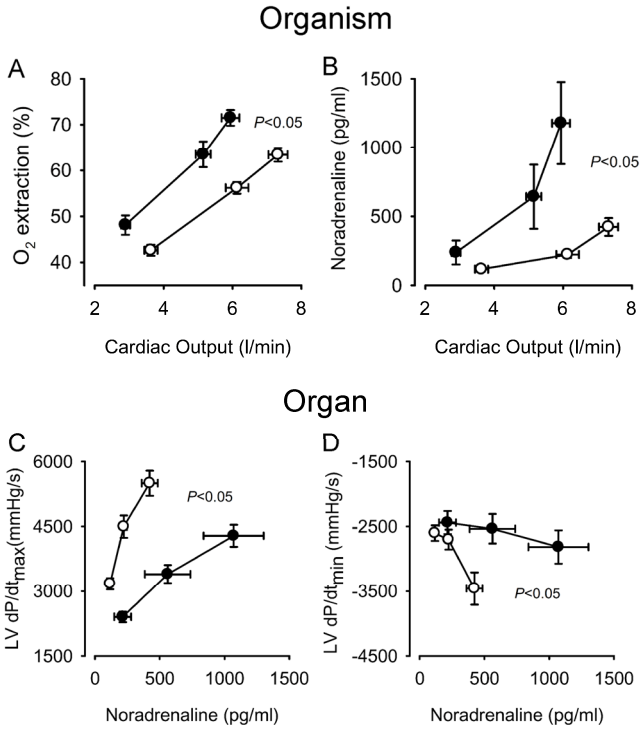

Figure 2.4. Functional changes at the whole-body and cardiac level. *Whole-body oxygen extraction (A) and circulating noradrenaline levels (B) in resting and exercising swine with cardiac dysfunction 3 weeks after MI (filled circles) or sham surgery (open circles), and maximum rates of rise (C) and fall (D) of left ventricular pressure were plotted as a function of circulating noradrenaline levels. In each group, data are shown during resting conditions and during treadmill running at 2 and 4 km h−1. The data show relatively little functional deficit in resting conditions, but functional deficits at higher endogenous sympathetic activation increasing with exercise intensity. Based on Haitsma et al. (2001) with permission from the European Society of Cardiology and van der Velden et al. (2004).*

consisting of increased vasodilator influences in conjunction with blunted vasoconstrictor influences, acted to minimize the impairments of myocardial oxygen balance (Fig. 2.3). These studies not only highlight the plasticity of the post-MI remodeled heart and coronary circulation, to minimize perturbations in myocardial oxygenation in the face of increased

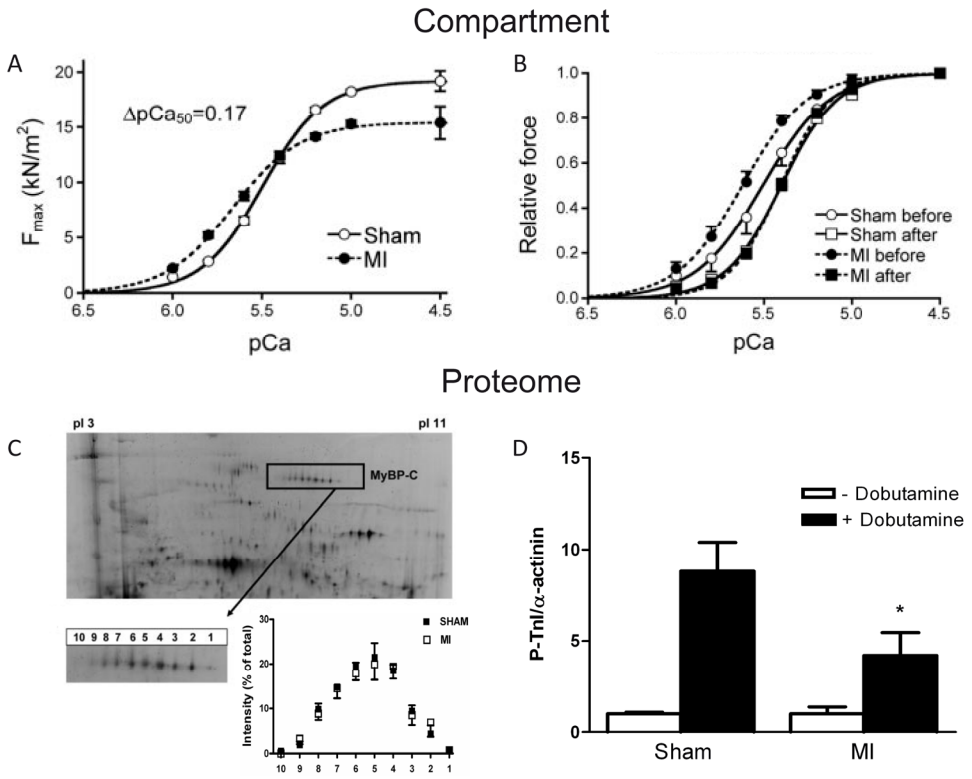

Figure 2.5. Myofilament function and protein phosphorylation. *A, determination of force development by skinned cardiomyocytes isolated from sham and post-MI pig hearts at different exogenous Ca^{2+} concentrations showed reduced maximal force and increased Ca^{2+} sensitivity in post-MI remodeled myocardium. B, Ca^{2+} sensitivity in the MI hearts was normalized to control (sham) values by pre-incubation of skinned cardiomyocytes with exogenous protein kinase A (PKA). Force development was measured before and after incubation with PKA. Force at maximal [Ca^{2+}] was set to 1. The observation that PKA abolished the difference in Ca^{2+} sensitivity between sham and post-MI cardiomyocytes suggests that the increase in myofilament Ca^{2+} sensitivity is caused by lower levels of PKA-mediated phosphorylation of sarcomeric proteins. C, two-dimensional gel electrophoresis showed no difference in the phosphorylation pattern of the PKA target protein cardiac myosin binding protein C (cMyBP-C) between sham and MI hearts. D, troponin I (TnI) phosphorylation did not differ under baseline conditions between sham and MI heart. However, following intravenous infusion of dobutamine the increase in TnI phosphorylation was attenuated in post-MI myocardium. Panels A and B were adapted from van der Velden et al. (2004), C was adapted from Duncker et al. (2009) and D shows data from Boontje et al. (2011).*

compressive forces and reduced capillary densities, but also illustrate the necessity to study these phenomena in an integrative manner in an intact animal model.

Neurohumoral activation following MI initially contributes to circulatory homeostasis, but will eventually contribute to the progressive deterioration in LV function. This concept is supported by studies showing detrimental effects of amplification of neurohumoral activity by phosphodiesterase-3 (PDE3) inhibitors in patients with heart failure (Packer *et al.*, 1991), while on the other hand β-adrenergic receptor blockade (CIBIS Investigators and Committees, 1994; CIBIS-II Investigators and Committees, 1999; MERIT-HF Study Group, 1999) and inhibitors of the RAAS system (Pfeffer *et al.*, 1992) have clearly shown long-term benefits in large cohorts of patients with heart failure. Starting from these observations in patients with heart failure, we took an integrative approach to study the cellular and molecular mechanisms underlying LV dysfunction observed in our swine model ~3 weeks after acute MI. In a first series of studies, we demonstrated the presence of LV remodeling (van Kats *et al.*, 2000) and dysfunction (Duncker *et al.*, 2001; Haitsma *et al.*, 2001), necessitating an increased oxygen extraction by the peripheral tissues (Fig. 2.4*A*) and causing an increase in neurohumoral activation (Fig. 2.4*B*) (Haitsma *et al.*, 2001). Despite the increased neurohumoral activation, β-adrenergic inotropic (Fig. 2.4*C*) and lusitropic (Fig. 2.4*D*) influences on the left ventricle were markedly blunted, particularly during treadmill exercise (Duncker *et al.*, 2005; van der Velden *et al.*, 2004). A loss of β-adrenergic signaling was also suggested by an attenuated response to PDE3 inhibition (Duncker *et al.*, 2001). To further investigate the cellular mechanisms underlying the global LV dysfunction, we performed studies in isolated permeabilized individual cardiomyocytes (van der Velden *et al.*, 2004). In myocytes from the remote LV zone in MI hearts, we observed abnormalities in myofilament force development, which correlated well with the degree of LV remodeling, and an increase in myofilament Ca^{2+} sensitivity (Fig. 2.5*A*) (van der Velden *et al.*, 2004). These alterations in myofilament function are likely to contribute to the systolic (Fig. 2.4*C*) and diastolic (Fig. 2.4*D*) LV dysfunction observed in swine during β-adrenergic receptor activation produced by treadmill exercise. The abnormalities in myofilament function could be prevented, at least in part, by treatment with chronic β1-adrenergic receptor blockade during the post-MI period (Duncker *et al.*, 2009). Analysis of myofilament proteins with one- and two-dimensional gel-electrophoresis failed to demonstrate significant alterations in phosphorylation status under basal conditions, including to our surprise the β-adrenergic target proteins cardiac myosin binding protein C (Fig. 2.5*C*) and troponin I (Fig. 2.5*D*) (Duncker *et al.*, 2009). When the heart was stimulated with the β-adrenergic receptor agonist dobutamine, the increase in troponin I phosphorylation was blunted in remodeled myocardium (Fig. 2.5*D*) (Boontje *et al.*, 2011). The increased Ca^{2+} sensitivity of force development of post-MI myocytes could be restored to normal (sham) values by incubation with the catalytic subunit of protein kinase A (PKA), the downstream kinase of the β1-

adrenergic receptor (Fig. 2.5*B*). Taken together, these observations suggest that PKA specific phosphorylation sites may be selectively
altered in post-MI hearts, which are the subject of ongoing studies within our laboratory.

To complement the top-down approach (from organism towards proteome) outlined above and to further investigate the mechanisms underlying the LV dysfunction following MI, we recently set out to investigate transcriptional control of LV remodeling and dysfunction. For this purpose, we performed microarray analysis to find genes that are differentially expressed in post-MI *versus* control hearts (Kuster *et al.*, 2011). Relations between the differentially expressed genes were assessed by Ingenuity Pathway Analysis. This program builds networks of interacting molecules by connecting as many differentially expressed genes as possible, and allowing for hub molecules of which the expression

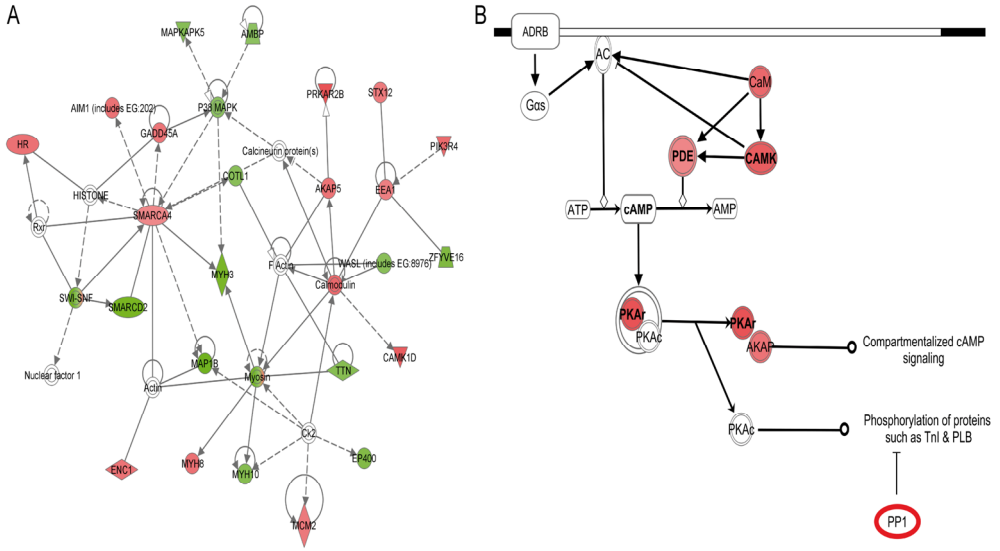

Figure 2.6. Network identification by Ingenuity Pathway Analysis. *A, one of the major networks identified by unsupervised analysis of genes differentially expressed in post-MI vs sham myocardium. Genes in red and green are up- and downregulated after MI, respectively. Genes in white, such as calcineurin, are not changed in expression but represent hubs between a large number of differentially expressed genes. The data show that a number of genes of the β-adrenergic pathway are changed in expression. B, simplified β-adrenergic signalling pathway identified by supervised data analysis, with upregulated genes in red and downregulated genes in green. Colour intensities correspond to the degree of change, with a deeper colour indicating a greater change. PP1 has been depicted with a red outline to indicate that we previously found an increase in PP1 protein level. Data are from Kuster et al. (2011).*

remains unchanged. Taken a non-supervised approach (Fig. 2.6*A*), an important network was identified that contained several genes encoding proteins involved in *β*-adrenergic signaling, including the regulatory subunit of PKA (PRKAR2B), A-kinase anchoring protein 5 (AKAP5), calmodulin and calmodulin kinase (CaMK), of which the expression was altered. In

addition, subsequent analysis of the β-adrenergic signaling network revealed increased expression of PDE4 (Fig. 2.6*B*). If confirmed at the protein level, the increased expression could contribute to the observed blunted PKA influence on myofilament Ca^{2+} sensitivity via (i) reduced cAMP production through increased CaMK-mediated inhibition of adenylyl-cyclase and increased cAMP breakdown by PDE4, and (ii) inactivation of the catalytic subunit of PKA by increased binding to the regulatory subunit of PKA.

2.4 Integrative Physiology 2.0

Systems biology approaches have not yet been applied to the study of cardiac remodeling, largely because of its tremendous complexity. Starting from observations in patients

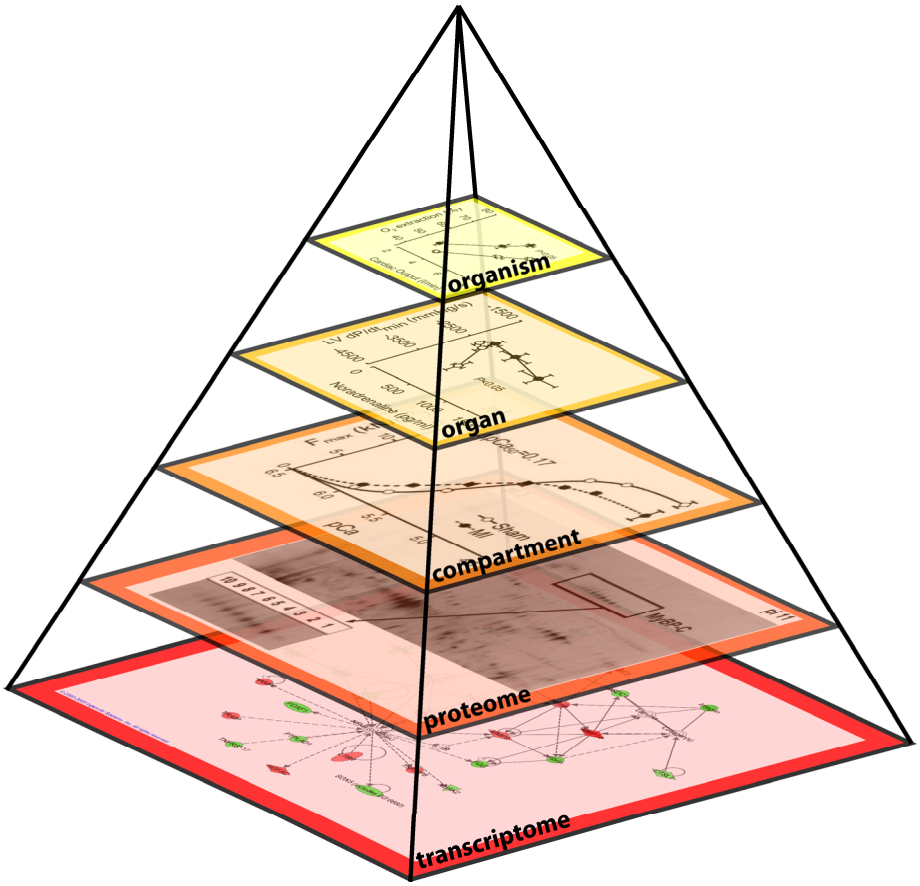

Figure 2.7. Illustration of our 'Integrative Physiology 2.0' approach. *Complex physiological processes such as cardiac remodeling must be studied in detail at different levels ranging from the transcriptome of cells all the way up to the intact organism, and possibly even further to population-based functional responses to pharmacons (not shown). At each level, data should be integrated with 'higher' and 'lower' levels, to build a multidimensional picture of the ongoing processes.*

showing detrimental effects of PDE3 inhibitors and beneficial effects of *β*-blockers, we have taken an integrative approach to studying the mechanisms underlying LV dysfunction after MI (Fig. 2.7). We began by narrowing our experimental focus to the well-defined clinical phenotype of post-MI LV remodeling and took a top-down approach, starting in the awake pig and ending with specific and generalized molecular investigations centered on transcriptomic and proteomic correlations (Fig. 2.7) based on current knowledge (Adams, 2010). Using a porcine model of post-MI remodeling, we first demonstrated the presence of LV remodeling and pump dysfunction in swine, necessitating increased oxygen extraction by the peripheral tissues and causing an increase in neurohumoral activation (*organism*). Despite the increased neurohumoral activation, *β*-adrenergic receptor mediated increases of LV function (*organ*) were blunted (Duncker *et al.*, 2005), which coincided with attenuated LV inotropic responses to PDE3 inhibition (Duncker *et al.*, 2001). Further studies at the cardiomyocyte level revealed abnormalities of myofilament force development that correlated well with the degree of LV remodeling (*cellular compartment*) (van der Velden *et al.*, 2004). The alterations in myofilament Ca^{2+} sensitivity appeared to be mediated by loss of PKA catalytic activity (*proteome*), and could be prevented by simultaneous treatment with *β*1-adrenergic receptor blockade, coinciding with an improvement in LV pump function (Duncker *et al.*, 2009). Non-supervised as well as supervised network analysis of microarray data (*transcriptome*) revealed significant alterations in expression of genes encoding proteins involved in *β*-adrenergic receptor signaling (Fig. 2.7). These preliminary findings will be followed up by further studies into translational and post-translation modifications. Since the completion of the Human Genome Project and the advent of the large scaled unbiased '-omics' techniques, the field of systems biology has emerged. Systems biology aims to move away from the traditional reductionist molecular approach, which focused on understanding the role of single genes or proteins, towards a more holistic approach by studying networks and interactions between individual components of networks. From a conceptual standpoint, systems biology elicits a 'back to the future' experience for any integrative physiologist, and we feel that systems biology can benefit from the knowledge and existing models of interaction between systems available in physiology. Conversely,
many of the new techniques and modalities employed by systems biologists yield tremendous potential for integrative physiologists to expand their tool arsenal to (quantitatively) study complex biological processes, such as cardiac remodeling and heart failure, in a truly holistic fashion. Such an approach may generate new hypotheses, concepts and eventually novel treatments for the process of cardiac remodeling and heart failure, which should subsequently be tested in a physiological setting. We therefore advocate that systems biology should not become/stay a separate discipline with '-omics' as its playing field, but should be integrated into physiology to create 'Integrative Physiology 2.0',

allowing interconnection and integration of processes at the various levels of complexity and organization within the pyramid of life.

2.5 Acknowledgement

The present study was supported by grants from the Netherlands Heart Foundation (2000T042 (D.M.), NHS2005B234 (D.K.) and 2005B220 (J.vdV.).

2.6 References

Adams KF (2010). Systems biology and heart failure: concepts, methods, and potential research applications. *Heart Fail Rev* **15**, 371-398.

Boontje NM, Merkus D, Zaremba R, Versteilen A, de Waard MC, Mearini G, de Beer VJ, Carrier L, Walker LA, Niessen HW, Dobrev D, Stienen GJ, Duncker DJ, & van der Velden J (2011). Enhanced myofilament responsiveness upon beta-adrenergic stimulation in post-infarct remodeled myocardium. *J Mol Cell Cardiol* **50**, 487-499.

Boushel R (2003). Metabolic control of muscle blood flow during exercise in humans. *Can J Appl Physiol* **28**, 754-773.

Brand T, Sharma HS, Fleischmann KE, Duncker DJ, McFalls EO, Verdouw PD, & Schaper W (1992). Proto-oncogene expression in porcine myocardium subjected to ischemia and reperfusion. *Circ Res* **71**, 1351-1360.

CIBIS Investigators and Committees (1994). A randomized trial of beta-blockade in heart failure. The Cardiac Insufficiency Bisoprolol Study (CIBIS). *Circulation* **90**, 1765-1773.

CIBIS-II Investigators and Committees (1999). The Cardiac Insufficiency Bisoprolol Study II (CIBIS-II): a randomised trial. *Lancet* **353**, 9-13.

Duncker DJ & Bache RJ (2008). Regulation of coronary blood flow during exercise. *Physiol Rev* **88**, 1009-1086.

Duncker DJ, Boontje NM, Merkus D, Versteilen A, Krysiak J, Mearini G, El Armouche A, de Beer VJ, Lamers JM, Carrier L, Walker LA, Linke WA, Stienen GJ, & van der Velden J (2009). Prevention of myofilament dysfunction by beta-blocker therapy in postinfarct remodeling. *Circ Heart Fail* **2**, 233-242.

Duncker DJ, Haitsma DB, Liem DA, Heins N, Stubenitsky R, & Verdouw PD (2001). Beneficial effects of the Ca^{2+} sensitizer EMD 57033 in exercising pigs with infarction-induced chronic left ventricular dysfunction. *Br J Pharmacol* **134**, 553-562.

Duncker DJ, Haitsma DB, Liem DA, Verdouw PD, & Merkus D (2005). Exercise unmasks autonomic dysfunction in swine with a recent myocardial infarction. *Cardiovasc Res* **65**, 889-896.

Duncker DJ & Merkus D (2007). Exercise hyperaemia in the heart: the search for the dilator mechanism. *J Physiol* **583**, 847-854.

Frey N & Olson EN (2003). Cardiac hypertrophy: the good, the bad, and the ugly. *Annu Rev Physiol* **65**, 45-79.

Guyton AC (1992). Kidneys and fluids in pressure regulation. Small volume but large pressure changes. *Hypertension* **19**, I2-I8.

Haitsma DB, Bac D, Raja N, Boomsma F, Verdouw PD, & Duncker DJ (2001). Minimal impairment of myocardial blood flow responses to exercise in the remodeled left ventricle early after myocardial infarction, despite significant hemodynamic and neurohumoral alterations. *Cardiovasc Res* **52**, 417-428.

Heineke J & Molkentin JD (2006). Regulation of cardiac hypertrophy by intracellular signalling pathways. *Nat Rev Mol Cell Biol* **7**, 589-600.

Katz AM (2008). The "modern" view of heart failure: how did we get here? *Circ Heart Fail* **1**, 63-71.

Katz AM (1988). Molecular biology in cardiology, a paradigmatic shift. *J Mol Cell Cardiol* **20**, 355-366.

Kuster DW, Merkus D, Kremer A, van IJcken WF, de Beer VJ, Verhoeven AJ, & Duncker DJ (2011). Left ventricular remodeling in swine after myocardial infarction: a transcriptional genomics approach. *Basic Res Cardiol* ***In press***.

Laughlin MH, McAllister RM, Jasperse JL, Crader SE, Williams DA, & Huxley VH (1996). Endothelium-medicated control of the coronary circulation. Exercise training-induced vascular adaptations. *Sports Med* **22**, 228-250.

Levy D, Garrison RJ, Savage DD, Kannel WB, & Castelli WP (1990). Prognostic implications of echocardiographically determined left ventricular mass in the Framingham Heart Study. *N Engl J Med* **322**, 1561-1566.

MERIT-HF Study Group (1999). Effect of metoprolol CR/XL in chronic heart failure: Metoprolol CR/XL Randomised Intervention Trial in Congestive Heart Failure (MERIT-HF). *Lancet* **353**, 2001-2007.

Merkus D, Haitsma DB, Sorop O, Boomsma F, de Beer VJ, Lamers JM, Verdouw PD, & Duncker DJ (2006). Coronary vasoconstrictor influence of angiotensin II is reduced in remodeled myocardium after myocardial infarction. *Am J Physiol Heart Circ Physiol* **291**, H2082-H2089.

Merkus D, Houweling B, van Den Meiracker AH, Boomsma F, & Duncker DJ (2005a). Contribution of endothelin to coronary vasomotor tone is abolished after myocardial infarction. *Am J Physiol Heart Circ Physiol* **288**, H871-H880.

Merkus D, Houweling B, van Vliet M, & Duncker DJ (2005b). Contribution of KATP+ channels to coronary vasomotor tone regulation is enhanced in exercising swine with a recent myocardial infarction. *Am J Physiol Heart Circ Physiol* **288**, H1306-H1313.

Mudd JO & Kass DA (2008). Tackling heart failure in the twenty-first century. *Nature* **451**, 919-928.

Murrant CL & Sarelius IH (2002). Multiple dilator pathways in skeletal muscle contraction-induced arteriolar dilations. *Am J Physiol Regul Integr Comp Physiol* **282**, R969-R978.

Narula J, Haider N, Arbustini E, & Chandrashekhar Y (2006). Mechanisms of disease: apoptosis in heart failure--seeing hope in death. *Nat Clin Pract Cardiovasc Med* **3**, 681-688.

Packer M, Carver JR, Rodeheffer RJ, Ivanhoe RJ, DiBianco R, Zeldis SM, Hendrix GH, Bommer WJ, Elkayam U, Kukin ML, & . (1991). Effect of oral milrinone on mortality in severe chronic heart failure. The PROMISE Study Research Group. *N Engl J Med* **325**, 1468-1475.

Pfeffer MA, Braunwald E, Moye LA, Basta L, Brown EJ, Jr., Cuddy TE, Davis BR, Geltman EM, Goldman S, Flaker GC, & . (1992). Effect of captopril on mortality and morbidity in patients with left ventricular dysfunction after myocardial infarction. Results of the survival and ventricular enlargement trial. The SAVE Investigators. *N Engl J Med* **327**, 669-677.

Rowell LB (2004). Ideas about control of skeletal and cardiac muscle blood flow (1876-2003): cycles of revision and new vision. *J Appl Physiol* **97**, 384-392.

Spinale FG (2007). Myocardial matrix remodeling and the matrix metalloproteinases: influence on cardiac form and function. *Physiol Rev* **87**, 1285-1342.

Tune JD, Gorman MW, & Feigl EO (2004). Matching coronary blood flow to myocardial oxygen consumption. *J Appl Physiol* **97**, 404-415.

Vakili BA, Okin PM, & Devereux RB (2001). Prognostic implications of left ventricular hypertrophy. *Am Heart J* **141**, 334-341.

van der Velden J, Merkus D, Klarenbeek BR, James AT, Boontje NM, Dekkers DH, Stienen GJ, Lamers JM, & Duncker DJ (2004). Alterations in myofilament function contribute to left ventricular dysfunction in pigs early after myocardial infarction. *Circ Res* **95**, e85-e95.

van Kats JP, Duncker DJ, Haitsma DB, Schuijt MP, Niebuur R, Stubenitsky R, Boomsma F, Schalekamp MA, Verdouw PD, & Danser AH (2000). Angiotensin-converting enzyme inhibition and angiotensin II type 1 receptor blockade prevent cardiac remodeling in pigs after myocardial infarction: role of tissue angiotensin II. *Circulation* **102**, 1556-1563.

van Veldhuisen DJ, van den Heuvel AF, Blanksma PK, & Crijns HJ (1998). Ischemia and left ventricular dysfunction: a reciprocal relation? *J Cardiovasc Pharmacol* **32 Suppl 1**, S46-S51.

Chapter 3

Nuclear protein extraction from frozen porcine myocardium

Diederik W. D. Kuster, Daphne Merkus, Huub J. J. Jorna, Dick H. W. Dekkers, Dirk J. Duncker & Adrie J. M. Verhoeven

J Physiol Biochem (2011) 67: 165-173

Abstract

Protocols for extraction of nuclear proteins have been developed for cultured cells and fresh tissue, but sometimes only frozen tissue is available. We have optimized the homogenization procedure and subsequent fractionation protocol for the preparation of nuclear protein extracts from frozen porcine left ventricular (LV) tissue. This method gave a highly reproducible protein yield (6.5 ± 0.7% of total protein; mean ± SE, n = 9) and a six-fold enrichment of the nuclear marker protein B23. The nuclear protein extracts were essentially devoid of cytosolic, myofilament and histone proteins. Compared to nuclear extracts from fresh LV tissue, some loss of nuclear proteins to the cytosolic fraction was observed. Using this method we studied the distribution of tyrosine phosphorylated STAT3 (PY-STAT3) in LV tissue of animals treated with the β-agonist dobutamine. Upon treatment, PY-STAT3 increased 30.2 ± 8.5 fold in total homogenates, but only 6.9 ± 2.1 fold (n = 4, P = 0.03) in nuclear protein extracts. Of all PY-STAT3 formed, only a minor fraction appeared in the nuclear fraction. This simple and reproducible protocol yielded nuclear protein extracts that were highly enriched in nuclear proteins with almost complete removal of cytosolic and myofilament proteins. This nuclear protein extraction protocol appears to be well-suited for nuclear proteome analysis of frozen heart tissue such as collected in biobanks.

3.1 Introduction

Preparation of nuclear protein extracts from tissue or cultured cells is an important tool for the study of gene regulation and the transcription factors (TFs) involved. Nuclear protein extracts are widely employed to study DNA binding of TFs in electrophoretic mobility shift experiments, or to study trafficking of TFs between the cytosol and the nucleus. Nuclear protein extracts are also well-suited for nuclear proteome analysis, as subcellular fractionation greatly reduces the complexity of the protein mixture, thus allowing detection of the low-abundant TFs (Ahmed & Rice, 2005; Barthelery *et al.*, 2008; Huber *et al.*, 2003). Preparation of nuclear protein extracts from fresh tissue samples or cultured cells is relatively straightforward. However, it is often desirable to utilize frozen tissue collected over a period in time as for example in biobanks.

In light of these considerations, we set out to develop a method for nuclear protein extraction from frozen cardiac muscle tissue, which is notoriously difficult to homogenize, and we compared this with standardized nuclear protein extraction from fresh heart tissue. Nuclear protein extracts from frozen heart tissue have already been applied for gel shift assays (Brown *et al.*, 2005; Chong *et al.*, 2004; Tahepold *et al.*, 2003; Zhao & Kukreja, 2003) and for the determination of nuclear translocation of TFs (Bukowska *et al.*, 2006; Carlson *et al.*, 2003; Fischer *et al.*, 2009; Gurusamy *et al.*, 2007; Li *et al.*, 2006; Lin *et al.*, 2004; Melling *et al.*, 2004; Wu *et al.*, 2007; Xi *et al.*, 2004). However, homogenization and fractionation protocols used in these studies vary widely. Most of these studies did not report the yield of nuclear proteins or the degree of contamination from other subcellular compartments. Recently a study was published which analyzed the nuclear extraction from frozen heart tissue with a commercial fractionation kit (Murray *et al.*, 2009). They found poor purification and high levels of contamination from other subcellular fractions. In the present study, we developed a simple and reproducible nuclear protein extraction method from frozen left ventricular tissue by systematically optimizing the homogenization and fractionation steps. We used cardiac tissue collected over time from pigs, a large laboratory animal, of which the cardiac physiology and anatomy closely resembles that of humans.

3.2 Material and Methods

3.2.1 Experimental animals

Studies were performed in accordance with the *Guide for the Care and Use of Laboratory Animals* (NIH Publication No. 85-23, revised 1996) and with approval of the Erasmus Medical Center Animal Care Committee. Cardiac tissue was collected from a total of 18 Yorkshire x Landrace swine. Animals were sedated by an intramuscular injection of a mixture of

ketamine and midazolam, anesthetized with intravenous pentobarbital (bolus + continuous infusion), intubated and ventilated (Sorop *et al.*, 2008; van der Velden *et al.*, 2004). The thorax and pericardium were opened and the heart was exposed. In a subset of four pigs, dobutamine was infused in consecutive doses of 2.5 and 10 µg/kg/min, for 10 min each, (Sorop *et al.*, 2008; van der Velden *et al.*, 2004) followed by a 10 min wash out period. Heart rate and LV contractility were determined as previously described (Sorop *et al.*, 2008; van der Velden *et al.*, 2004). Then the heart was arrested by application of an electroshock from a 9 Volt battery (Lameris *et al.*, 2000) and immediately excised. The left ventricle was divided into subendocardial and subepicardial tissue from the anterior, lateral, posterior and septal area of the left ventricle wall. Subsequently, cardiac tissue was snap-frozen in liquid nitrogen (i.e. within 5 min of excising the heart) and stored at -80 °C.

3.2.2 Nuclear protein extraction from frozen tissue

Frozen heart tissue from nine pigs collected over a period of 10 years was used for nuclear protein extraction. Approximately 100 mg of frozen left ventricular subendocardial tissue from the anterior region was pulverized using a Mikro-Dismembrator U (1700 rpm, 4 min; Sartorius, Nieuwegein, Netherlands) and the powder was immediately suspended in 4 ml ice-cold DPBS (Lonza, Verviers, Belgium) containing protease and phosphatase inhibitors (Complete, Roche Diagnostics, Almere, Netherlands, and Phosphatase Inhibitor Cocktail 1 & 2, Sigma, St. Louis, IL, USA, respectively). All further steps were carried out at 4 °C. After homogenization with a handheld glass-glass Dounce Tissue grinder (5 times loose, 5 times tight pestle; GPE Ltd, Leighton Buzzard, UK), the suspension was centrifuged at 1,850 x *g* for 15 min. The supernatant was taken as the cytosolic fraction. The pellet was resuspended in 10 volumes of hypotonic CER I buffer (NE-PER kit, Thermo Scientific, Rockford, IL, USA) containing protease (Protease Inhibitor Mix, Amersham Biosciences, Piscataway, NJ, USA) and phosphatase inhibitors and incubated for 10 min. Then, 55 µl of detergent-containing CER II solution was added per 100 µl of the original pellet volume. This mixture was incubated for 1 min, followed by centrifugation at 13,000 x *g* for 5 min, and the supernatant representing the organelle fraction was collected. The pellet was resuspended in 5 volumes of high-salt NER buffer containing protease and phosphatase inhibitors, and then incubated for 40 min and vortexed every 10 min. Thereafter, the suspension was centrifuged at 13,000 x *g* for 10 min, and the supernatant was saved as the nuclear protein extract. The final pellet containing myofilament and histone proteins was resuspended in 500 µl DPBS with protease and phosphatase inhibitors. All fractions were snap-frozen in liquid nitrogen, and stored at -80°C until further analysis.

3.2.3 Nuclear protein extraction from fresh LV tissue

Fresh heart tissue from five pigs was used. Nuclear protein extraction protocol was performed with the NE-PER kit (Thermo Scientific) according to the manufacturer's instructions. In short, the heart was excised and a piece of left ventricular subendocardial tissue from the anterior region was taken and rinsed with ice-cold PBS to remove blood. The tissue was cut into small pieces with a razorblade and placed in 1 ml hypotonic CER I buffer containing protease and phosphatase inhibitors. The tissue was homogenized by Teflon-glass Potter homogenization. The suspension was incubated on ice for 10 min. Then, 55 µl of detergent-containing CER II solution was added per 1 ml of CER I buffer. This mixture was incubated for 1 min, followed by centrifugation at 13,000 x *g* for 5 min, and the supernatant representing the cytosolic fraction was collected. The pellet was resuspended in 500 µl NER buffer per 1 ml CER I, containing protease and phosphatase inhibitors, and then incubated for 40 min and vortexed every 10 min. Thereafter, the suspension was centrifuged at 13,000 x *g* for 10 min, and the supernatant was saved as the nuclear protein extract. The final pellet containing the myofilament and histone protein was resuspended in 500 µl DPBS with protease and phosphatase inhibitors. All fractions were snap-frozen in liquid nitrogen, and stored at -80°C until further analysis.

3.2.4 Immunohistochemistry

Cryocoupes (5 µm) were cut from left ventricular tissue samples embedded in TissueTek. Sections were probed with B23 antibody (Santa Cruz Biotechnology Inc., Santa Cruz, CA, USA) at 1:4000 dilution, followed by an anti-mouse IgG horseradish peroxidase-conjugated secondary antibody (DAKO, Carpinteria, CA, USA) at 1:100 dilution. Peroxidase-labeled immune complexes were visualized by incubation with 3,3'-diaminobenzidine tetrahydrochloride (DAKO) and the sections were counterstained with hematoxylin.

3.2.5 Immunoblotting

The protein fractions were prepared in Laemmli's loading buffer (Laemmli, 1970), and protein concentration was determined using the Bio-Rad RC DC protein assay kit (Bio-Rad, Hercules, CA, USA) using bovine serum albumin as standard. Equal quantities of protein were loaded onto 12 % SDS-polyacrylamide gels. After electrophoresis, proteins were transferred overnight to Immun-Blot (for ECL, Bio-Rad) or Immobilon-FL (for Odyssey, Millipore, Bedford, MA) polyvinylidene difluoride membranes. Protein transfer onto the blot was checked with Ponceau S staining.

For ECL, blots were blocked for 30 min with 0.5% milk powder (Campina Melkunie BV, Eindhoven, Netherlands) in TBS/0.1% Tween-20. Then, primary antibodies were added to the block buffer at the dilutions described in Table 3.1, and the blots were incubated for

90 min, or overnight in the case of PY-STAT3. After washing extensively with TBS/0.1% Tween-20, the blots were incubated with the indicated amount (Table 3.1) of HRP conjugated secondary antibodies in block buffer for 1 h, or for 3 h in the case of PY-STAT3. After washing the blots, ECL signals were generated with the Supersignal West Femto Maximum Sensitivity Kit (Thermo Scientific) on Hyperfilm ECL (Amersham).

For quantification, the Odyssey system using fluorescently labeled secondary antibodies was applied, as this technique is linear over a larger dynamic range than ECL (Mathews *et al.*, 2009). Blots were blocked for 1 h with Odyssey blocking buffer (Li-Cor, Bad Homburg, Germany) diluted 1:1 with DPBS. Blots were incubated for 1 h with the primary antibodies (Table 3.1) in block buffer containing 0.1% Tween-20. After extensive washing in DPBS/0.1% Tween-20, the blots were incubated with IRDye800CW-coupled secondary antibodies (Table 3.1) for 1 h in block buffer containing 0.1% Tween-20 and 0.01% SDS. Finally, images were generated by scanning the blots on the Odyssey Infrared Imaging System (Li-Cor).

Table 3.1 Antibodies and dilutions used for immunoblotting and visualization by ECL and Odyssey

Antibody			ECL		Odyssey	
antigen	**sp[a)]**	**supplier**	**primary**	**secondary[b)]**	**primary**	**secondary[b)]**
GAPDH	M	Chemicon	1:3,200,000	1:8000	1:200,000	1:2000
SERCA2	R	Santa Cruz	1:20,000	1:8000	1:2000	1:2000
prohibitin	R	Abcam	1:8000	1:8000	1:2000	1:2000
α-actin	M	Sigma	1:2000	1:2000	1:1000	1:2000
histone H3	R	Eurogentec	1:200,000	1:8000	1:100,000	1:2000
B23	M	Santa Cruz	1:100,000	1:8000	1:8000	1:2000
PY-STAT3	M	Cell Signal	1:500	1:2000	-	-

a) sp, species. Mouse (M), rabbit (R) antibodies; b) secondary antibodies for ECL were HRP-conjugated goat anti-mouse or anti-rabbit IgG from Thermo Scientific, and for Odyssey were IRDye800CW conjugated goat anti-mouse or anti-rabbit IgG from Li-Cor.

3.2.6 Statistical Analysis

Results are expressed as mean ± SE. Unpaired Student's *t* test was used to compare means. Results were considered statistically significant at $P < 0.05$.

3.3 Results

3.3.1 Nuclear protein extraction procedure

To follow the nuclear proteins during homogenization and fractionation, and to determine the recovery of nuclear proteins in the nuclear protein extract, we used the abundant nuclear protein nucleophosmin (B23) as a nuclear marker protein (Duan *et al.*, 2007; van Deursen *et al.*, 2008). By immunohistochemistry on frozen cardiac tissue, we showed that localization of B23 is almost completely restricted to the nuclei (Fig 3.1).

Homogenization of the frozen LV tissue was found to be a critical step in the nuclear protein extraction protocol. Following Polytron homogenization as described by Lin *et al.* (Lin *et al.*, 2004) and Gurusamy *et al.* (Gurusamy *et al.*, 2007), most the B23 protein appeared in the cytosolic fraction (data not shown). This was prevented by more gentle homogenization of heart tissue cut into small pieces, using a handheld glass-glass Dounce homogenizer. However, this method resulted in a large intra-assay variation in the amount of total nuclear protein (7.1 ± 1.6 %, range 2.6-14.6 %; n = 8) and the amount of B23 recovered in the nuclear fraction, as determined by immunoblotting (6.6 ± 1.9 arbitrary units, range 2.9-19.3; n = 8). The reproducibility of total protein and B23 recovery in the nuclear protein fraction was markedly improved upon introduction of a tissue pulverization step at liquid nitrogen temperature before Dounce homogenization in PBS (see below).

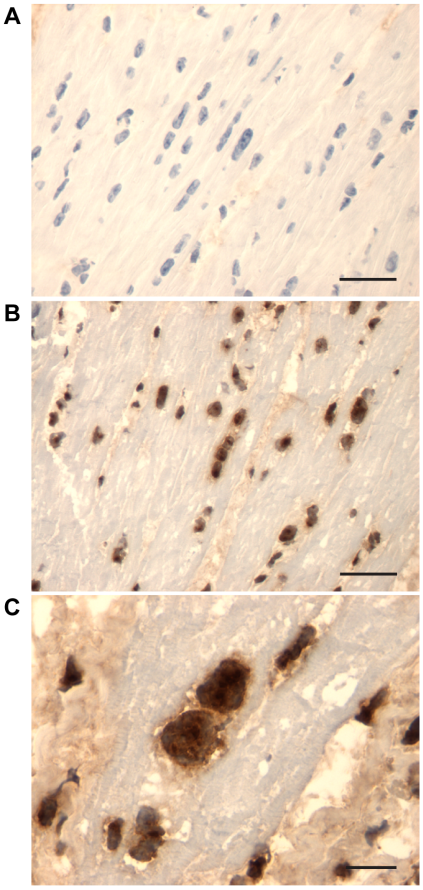

Figure 3.1 Subcellular localization of B23 in cardiac tissue. *Cryocoupes of cardiac tissue were immunostained (brown) without (A) or with anti B23 antibody (B, C), and counterstained with hematoxylin (blue). Bar represents 50 µm (A and B) or 100 µm (C).*

Next, we tested several fractionation protocols based on differential centrifugation at different sucrose densities (Cox & Emili, 2006; Kislinger *et al.*, 2005). In our hands these laborious protocols gave variable degrees of B23 and total protein recovery in the nuclear fraction (data not shown). Instead, we tested whether the commercial nuclear protein extraction kit from Thermo Scientific, which was specifically designed to isolate nuclear and cytoplasmic proteins from fresh tissue, could be made suitable for frozen tissue. After pulverization and homogenization in PBS, we introduced an additional centrifugation step, which leaves the contents of the nuclei damaged by freeze-thawing in the soluble fraction together with the cytosolic proteins (denoted further as the cytosolic fraction). The pellet containing the nuclei was then resuspended in a small volume of CER I buffer, and the extraction procedure was continued according to the manufacturer's instructions. The fractionation protocol is based on swelling of the cells and organelles in hypotonic buffer, followed by bursting of the swollen cells and organelles by detergent. The nucleus is spared from this hypotonic swelling, as its nuclear pores allows for the free diffusion of water and electrolytes in and out of the nucleus. The nuclear proteins were extracted from the nucleus by incubation in high salt buffer. This homogenization and fractionation protocol is relatively simple and showed the highest reproducibility of all methods tested. A schematic overview of the overall nuclear protein extraction procedure on frozen LV tissue is depicted in Figure 3.2A, and compared with a standard nuclear protein extraction protocol on fresh

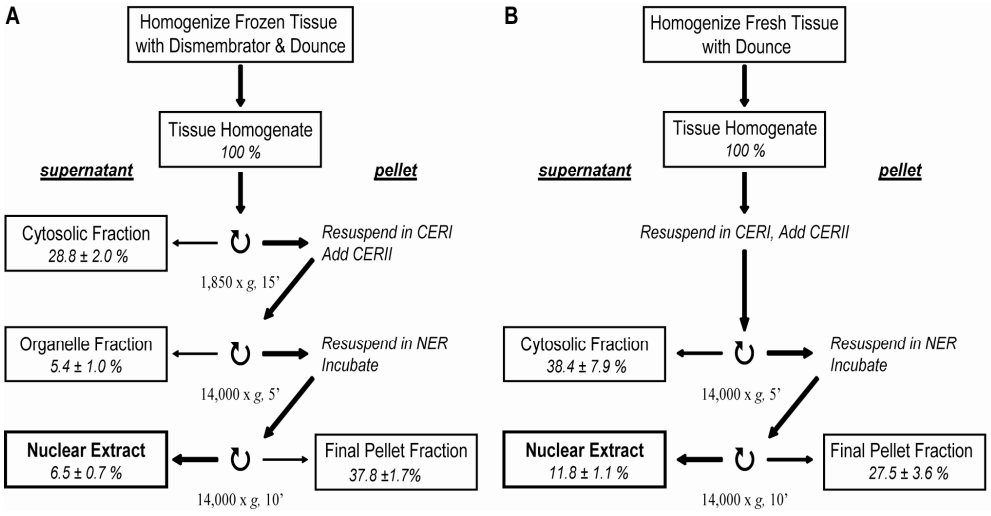

Figure 3.2 Nuclear protein extraction protocols from frozen and fresh cardiac tissue. *Protocols for the extraction of nuclear protein from frozen (A) and fresh (B) LV tissue are schematically depicted. The amount of protein in each fraction is expressed as a percentage of total protein in the homogenate. Data are mean ± SE for nine (frozen) and five (fresh) extractions performed on independent LV tissue samples.*

cardiac tissue (Fig 3.2B). The final pellet fraction left after incubation with nuclear extraction reagent principally contains myofilament proteins but also histone proteins, as the salt concentration is too low to enable their extraction from the DNA (von Holt *et al.*, 1989).

3.3.2 Nuclear protein enrichment and contamination

Nuclear fractions were obtained that contained 6.5 ± 0.7 % (range 3.9-8.6 %, n = 9) of the total protein (Fig. 3.2A) with a more than 6-fold enrichment of B23 (Table 3.2). B23 enrichment was similar in nuclear protein extracts from frozen and fresh tissue (Table 3.2). However, compared to the extraction procedure on fresh cardiac tissue, the total protein yield in the nuclear fraction was significantly lower ($P < 0.001$, Fig 3.2). In extracts from frozen tissue more B23 was present in the cytosolic fraction than with fresh tissue, probably due to damage of some nuclei during freezing and thawing (Fig 3.3). As expected from the relative content of cytosolic and myofilamental proteins in heart tissue, most of the total cellular protein was recovered in the cytosolic and final pellet fractions independently of whether frozen or fresh tissue was used. The relative recovery in these fractions differed between frozen and fresh tissue. It should be noted, however, that due to freeze-thawing the cytosolic fraction is likely to be contaminated with some proteins derived not only from nuclei but also from damaged organelles. With fresh tissue, organelle marker proteins were found in the cytosolic fraction. Total protein recovery in all fractions combined was similar for frozen and fresh tissue extracts (78.5 ± 2.7 vs. 80.6 ± 6.3 %).

Table 3.2 Quantification of marker proteins in their specific marker compartment and in the nuclear protein extract

	Marker Compartment		**Nuclear Extract**
Frozen tissue	*compartment*	*RE*	*RE*
GAPDH	cytosol	2.5 ± 0.3	0.0 ± 0.0
SERCA2	organelles	8.0 ± 1.6	0.9 ± 0.3
prohibitin	organelles	5.8 ± 0.8	0.7 ± 0.2
α-actin	final pellet	3.0 ± 0.1	0.1 ± 0.1
histone H3	final pellet	4.7 ± 0.4	0.2 ± 0.1
B23	nuclei	6.2 ± 1.7	6.2 ± 1.7
Fresh tissue			
B23	nuclei	7.6 ± 1.6	7.6 ± 1.6

Data are mean ± SE from 4 independent experiments. Quantitative data were obtained with the Odyssey system. RE, relative enrichment: is the fold increase in protein abundance relative to the total homogenate.

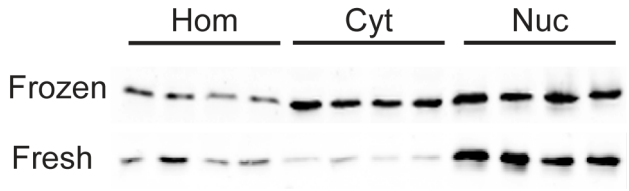

Figure 3.3 Distribution of B23 in the cytosolic and nuclear fractions from fresh and frozen tissue. *Fractionation was performed on four different frozen and fresh LV tissue samples. Of each fraction, 10 µg was analyzed by immunoblotting. Hom, total homogenate; Cyt, cytosolic fraction; Nuc, nuclear protein extract*

To determine the contamination of the nuclear protein extracts from frozen tissue with proteins from other subcellular compartments, we tested each fraction for the presence of different subcellular marker proteins (Fig 3.4). GAPDH ended up almost exclusively in the cytosolic fraction, with no detectable contamination of the nuclear protein extract. The SR and mitochondria markers SERCA2 and prohibitin were 8- and 6-fold enriched in the organelle fraction. Nevertheless, some SERCA2 and prohibitin was detected in the nuclear fraction, but this represented only a small percentage (Table 3.2). Similar results were obtained using ATP synthase subunit β as marker for mitochondrial marker (data not shown). The myofilament marker α-actin was recovered almost exclusively in the final pellet fraction, with only a minor contamination in the nuclear protein extract. The nucleosome marker histone H3 fractionated almost exclusively to the final pellet fraction, which is expected as higher salt concentrations are needed to extract histones from the DNA (von Holt *et al.*, 1989).

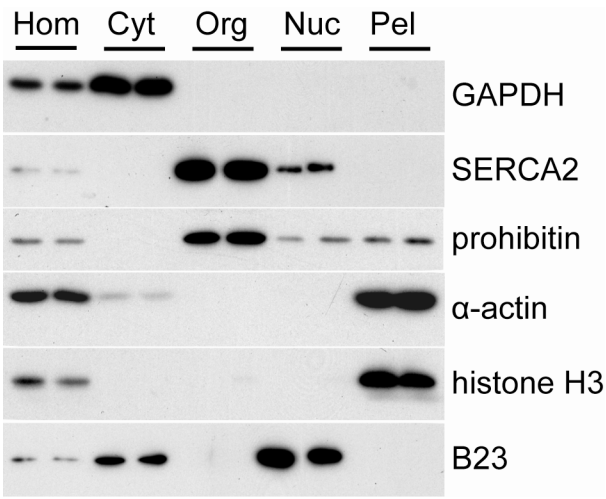

Figure 3.4 Subcellular markers in subcellular fractions from frozen LV tissue. *Fractionation was performed in parallel on two different frozen LV tissue samples. Of each fraction 10 µg was analyzed by immunoblotting. Hom, total homogenate; Cyt, cytosolic fraction; Org, organellar fraction; Nuc, nuclear protein extract; Pel, final pellet fraction.*

3.3.3 Nuclear appearance of PY-STAT3

We employed our method to address the question whether phosphorylation of the TF STAT3 to PY-STAT3 leads to its nuclear accumulation, where it may affect gene expression. In recent years, evidence has emerged that phosphorylation of STAT3 not necessarily leads to nuclear translocation (Mukhopadhyay *et al.*, 2008;

Shah *et al.*, 2006). It is therefore necessary to demonstrate the nuclear accumulation of PY-STAT3 when studying PY-STAT3-dependent gene expression. Stimulation of heart tissue with β-adrenergic receptor agonists leads to STAT3 phosphorylation (Liu *et al.*, 2006; Zhang *et al.*, 2008) and increased transcriptional activity (Zhang *et al.*, 2008). Intravenous infusion with the β-adrenergic receptor agonist dobutamine in swine resulted in a significant increase in heart rate (from 121 ± 10 before to 170 ± 7 beats per minute after dobutamine infusion, n = 4) and LV contractility (LV dP/dt_{max} from 1778 ± 223 before to 4955 ± 1052 mm Hg/sec after dobutamine infusion, n = 4). From treated and control sham-operated animals, total homogenates and nuclear protein extracts were prepared from frozen LV tissue samples. Tyrosine phosphorylated STAT3 was 30.2 ± 8.5 fold higher (n=4, P = 0.01) in the total homogenates from dobutamine-treated animals compared to controls (Figure 3.5A). In nuclear protein extracts PY-STAT3 was 6.9 ± 2.1 fold higher (n=4; P = 0.03) in animals treated with dobutamine than in controls (Figure 3.5B). In Figure 3.5C, the distribution of PY-STAT3 in the different fractions is shown. PY-STAT3 was detectable in all fractions, but the majority of PY-STAT3 was present in the cytosolic fraction. In contrast, the amount of B23 in this fraction was relatively low, which indicates that the presence of PY-STAT3 in this fraction is not merely due to leakage from damaged nuclei.

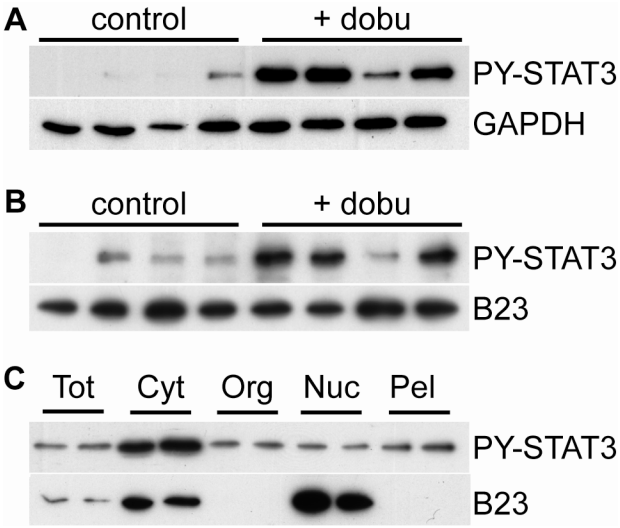

Figure 3.5 Effect of dobutamine on PY-STAT3 distribution. *PY-STAT3 amount was determined in total homogenates (A) and in nuclear protein extracts (B) from frozen LV tissue of 4 swine treated without (control) or with dobutamine (+dobu). GAPDH and B23 was used as loading control, respectively. Ten µg of protein was analyzed by immunoblotting. (C) Nuclear protein extraction was performed in parallel on two frozen LV samples of swine treated with dobutamine. Hom, total homogenate; Cyt, cytosolic fraction; Org, organellar fraction; Nuc, nuclear protein extract; Pel, final pellet fraction.*

3.4 Discussion

In this report we describe an optimized nuclear protein extraction protocol for frozen porcine heart tissue. With this relatively simple protocol we can reproducibly obtain nuclear protein extracts with high enrichment of nuclear proteins, which are essentially devoid of cytosolic, myofilament and histone proteins. The protein yields of the nuclear fractions are higher in extracts from fresh tissue, but this can be explained by loss of proteins to the cytosolic fraction from nuclei damaged during freeze-thawing, as illustrated by increased appearance of B23 in the cytosolic fraction (Fig 3.3). We have used B23 as nuclear marker protein. B23 has been reported to shuttle between the cytoplasm and the nucleus in isolated chick or interspecies (mouse-chick) heterokaryon fibroblast cell lines (Borer *et al.*, 1989). If shuttling also occurs in porcine cardiomyocytes, the cytosolic appearance of B23 may not only be due to loss of nuclear proteins from damaged nuclei, but also to active shuttling, thereby leading to an underestimation of the enrichment of nuclear proteins by our extraction procedure. We show however, that B23 was almost exclusively localized in the nuclei of porcine LV tissue (Fig. 3.1). Furthermore, in the nuclear extracts from fresh tissue, where the nuclei are not damaged by freeze-thawing, almost no B23 is seen in the cytosolic fraction (Fig. 3.3).

When studying transcription factors it is critical that the cytosolic proteins are removed from the nuclear protein extracts, as a number of TFs are present in their inactive form in the cytosol (e.g. NFAT). Using this protocol, the cytosolic marker protein GAPDH was not observed in the nuclear fraction. Since most of the abundant cytoplasmic proteins, i.e. the cytosolic and myofilamental proteins, as well as the most abundant nuclear proteins, i.e. the histones, are removed, the resulting nuclear protein extract appears to be aptly suited for further analysis of TF abundance and function. We are planning to employ this method to nuclear proteome profiling on remodeled (van der Velden *et al.*, 2004) and hibernating (Sorop *et al.*, 2008) myocardium. Since there is minimal contamination of the nuclear protein extract with cytosolic proteins, this method is highly useful for the analysis of nuclear presence of TFs in different conditions.

We tested the applicability of the method by studying the distribution of PY-STAT3 in porcine myocardium after β-adrenergic receptor stimulation. This stimulation causes phosphorylation of STAT3 and an increase in its transcriptional activity (Zhang *et al.*, 2008). However, only a small part of the PY-STAT3 pool was found in nuclear protein extracts from dobutamine-treated animals (Fig. 3.5C), indicating that only a minority of PY-STAT3 translocates to the nucleus. Also, the increase in PY-STAT3 is much higher in the tissue homogenate than in the nuclear protein extracts from dobutamine treated animals. This

demonstrates the necessity to perform nuclear protein extractions when studying the role of PY-STAT3 in the regulation of gene expression.

In a recent study, Murray et al. (Murray *et al.*, 2009) tested a nuclear extraction protocol on frozen heart tissue, and reported nuclear extracts with major contamination from cytosolic GAPDH and mitochondrial ATP synthase subunit β marker proteins. One difference with our study is the use of a different tissue homogenization method, which we found to be a crucial step in ensuring proper separation of the fractions. Murray et al. also used a different nuclear extraction kit, using DNAse to cut DNA and release all DNA bound proteins. In contrast, the kit we used employs salt extraction, which likely explains the absence of histone proteins in the nuclear extract.

An inherent limitation of whole tissue homogenization is that it does not allow delineation between nuclear protein extracts from different cell types present in cardiac tissue, including fibroblasts, vascular smooth muscle cells and endothelial cells in addition to cardiomyocytes. Future studies using laser capture approaches are needed to study nuclear extracts from specific cell types within the heart, but may yield too low levels of transcription factors to be quantified reliably.

In conclusion, the preparation of nuclear protein extracts from frozen tissue allows for the study of nuclear localization of TFs, and of TF function in gene regulation, years after tissue has been collected. We used tissue samples that had been stored for 1 week to 10 years, and observed no effect of the time of storage on the amount of nuclear protein recovered (data not shown). In addition, using frozen tissue allows for the preparation of nuclear protein extracts from several LV biopsies in parallel, thereby reducing potential day-to-day variability. This method will enable the study of nuclear protein profiles of heart tissue from experimental animals present in tissue banks, but may also be applicable to analysis of human heart biopsies collected in biobanks.

3.5 Acknowledgement

This work was supported by a grant from the Netherlands Heart Foundation (NHS2005B234).

3.6 References

Ahmed N & Rice GE (2005). Strategies for revealing lower abundance proteins in two-dimensional protein maps. *J Chromatogr B Analyt Technol Biomed Life Sci* **815**, 39-50.

Barthelery M, Salli U, & Vrana KE (2008). Enhanced nuclear proteomics. *Proteomics* **8**, 1832-1838.

Borer RA, Lehner CF, Eppenberger HM, & Nigg EA (1989). Major nucleolar proteins shuttle between nucleus and cytoplasm. *Cell* **56**, 379-390.

Brown M, McGuinness M, Wright T, Ren X, Wang Y, Boivin GP, Hahn H, Feldman AM, & Jones WK (2005). Cardiac-specific blockade of NF-kappaB in cardiac pathophysiology: differences between acute and chronic stimuli in vivo. *Am J Physiol Heart Circ Physiol* **289**, H466-H476.

Bukowska A, Lendeckel U, Hirte D, Wolke C, Striggow F, Rohnert P, Huth C, Klein HU, & Goette A (2006). Activation of the calcineurin signaling pathway induces atrial hypertrophy during atrial fibrillation. *Cell Mol Life Sci* **63**, 333-342.

Carlson DL, White DJ, Maass DL, Nguyen RC, Giroir B, & Horton JW (2003). I kappa B overexpression in cardiomyocytes prevents NF-kappa B translocation and provides cardioprotection in trauma. *Am J Physiol Heart Circ Physiol* **284**, H804-H814.

Chong AJ, Shimamoto A, Hampton CR, Takayama H, Spring DJ, Rothnie CL, Yada M, Pohlman TH, & Verrier ED (2004). Toll-like receptor 4 mediates ischemia/reperfusion injury of the heart. *J Thorac Cardiovasc Surg* **128**, 170-179.

Cox B & Emili A (2006). Tissue subcellular fractionation and protein extraction for use in mass-spectrometry-based proteomics. *Nat Protoc* **1**, 1872-1878.

Duan S, Yao Z, Hou D, Wu Z, Zhu WG, & Wu M (2007). Phosphorylation of Pirh2 by calmodulin-dependent kinase II impairs its ability to ubiquitinate p53. *EMBO J* **26**, 3062-3074.

Fischer UM, Radhakrishnan RS, Uray KS, Xue H, & Cox CS, Jr. (2009). Myocardial function after gut ischemia/reperfusion: does NF kappaB play a role? *J Surg Res* **152**, 264-270.

Gurusamy N, Malik G, Gorbunov NV, & Das DK (2007). Redox activation of Ref-1 potentiates cell survival following myocardial ischemia reperfusion injury. *Free Radic Biol Med* **43**, 397-407.

Huber LA, Pfaller K, & Vietor I (2003). Organelle proteomics: implications for subcellular fractionation in proteomics. *Circ Res* **92**, 962-968.

Kislinger T, Gramolini AO, MacLennan DH, & Emili A (2005). Multidimensional protein identification technology (MudPIT): technical overview of a profiling method optimized

for the comprehensive proteomic investigation of normal and diseased heart tissue. *J Am Soc Mass Spectrom* **16**, 1207-1220.

Laemmli UK (1970). Cleavage of structural proteins during the assembly of the head of bacteriophage T4. *Nature* **227**, 680-685.

Lameris TW, de Zeeuw S, Alberts G, Boomsma F, Duncker DJ, Verdouw PD, Veld AJ, & van Den Meiracker AH (2000). Time course and mechanism of myocardial catecholamine release during transient ischemia in vivo. *Circulation* **101**, 2645-2650.

Li B, Dedman JR, & Kaetzel MA (2006). Nuclear Ca2+/calmodulin-dependent protein kinase II in the murine heart. *Biochim Biophys Acta* **1763**, 1275-1281.

Lin CC, Lin JL, Lin CS, Tsai MC, Su MJ, Lai LP, & Huang SK (2004). Activation of the calcineurin-nuclear factor of activated T-cell signal transduction pathway in atrial fibrillation. *Chest* **126**, 1926-1932.

Liu AM, Lo RK, Wong CS, Morris C, Wise H, & Wong YH (2006). Activation of STAT3 by G alpha(s) distinctively requires protein kinase A, JNK, and phosphatidylinositol 3-kinase. *J Biol Chem* **281**, 35812-35825.

Mathews ST, Plaisance EP, & Kim T (2009). Imaging systems for westerns: chemiluminescence vs. infrared detection. *Methods Mol Biol* **536**, 499-513.

Melling CW, Thorp DB, & Noble EG (2004). Regulation of myocardial heat shock protein 70 gene expression following exercise. *J Mol Cell Cardiol* **37**, 847-855.

Mukhopadhyay S, Shah M, Xu F, Patel K, Tuder RM, & Sehgal PB (2008). Cytoplasmic provenance of STAT3 and PY-STAT3 in the endolysosomal compartments in pulmonary arterial endothelial and smooth muscle cells: implications in pulmonary arterial hypertension. *Am J Physiol Lung Cell Mol Physiol* **294**, L449-L468.

Murray CI, Barrett M, & Van Eyk JE (2009). Assessment of ProteoExtract subcellular fractionation kit reveals limited and incomplete enrichment of nuclear subproteome from frozen liver and heart tissue. *Proteomics* **9**, 3934-3938.

Shah M, Patel K, Mukhopadhyay S, Xu F, Guo G, & Sehgal PB (2006). Membrane-associated STAT3 and PY-STAT3 in the cytoplasm. *J Biol Chem* **281**, 7302-7308.

Sorop O, Merkus D, de Beer VJ, Houweling B, Pistea A, McFalls EO, Boomsma F, van Beusekom HM, van der Giessen WJ, VanBavel E, & Duncker DJ (2008). Functional and structural adaptations of coronary microvessels distal to a chronic coronary artery stenosis. *Circ Res* **102**, 795-803.

Tahepold P, Vaage J, Starkopf J, & Valen G (2003). Hyperoxia elicits myocardial protection through a nuclear factor kappaB-dependent mechanism in the rat heart. *J Thorac Cardiovasc Surg* **125**, 650-660.

van der Velden J, Merkus D, Klarenbeek BR, James AT, Boontje NM, Dekkers DH, Stienen GJ, Lamers JM, & Duncker DJ (2004). Alterations in myofilament function contribute to left ventricular dysfunction in pigs early after myocardial infarction. *Circ Res* **95**, e85-e95.

van Deursen D, Botma GJ, Jansen H, & Verhoeven AJ (2008). Down-regulation of hepatic lipase expression by elevation of cAMP in human hepatoma but not adrenocortical cells. *Mol Cell Endocrinol* **294**, 37-44.

von Holt C, Brandt WF, Greyling HJ, Lindsey GG, Retief JD, Rodrigues JD, Schwager S, & Sewell BT (1989). Isolation and characterization of histones. *Methods Enzymol* **170**, 431-523.

Wu Y, Tu X, Lin G, Xia H, Huang H, Wan J, Cheng Z, Liu M, Chen G, Zhang H, Fu J, Liu Q, & Liu DX (2007). Emodin-mediated protection from acute myocardial infarction via inhibition of inflammation and apoptosis in local ischemic myocardium. *Life Sci* **81**, 1332-1338.

Xi L, Taher M, Yin C, Salloum F, & Kukreja RC (2004). Cobalt chloride induces delayed cardiac preconditioning in mice through selective activation of HIF-1alpha and AP-1 and iNOS signaling. *Am J Physiol Heart Circ Physiol* **287**, H2369-H2375.

Zhang H, Feng W, Liao W, Ma X, Han Q, & Zhang Y (2008). The gp130/STAT3 signaling pathway mediates beta-adrenergic receptor-induced atrial natriuretic factor expression in cardiomyocytes. *FEBS J* **275**, 3590-3597.

Zhao TC & Kukreja RC (2003). Protein kinase C-delta mediates adenosine A3 receptor-induced delayed cardioprotection in mouse. *Am J Physiol Heart Circ Physiol* **285**, H434-H441.

Chapter 4

Left ventricular remodeling in swine after myocardial infarction: a transcriptional genomics approach

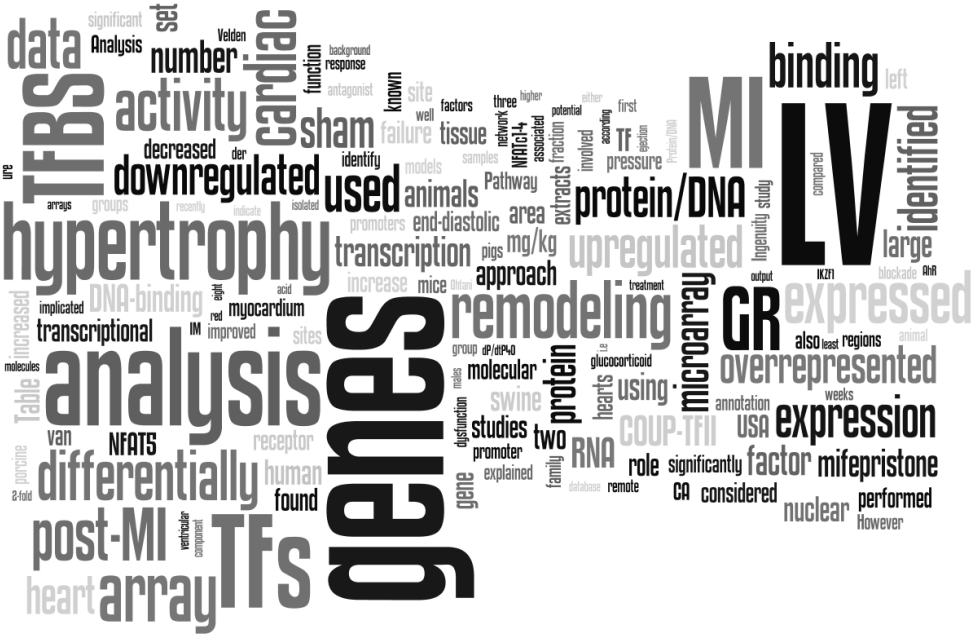

Diederik W. D. Kuster, Daphne Merkus, Andreas Kremer, Wilfred F.J. van Ijcken, Vincent J. de Beer, Adrie J.M. Verhoeven & Dirk J. Duncker

Basic Res Cardiol (2011) In press

Abstract

Despite the apparent appropriateness of left ventricular (LV) remodeling following myocardial infarction (MI), it poses an independent risk factor for development of heart failure. There is a paucity of studies into the molecular mechanisms of LV remodeling in large animal species. We took an unbiased molecular approach to identify candidate transcription factors (TFs) mediating the genetic reprogramming involved in post-MI LV remodeling in swine.

LV tissue was collected from remote, non-infarcted myocardium, 3 weeks after MI-induction or sham-surgery. Microarray analysis identified 285 upregulated and 278 downregulated genes (FDR<0.05). Of these differentially expressed genes, the promoter regions of the human homologues were searched for common TF binding sites (TFBS). Eighteen TFBS were overrepresented >2-fold ($p<0.01$) in upregulated and 13 in downregulated genes. LV nuclear protein extracts were assayed for DNA-binding activity by protein/DNA array. Out of 345 DNA probes, thirty showed signal intensity changes >2-fold. Five TFs were identified in both TFBS and protein/DNA array analyses, which showed matching changes for COUP-TFII and glucocorticoid receptor (GR) only. Treatment of swine with the GR antagonist mifepristone after MI reduced the post-MI increase in LV mass but LV dilation remained unaffected.

Using an unbiased approach to study post-MI LV remodeling in a physiologically relevant large animal model, we identified COUP-TFII and GR as potential key mediators of post-MI remodeling.

4.1 Introduction

Heart failure is currently the only major cardiovascular syndrome of which the prevalence is steadily increasing. For a significant part this is the result of improved survival of patients encountering an acute myocardial infarction (MI) in conjunction with an ageing population (Velagaleti *et al.*, 2008). Loss of viable myocardium elicits a cascade of compensatory mechanisms, including neurohumoral activation, fluid retention and left ventricular (LV) remodeling, in an attempt to maintain normal pump function (Sutton & Sharpe, 2000; Katz, 2008). However, despite its apparent appropriateness, post-MI remodeling –consisting of LV hypertrophy and dilation- constitutes an independent risk factor for the development of heart failure (White *et al.*, 1987). Mechanisms that have been implicated in the pathology of post-MI remodeling and heart failure include myofilament dysfunction (van der Velden *et al.*, 2004; Schoenauer *et al.*, 2011), alterations in excitation-contraction coupling (Heusch & Schulz, 2011) and mitochondrial function (Javadov *et al.*, 2011), decreased expression of atrophy mediators (Conraads *et al.*, 2010), inflammatory responses (Kleinbongard *et al.*, 2010; Chorianopoulos *et al.*, 2010; Garlie *et al.*, 2011) and alterations in extracellular matrix (Saygili *et al.*, 2009; Hammoud *et al.*, 2011) and cell-cell interactions (Krusche *et al.*, 2011).

The molecular pathways underlying LV remodeling and its progression towards heart failure remain incompletely understood. The majority of studies into the molecular mechanisms of LV remodeling have been reductionistic in nature and have principally been performed in mice. These studies have yielded a wealth of information regarding the role of individual genes and proteins in LV remodeling (Mudd & Kass, 2008). However, there are marked differences in cardiac physiology between rodents and large mammals (Hasenfuss, 1998; Dixon & Spinale, 2009). Nevertheless, there is a paucity of studies into the molecular mechanisms of cardiac remodeling in large animal species mainly because the use of large animal models in molecular '–omics' studies was limited by a lack of suitable tools together with incomplete annotation of the genome, transcriptome and proteome. However, porcine gene-expression arrays in conjunction with improved annotation have recently become available (Couture *et al.*, 2009), allowing analysis of the molecular alterations in LV remodeling in pigs.

To identify candidate transcription factors (TFs) that mediate the genetic reprogramming involved in LV remodeling in the pig, we took an unbiased molecular approach (Fig 4.1). First, global changes in gene expression were studied by microarray analysis of the remote non-infarcted LV tissue early after induction of MI. To identify the responsible transcription factors, these data were subsequently combined with transcription factor binding site (TFBS) analysis as well as with protein-DNA arrays using LV nuclear protein extracts. Rationale for this approach was that the coordinate upregulation

and downregulation of a high number of different genes is likely achieved through altered function of a limited set of TFs. This integrated approach led to the identification of COUP-TFII and the glucocorticoid receptor as potential mediators of post-MI LV remodeling.

4.2 Methods

4.2.1 Experimental animals

Animal experiments were performed in accordance with the *Guide for the Care and Use of Laboratory Animals* (NIH Publication No. 85-23, revised 1996) and with approval of the Erasmus Medical Center Animal Care Committee. 51 pre-adolescent (2-3 months old) Yorkshire x Landrace swine (22.0±0.4 kg) of either sex were used; males had been neutered.

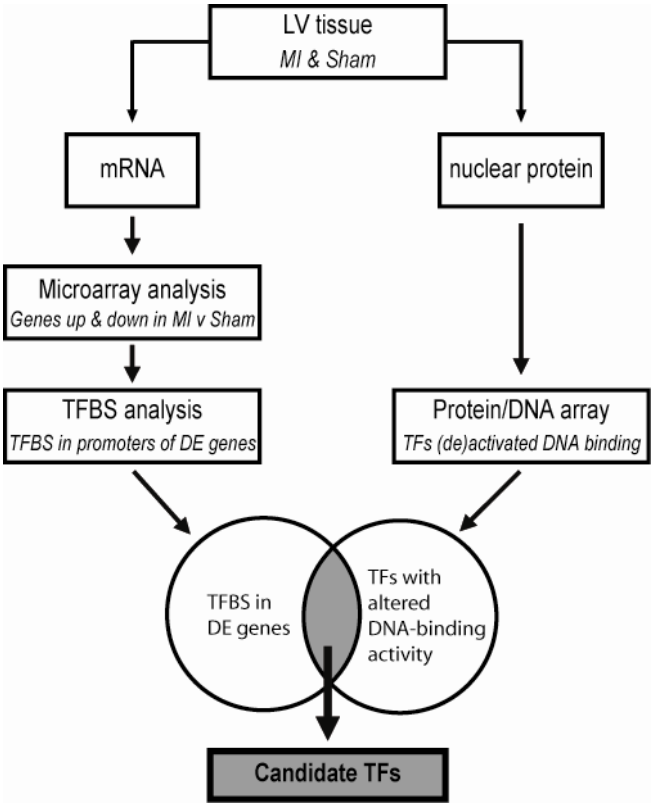

***Figure 4.1: Workflow of our transcriptional genomics approach**. RNA and nuclear proteins were isolated from LV tissue. The RNA was used in microarray analysis followed by TFBS analysis of differentially expressed genes. Nuclear protein extracts were used for protein/DNA array analysis to identify TFs that were increased or decreased in DNA-binding activity in post-MI hearts. Candidate TFs were identified by combining these two data sets. LV, left ventricular; MI, myocardial infarction; TFBS, transcription factor binding site; DE, differentially expressed; TF, transcription factor.*

4.2.2 Surgery

Animals were sedated with ketamine (20 mg/kg, Intramuscularly [IM]) and midazolam (0.5 mg/kg, IM), anesthetized with thiopental (10 mg/kg, intravenously [IV]), intubated and ventilated with O_2/N_2 (1/2 v/v) enriched with 0.1-1% (vol/vol) isoflurane (van der Velden *et al.*, 2004; Sorop *et al.*, 2008). Following a thoracotomy through the fourth left intercostal space, the heart was exposed via a small pericardial incision, the left circumflex artery (LCx) was dissected and a suture was placed around it. Subsequently, the LCx was permanently ligated in 31 swine designated to the MI group

(producing a transmural infarction in the lateral wall encompassing 20-25% of the left ventricle (van Kats *et al.*, 2000)), while the suture was removed in the 20 swine designated to the sham group (van Kats *et al.*, 2000; van der Velden *et al.*, 2004; Duncker *et al.*, 2009). Then the pericardium and the chest were closed and animals were allowed to recover, receiving analgesia (0.3 mg buprenorphine IM) for 2 days and antibiotic prophylaxis (25 mg/kg amoxicillin and 5 mg/kg gentamycin IV) for 5 days.

4.2.3 Echocardiography and Hemodynamic Measurements

Three weeks after surgery, animals were sedated with ketamine (20 mg/kg, IM) and midazolam (0.5 mg/kg, IM) and underwent echocardiography for the determination of LV end-diastolic cross-sectional area (EDA) and end-systolic cross-sectional area (ESA) (Duncker *et al.*, 2009). 2D ejection fraction was calculated as 100 · (EDA-ESA)/EDA %. After induction of anesthesia with pentobarbital (10-15 mg/kg per hour, IV) swine were instrumented for measurement of mean arterial pressure, heart rate, cardiac output, rate of rise in LV pressure at 40 mm Hg (LV dP/dt_{P40}), time constant of relaxation (tau) and LV end diastolic pressure (van Kats *et al.*, 2000; van der Velden *et al.*, 2004; Duncker *et al.*, 2009). After completion of all measurements, animals underwent a sternotomy and the heart was arrested and immediately excised. The left ventricle was divided into subendocardial and subepicardial tissue from the anterior, lateral, posterior and septal area of the left ventricle wall and cardiac tissue was snap-frozen in liquid nitrogen (i.e. within 3-5 min of excising the heart) and stored at -80 °C. For protein and RNA analysis, subendocardial tissue from the anterior wall was used, which is the remote non-infarcted area in MI animals.

4.2.4 Total RNA isolation

RNA was extracted from LV tissue from eight MI and eight sham animals (four males and four females per group). Frozen tissue samples were pulverized with a mortar and pestle and TRI Reagent (Invitrogen, Carlsbad, CA, USA) was added immediately to the powder. RNA was isolated according to manufacturer's instructions. RNA was cleaned with RNeasy clean-up kit (Qiagen, Valencia, CA, USA). Purity and quality of isolated RNA were assessed by RNA 6000 Nano assay on a 2100 Bioanalyzer (Agilent Technologies, Santa Clara, CA, USA). All samples showed a RNA integrity number >8.

4.2.5 Microarray analysis

Sixteen microarrays, 8 for sham and 8 for post-MI hearts, were run in three independent batches. From each heart, RNA (3 µg) was used for synthesis of biotinylated cRNA. Labeled cRNA was hybridized to the GeneChip Porcine Genome Array (Affymetrix, Santa Clara, CA, USA) according to the manufacturer's instructions. The Affymetrix QC reports showed high quality of the samples and arrays, indicated by percentage of present calls, noise,

background, and by a 3':5' signal ratio for glyceraldehyde-3-phosphate dehydrogenase mRNA of <1.4.

Raw intensity values of all samples were normalized in R (http://www.r-project.org). The data were corrected for variability across batches and arrays by quantile normalization according to experimental group, followed by Robust Micro-array Average normalization, using the Affy package developed by Bioconductor (Gentleman *et al.*, 2004). The normalized expression values were loaded into Partek genomic suite (Partek Inc, St. Louis, MO, USA) and multivariate principal component analysis was performed (Ringner, 2008). All the microarray data have been submitted to the National Center for Biotechnology Information (NCBI) Gene Expression Omnibus database (GEO) (http://www.ncbi.nlm.nih.gov/geo) with GEO accession number GSE27962.

The class comparison tool of BRB-ArrayTools software (http://linus.nci.nih.gov/BRB-ArrayTools.html) was used for generation of lists of differentially expressed genes (Simon *et al.*, 2007). Genes were considered significantly different between MI and sham at a false discovery rate (FDR) < 0.05. Because the annotation of the porcine genechip is far from complete, the annotation of ANEXdb (Couture *et al.*, 2009) was used. This open source application aligns Affymetrix porcine GeneChip target sequences to the Iowa Porcine Assembly, which is an assembly of all publicly available porcine-expressed consensus sequences. This was subsequently aligned to the NCBI RefSeq RNA database, to give the homologous human RefSeq IDs .

4.2.6 Transcription factor binding site analysis

The genomic sequences of the human homologues of the differentially expressed genes were selected, and regions between position 500 upstream and 100 downstream of the transcription start site were searched for putative transcription factor binding sites (TFBS) using F-match implemented in the Explain Analysis System (Biobase GmbH, Wolfenbüttel, Germany) (Kel *et al.*, 2006; Kel *et al.*, 2008). The rationale for searching differentially expressed genes for common TFBS is the assumption that co-expressed genes are coordinately regulated by a limited set of TFs. Promoter regions of the differentially expressed genes were scanned for so-called positional weight matrices (Kel *et al.*, 2006), constructed from collections of known binding sites for a given TF. TFBS were searched using the entire vertebrate non-redundant set of transcription factors matrix from the TRANSFAC database (Wingender *et al.*, 2000). To reduce false positive results in TFBS analysis, the choice of an appropriate control data set is of paramount importance. To identify TFBS that cause the increased expression of the upregulated genes, the promoters of the upregulated genes were taken as input set, while the promoters of the downregulated genes were taken as background set. For the identification of overrepresented TFBSs in downregulated genes, the promoters of downregulated were

used as input set and the promoters of upregulated genes as background set. The number of binding sites in the promoter region of upregulated and downregulated genes per 600 basepairs for each TF is indicated. Overrepresentation was determined using a one-tailed Fisher exact probability test and considered significant when more than 2-fold and at $p < 0.01$.

4.2.7 Protein/DNA array

With the protein/DNA array (Combo array, Panomics/Affymetrix, Milan, Italy), nuclear protein extracts were semi-quantitatively assayed by DNA binding activity for 345 TFs. Nuclear protein extracts were prepared from LV tissue as previously described (Kuster *et al.*, 2010). Protein/DNA array analysis was performed according to the manufacturer's instructions. Briefly, 5 µg of nuclear protein of a pool of 4 MI extracts and a pool of 4 sham extracts was used for binding to a mix of biotin-labeled TF-specific DNA probes in solution. Subsequently, all unbound DNA probes were washed away. The TF-bound probes were denatured and then hybridized to the array membrane. After addition of steptavidin-HRP, signals were generated by enhanced chemiluminescence (ECL) and exposure to Hyperfilm ECL (Amersham Biosciences, Piscataway, NJ, USA). Various exposure times were used to obtain signals over a large dynamic range. Signal intensities were quantified using a Bio-Rad calibrated GS-800 scanner and Quantity One software (Bio-Rad, Hercules, CA, USA). Only non-saturated signals were used for further analysis. TF binding activity was considered significant when at least 2-fold signal difference between MI and sham.

4.2.8 Ingenuity Pathway analysis

Pathway Analysis (Ingenuity Systems, Redwood City, CA, USA) was performed to detect the biological functions and molecular networks of the differentially expressed genes, using the human Refseq IDs as input. Biological groups were identified with which the genes are significantly associated ($p<0.001$). Interconnectivity of the genes was visualized by the molecular networks constructed by the program. These networks are constructed by connecting as many genes as possible, also using unchanged hub molecules. For linking TFs from the protein/DNA array to genes identified in the microarray analysis, the TFs were used as input for Pathway Analysis. In the build function and with the grow tool, the genes were linked to the TFs if they are known from the literature to be either expressed/ transcribed by, or have an experimentally validated binding site for the TFs.

4.2.9 Statistics

Data are presented as mean ± SEM. Differences between two groups were analyzed by unpaired Student's *t*-test. Differences between three groups were analyzed by one-way ANOVA followed by Student Newman-Keuls *post-hoc* test using GraphPad Prism version

5.01 (GraphPad Software, San Diego, CA, USA). $P<0.05$ was considered to be statistically significant.

4.3 Results

4.3.1 LV remodeling and dysfunction after MI

Three weeks after MI-induction or sham surgery, LV eccentric hypertrophy was evident from a 15% higher LV to body weight ratio and a 70% larger LV end-diastolic lumen area in MI animals (Table 4.1). LV remodeling was associated with a maintained stroke volume and cardiac output, but the 2D-ejection fraction was lower in MI (37±3%) than in sham (67±3%) swine ($P<0.05$) due to the increase in LV end-diastolic lumen area. LV systolic dysfunction was also reflected in the 20% lower LV dP/dt_{P40}, while perturbed LV relaxation was suggested by the 20% higher time constant of relaxation tau. Finally, the elevations in LV end-diastolic pressure in conjunction with right ventricular hypertrophy suggest the presence of LV backward failure.

Table 4.1: Anatomic, echocardiographic and hemodynamic data

	Sham	MI
Anatomic data	(n=20)	(n=24)
Body weight (kg)	30±1	32±1
RVW/BW (g/kg)	0.99±0.05	1.35±0.06‡
LVW/BW (g/kg)	2.87±0.09	3.38±0.06‡
Echocardiographic data	(n=9)	(n=13)
LV EDA (mm^2)	921±47	1551±157†
LV ESA (mm^2)	306±34	985±128‡
2D-Ejection Fraction (%)	67±3	37±3‡
Hemodynamic data	(n=18)	(n=20)
MAP (mm Hg)	93±5	94±4
Heart rate (bpm)	115±4	116±7
Cardiac Output (l/min)	3.4±0.2	3.3±0.2
Stroke Volume (ml)	30±2	30±2
LV dP/dt_{P40} (mm Hg/s)	1743±88	1411±51†
Tau (ms)	36±2	43±2*
LV EDP (mm Hg)	7.7±0.8	13.0±1.4†

*Values are mean ± SEM. BW, body weight; RVW and LVW, right and left ventricle weight; EDA and ESA, end-diastolic and end-systolic cross-sectional area; MAP, mean aortic pressure; LV dP/dt_{P40}, rate of rise in LV pressure at 40 mm Hg; EDP, end-diastolic pressure. * $P<0.05$; † $P<0.01$; ‡ $P<0.001$ versus sham*

4.3.2 Gene expression analysis

Global differences in gene expression in the remote non-infarcted part of the LV were determined by microarray analysis. In principal component analysis 33.7% of the variation in the data sets was explained by the first two components, with principal component 1

clearly separating MI from sham animals (Fig. 4.2A). There was no apparent clustering based on gender, which may be explained by the use of pre-adolescent pigs and neutered males. In MI swine, 285 genes were upregulated and 278 were downregulated (FDR <0.05) compared to myocardium from sham swine.

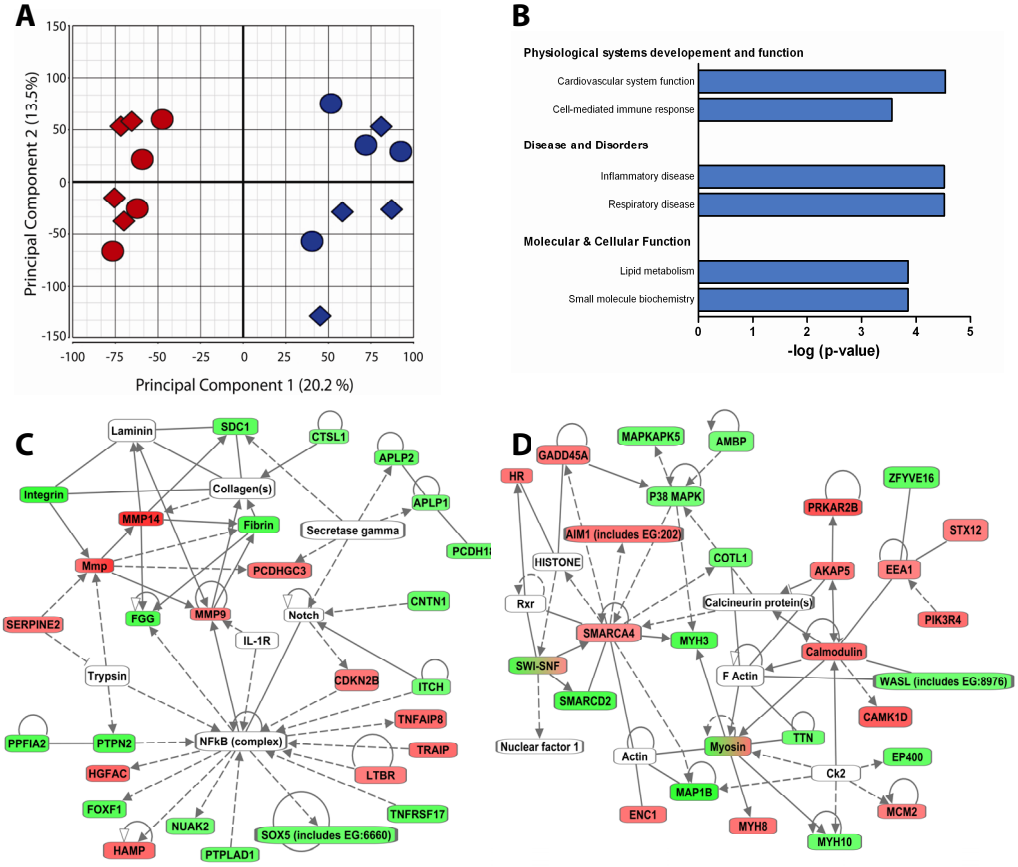

Figure 4.2. Differential gene expression. *(A) Principal component analysis of the data from the individual microarrays shows separation into two groups, with the sham (blue) and post-MI (red) samples forming separate clusters. Females (diamonds) and males (circles) do not form separate clusters. (B) Clustering of the differentially expressed genes into biological groups was performed with Ingenuity Pathway Analysis (P<0.001). (C&D) The top two networks of differentially expressed genes. Rectangles in green and red represent genes downregulated and upregulated after MI compared with sham. Dual-colored rectangles depict a group of genes, some of which are upregulated and some are downregulated after MI. White rectangles are hub molecules, of which the expression is not altered, but that generally have a large number of connections with the genes. Uninterrupted and dashed lines indicate physical and indirect interactions between molecules.*

To test whether differentially expressed genes clustered into 'biological process' groups, Ingenuity Pathway Analysis was used (Fig. 4.2B). Besides 'Cardiovascular System Development and Function', genes involved in 'Cell-Mediated Immune Response' and 'Inflammatory Disease Genes' were significantly overrepresented among differentially expressed genes. These findings are in accordance with the concept that inflammation plays an important role in post-MI LV remodeling (Nian *et al.*, 2004). In addition, 'Lipid Metabolism' was significantly overrepresented, which may reflect the changes in energy metabolism associated with LV hypertrophy (Zhang *et al.*, 1995). The genes that attribute to the subgroup clustering in Figure 4.2B are listed in supplemental Table 4.1.

Ingenuity Pathway Analysis was also used to visualize relationships between the differentially expressed genes. Fig. 4.2C displays the network with the highest number of genes. In this network NF-κB is a central hub molecule whose expression is not changed at the mRNA level, but which is known to be activated after MI in murine models (Kawano *et al.*, 2006) and in the failing human heart (Wong *et al.*, 1998). Calcineurin is a central hub molecule in the network with the second highest number of differentially expressed genes (Fig. 4.2D), and its role in cardiac hypertrophy in murine models has been well established (Molkentin *et al.*, 1998). In this network the 'Calmodulin – A kinase anchor protein 5 (AKAP5) – protein kinase A regulatory subunit 2B (PRKAR2B) – axis' is present, which was upregulated after MI. The latter observations are consistent with previous data from our laboratory, showing perturbations in PKA signaling in post-MI hearts (van der Velden *et al.*, 2004).

4.3.3 Transcription Factor Binding Site analysis

To identify which TFs are involved in the coordinate regulation of expression of differentially expressed genes, we scanned promoter regions of the homologous human genes for overrepresentation of transcription factor binding sites (TFBS). Eighteen TFBS were significantly overrepresented in promoter regions of the upregulated genes, while 13 were overrepresented in the downregulated genes (Table 4.2). These included a number of TFs involved in cell differentiation and proliferation (e.g., serum response factor (SRF) and BTB and CNC homology 1 (BACH1)), and a number of nuclear receptors (e.g., aryl hydrocarbon receptor (AhR), glucocorticoid receptor (GR), chicken ovalbumin upstream promoter transcription factor II COUP-TFII). For members of the FOX family of TFs, a different binding site was overrepresented in the promoters of upregulated and downregulated genes. TFBS for the nuclear factor of activated T-cells (NFAT) family of TFs were overrepresented in the downregulated genes. For each TFBS, the site was found on average in the proximal

Table 4.2. Transcription factor binding sites overrepresented in upregulated or downregulated genes

Matrix name	Transcription Factor	Up/Down	Frequency (sites/600 bp)		p-value
			Up genes	Down genes	
V$HOXA3_01	HOXA3/4	5.6	0.11	0.02	0.001
V$SPIB_01	SPIB	4.7	0.12	0.03	0.001
V$PAX4_01	PAX4	4.4	0.11	0.03	0.002
V$PAX3_B	PAX3	4.2	0.11	0.03	0.003
V$SRF_Q5	SRF	4.1	0.12	0.03	0.003
V$GR_Q6	GR (NR3C1)	3.2	0.13	0.04	0.006
V$TBX5_02	TBX5	3.1	0.16	0.05	0.002
V$SMAD_Q6	SMAD1-8	2.8	0.18	0.06	0.002
V$HNF4_01	HNF4gamma,HNF-4,HNF-4α	2.8	0.12	0.04	0.01
V$FOXD3_01	FOXC1/D1/D3/F1/F2/H1/I1/ J1/J2FOXL1/O1/O3/O4	2.8	0.19	0.07	0.002
V$AR_03	AR	2.7	0.13	0.05	0.009
V$MYC_Q2	c-Myc,N-Myc,Max	2.4	0.28	0.13	0.002
V$HNF3B_01	HNF-3beta	2.3	0.17	0.08	0.008
V$SOX10_Q6	Sox2/4-6/9-12/18/20	2.3	0.20	0.09	0.005
V$ARNT_02	Arnt	2.3	0.27	0.12	0.005
V$ARP1_01	COUP-TFI/II (NR2F1/2)	2.2	0.37	0.17	0.0003
V$E47_02	MRF2,MASH-1,Myf5/6,MyoD ,Myogenin, HTF4γ,E47	2.1	0.28	0.13	0.002
V$NFAT_Q6	NFATC1-4	−4.8	0.02	0.11	0.002
V$AHRARNT_0	AhR,ARNT	−3.1	0.03	0.11	0.009
V$TCF11MAFG _0	BACH1/2,MAF,MAFB/E/G/K, NFE2,NFE2L1-3	−3.1	0.03	0.11	0.009
V$OLF1_01	EBF1/3	−3.1	0.03	0.11	0.009
V$YY1_02	YY1	−2.7	0.7	0.16	0.005
V$XFD3_01	EP300,MEIS1,RRN3, SMAD2,TGIF1	−2.7	0.06	0.15	0.005
V$STAT3STAT3	STAT3	−2.7	0.07	0.19	0.002
V$FAC1_01	BPTF	−2.6	0.07	0.17	0.003
V$CMYB_01	MYB,MYBL2	−2.4	0.06	0.15	0.009
V$FREAC3_01	FOXC1/D1/D3/F1/F2/H1/I1/ J1/J2FOXL1/O1/O3/O4	−2.4	0.07	0.17	0.007
V$PAX8_01	PAX8	−2.4	0.07	0.16	0.007
V$ATF1_Q6	ATF1-4,ATF7,CREB1, CREM	−2.1	0.1	0.21	0.007
V$HELIOSA_02	IKZF1	−2.1	0.12	0.24	0.006

Matrix name: TFBS matrix from TRANSFAC database; Transcription Factor: TFs that can bind to the matrix element; Up/Down: factor overrepresentation of the TFBS in upregulated versus downregulated genes (+ sign) or in downregulated versus upregulated genes (−sign).

promoter region of 10-30 % of the differentially expressed genes, whereas 37 % of upregulated genes contained a site for COUP-TFII (Table 4.2).

4.3.4 Protein/DNA array

To identify TFs with altered activity in remodeled myocardium, we performed protein/DNA array analysis of pooled LV nuclear extracts from eight post-MI hearts versus eight sham swine. Signals above background were detected for 186 out of the 345 probes in the array. DNA-binding activity of 10 TFs was found to be at least 2-fold higher, while binding activity of 20 TFs was at least 2-fold less, in remodeled myocardium of post-MI hearts compared to sham. Table 4.3 shows the top 5 of affected TFs (see Supplemental Table 4.2 for the full list). Two TFs were active only in one protein pool (Ikaros family zinc finger 1 (IKZF1) in MI and retinoic acid receptor (RAR) in sham), but signal intensity just surpassed the detection limit of the array.

Table 4.3. Top 5 transcription factors showing increased or decreased DNA-binding activity in nuclear extracts from MI myocardium

Probe name	Transcription factor	Ratio MI/sham
LyF	IKZF1	∞*
AIC/CBF	COUP-TFI/II (NR2F1/2)	9.8
AF-1	COUP-TFII (NR2F2)	4.6
PEPCK PR	GR (NR3C1)	2.5
ACP BP	HIVEP1‡	2.5
RAR(DR5)	RAR	−∞†
ORE	NFAT5	−9.9
HNF-3	FOXA1/2/3	−7.4
NF-Y	NF-Y	−6.7
MEF-1	MyoD§	−6.5

**, signal was only detectable on post-MI array; †, signal was only detectable on sham array. ‡HIVEP1 is the most likely candidate to bind to the ACPBP binding element (Brady et al., 1995); §MyoD is the most likely candidate to bind to the MEF-1 element (Neuhold & Wold, 1993)*

Ingenuity Pathway Analysis was performed to link the TFs identified from the protein/DNA array to the differentially expressed genes from the microarray analysis (Fig 4.3). The two TFs with the highest number of connections to the genes were CCAAT/enhancer-binding protein alpha (C/EBPα) and GR (also known as NR3C1). Most of the identified TFs had few or no links to the differentially expressed genes.

Five TFs were identified in both the *in silico* TFBS analysis and the protein/DNA array. Paired box protein 8 (PAX8) and IKZF1 were overrepresented in the down-regulated genes after MI, while their DNA-binding activity was increased in remodeled myocardium, which could be explained if these TFs were repressors of gene expression. However, PAX8 is considered an activator of expression(Ohno *et al.*, 1999) and IKZF1 can act both as activator

and repressor (Georgopoulos, 2002). The transcriptional activator myogenic differentiation (MyoD) (Tapscott, 2005) was decreased in DNA-binding activity, while a TFBS where MyoD could bind to was overrepresented in upregulated genes. For two TFs corresponding data were found in TFBS and protein/DNA array analysis, i.e. COUP-TFII (also known as NR2F2) and GR. As connections with the microarray data set were more abundant for GR than for COUP-TFII and since a pharmacological antagonist of COUP-TFII is, to our knowledge, not currently available we selected GR for validation of our transcriptional genomics approach.

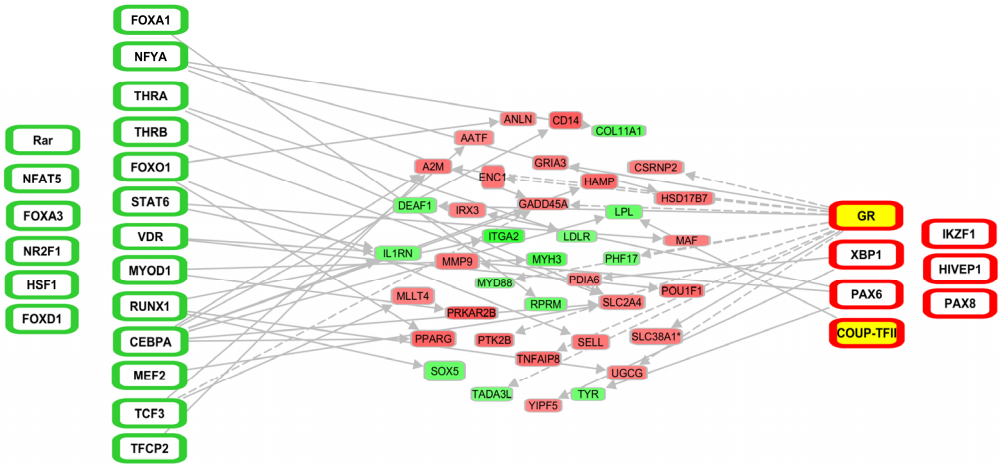

Figure 4.3. Linking of TFs identified by protein/DNA array to differentially expressed genes. *TFs that show less (green outline) or more (red outline) DNA-binding activity in post-MI LV tissue are depicted at the far left and right and are connected with upregulated (red) and downregulated (green) genes depicted in the center. TFs in yellow show matching changes in both protein/DNA array and TFBS analysis. A line was drawn between a TF and a gene if it was known from the literature that the TF can cause the expression of the gene. Uninterrupted and dashed lines indicate physical and indirect interactions between molecules.*

4.3.5 Pharmacological blockade of GR

To test if GR is a critical mediator of LV remodeling, the GR antagonist mifepristone (Cadepond *et al.*, 1997) (Mifegyne, Nordic Pharma BV, Baarn, the Netherlands) was administered to a subset of 7 MI pigs from day one after the MI. The animals received a daily dose of 200 mg p.o. for the first three days of treatment, and 100 mg/kg p.o. thereafter until the day of sacrifice. Mifepristone attenuated LV hypertrophy by 65% as reflected in the lower LVW/BW ratio measured at three weeks after MI (Fig 4.4). However, mifepristone treatment of MI pigs had no effect on LV end-diastolic dimensions and did not improve 2D-ejection fraction or $LVdP/dt_{P40}$ compared to untreated MI pigs (Fig. 4.4). In addition,

mifepristone had no significant effect on stroke volume, cardiac output, tau, LV end-diastolic pressure, or right ventricular hypertrophy (see Supplemental Table 4.3).

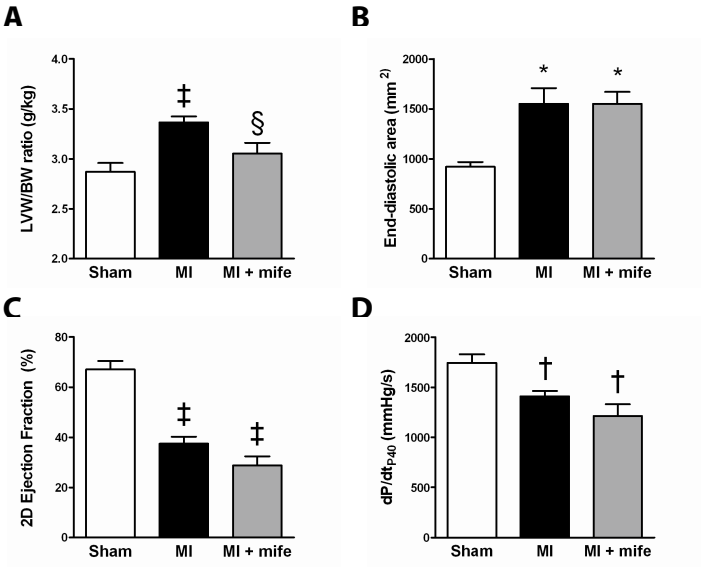

Figure 4.4. Effect of GR antagonist mifepristone on cardiac remodeling and function following MI. *Sham (n=20), MI (n=23) and MI+mifepristone (n=7) animals were studied. (A) LVW/BW ratios. (B) LV-dilation as indicated by LV end-diastolic area. (C) LV 2D-Ejection Fraction. (D) LV dP/dt$_{P40}$. *P<0.05, †P<0.01; ‡P<0.001 vs. sham; §P<0.05 vs MI. Measurements are mean ±SEM.*

4.4 Discussion

The present study is the first integrative unbiased investigation into the transcriptional control of post-MI LV hypertrophic remodeling in a large animal model, combining microarray data with TFBS data-mining and nuclear protein/DNA array data. Our approach identified two potential key players in LV remodeling, i.e. COUP-TFII and GR. Subsequent GR blockade revealed a critical role of this nuclear receptor in post-MI LV hypertrophy in swine, although it failed to blunt post-MI LV dilation.

In silico scanning of microarray data for TFBS in promoters regions of genes, identified a number of TFBS that were significantly overrepresented in either upregulated or downregulated genes. A number of these TFs have already been implicated in murine models of cardiac hypertrophy. SRF is part of the fetal gene program initiated after hypertrophy, and its transcriptional activity is higher in neonatal cardiomyocytes treated with hypertrophic stimuli (Davis *et al.*, 2003). Furthermore, SRF overexpression in a transgenic mouse model caused hypertrophy and cardiomyopathy (Zhang *et al.*, 2001). BACH1 has been implicated in cardiac hypertrophy as knock-out mice display less

hypertrophy following pressure-overload (Mito *et al.*, 2008). In our analysis BACH1 was overrepresented in downregulated genes, which is in line with its function as a transcriptional repressor (Dhakshinamoorthy *et al.*, 2005). Finally, AhR is considered to be a negative regulator of cardiac hypertrophy, as $AhR^{-/-}$ mice develop significant cardiac hypertrophy (Thackaberry *et al.*, 2002), and TFBS analysis showed that binding sites for AhR were overrepresented in downregulated genes after MI. Hannenhalli *et al*. recently identified TFBS overrepresented in differentially expressed genes in human end-stage systolic heart failure (Hannenhalli *et al.*, 2006). In that study, an important role for the family of FOX transcription factors was found, a number of which were also identified in our data set (see Table 4.2). Except for the FOX family of TFs, their dataset (Hannenhalli *et al.*, 2006) shows remarkable little overlap with ours, which might be explained by the distinction between early LV hypertrophy versus end-stage heart failure, as well as the older age of the human patients compared with the swine used in this study and the usage of medication in the human patient population.

Protein/DNA array analysis simultaneously assays the DNA-binding activity of a large set of TFs and has previously been applied to cultured cardiomyocytes (Davis *et al.*, 2005; Venkatesan *et al.*, 2010), but not to studies on TF activity in LV remodeling. Of the TFs identified in the protein/DNA array that were not confirmed by the TFBS analysis, only retinoic acid receptor (RAR) has been implicated in hypertrophy, although its role is controversial. RAR was found to suppress the α-adrenergic receptor-dependent hypertrophy in isolated cardiomyocytes (Zhou *et al.*, 1995), whereas overexpression of RAR in the heart caused dilated cardiomyopathy in mice (Colbert *et al.*, 1997). Furthermore, a recent report suggests that retinoic acid induces a cardiac phenotype that is more compatible with physiological hypertrophy (Freire *et al.*, 2010).

Overrepresentation of the TFBS for the NFATc1-4 family in downregulated genes was unexpected, as NFATs are considered transcriptional activators and NFATc1-4 are activated in cardiac hypertrophy, at least in rodents (Molkentin *et al.*, 1998). Indeed, NFAT transcriptional activity was reported to be increased in mice three weeks after MI (Heineke *et al.*, 2005). This discrepancy might be explained by NFAT5 binding to the TFBS of NFATc1-4. In contrast to NFATc1-4, NFAT5 does not have its own entry in the TRANSFAC database and would therefore not be identified in the TFBS analysis. NFAT5 binds to the 5'-TGGAAA(C/A/T)A(T/A)-3' motif, which contains the NFATc1-4 cognate element 5'-(T/A/C)GGAA(A/G)-3' (Morancho *et al.*, 2008). In line with this notion, using protein/DNA array, we found NFAT5 DNA-binding activity to be reduced in MI hearts. Similarly, NFAT5 DNA-binding activity is decreased in pacing induced heart failure in dogs (Srivastava *et al.*, 2002). In contrast to NFATc1-4, NFAT5 is not activated by calcineurin-mediated dephosphorylation (Morancho *et al.*, 2008). NFAT5 could play a role in cardiomyocyte survival, as expression of a dominant negative protein in neonatal cardiomyocytes

decreased cell viability (Ito *et al.*, 2007). Interestingly, no known NFAT5 target genes were identified among the differentially expressed genes in our microarray analysis. Further studies into the role of NFAT5 in cardiac remodeling are warranted.

For two TFs, matching data were found in TFBS and protein/DNA array analysis, i.e. COUP-TFII and GR. COUP-TFs are involved in suppression of genes involved in fatty acid oxidation after pressure overload induced hypertrophy (Sack *et al.*, 1997). We found COUP-TFII DNA-binding activity to be increased in post-MI hearts and COUP-TFII binding sites to be overrepresented in promoter regions of upregulated genes. As COUP-TFs are mainly considered as repressors of gene expression (Pereira *et al.*, 2000), our data could be interpreted to suggest that the increase in COUP-TF binding activity in post-MI hearts represents a compensatory reaction, possibly as a response to the elevated expression of target genes. Unfortunately no inhibitors of COUP-TF are, to our knowledge, available, so its contribution to LV remodeling could not be validated pharmacologically *in vivo*. The second TF identified by our integrative approach was GR, which was extensively linked to the microarray data (Fig. 4.3). We found that the increase in cardiac mass was blunted by GR blockade with mifepristone. These findings indicate that glucocorticoids via the GR contribute to post-infarct hypertrophy of the remote myocardium.

Glucocorticoids have been prescribed as anti-inflammatory agents and a large body of data has accrued on its adverse effects on the heart. It was first recognized that the GR agonist dexamethasone, given as treatment for chronic lung disease in pre-term children, can result in cardiac hypertrophy (Werner *et al.*, 1992). In a large population-based study it was shown that patients using glucocorticoids were at increased risk of developing cardiovascular disease and a dose-dependent increase in risk for development of heart failure was observed (Wei *et al.*, 2004). Hyperproduction of cortisol in Cushing's syndrome is associated with cardiac hypertrophy, which is reversed upon correction of hypercortisolism (Pereira *et al.*, 2010). A role for local cardiac glucocorticoid production in mediating LV hypertrophy in response to hemodynamic overload was recently suggested by Ohtani *et al.*(Ohtani *et al.*, 2009) who reported that GR expression was upregulated in pressure-overload hypertrophied LV of rats. Furthermore, cardio-specific elevation of glucocorticoid production augmented the hypertrophy response to pressure overload in mice (Ohtani *et al.*, 2009). Taken together these studies indicate that pharmacologically (Werner *et al.*, 1992; Wei *et al.*, 2004), pathologically (Pereira *et al.*, 2010), or genetically (Ohtani *et al.*, 2009) induced hypercortisolism is able to produce or augment hypertrophy. However, these studies do not answer the question whether glucocorticoid signaling contributes to LV hypertrophy under conditions of eucortisolism.

In mice with a recent MI, blocking GR with mifepristone was recently shown to significantly increase angiogenesis (Small *et al.*, 2005). This increased angiogenesis was associated with improved infarct healing and a thicker scar area, which likely contributed to

the improved 2D ejection fraction at 1-4 weeks after MI (McSweeney *et al.*, 2010). Unfortunately, the authors did not report on LV end-diastolic dimensions or LV weights. In contrast, we show here that GR contributes to post-MI LV hypertrophy, as mifepristone attenuated LV hypertrophy in MI pigs, while post-infarct LV dilatation and 2D ejection fraction as well as LV systolic and diastolic dysfunction were not affected. Thus, treatment with mifepristone specifically blunted the post-MI increase in LV mass, but failed to reverse the LV dilation and dysfunction. Although this observation is not readily explained, it could be speculated that GR blockade may have led to a pro-inflammatory state with a NF-κB mediated increase in activity of metalloproteinases (MMPs) in the remote area of the LV. Increased activity of MMPs has been implicated in post-MI LV remodeling (Spinale, 2007) and the pro-hypertrophic calcineurin/NFAT pathway leads to upregulation of MMPs (Saygili *et al.*, 2009). Whether this mechanism was indeed operative should be the subject of future studies. Mifepristone was used to validate our transcriptional genomics approach. Besides a GR antagonist, mifepristone also acts as a progesterone receptor antagonist (Cadepond *et al.*, 1997). In our study mifepristone was used to treat young prepubescent animals of either sex. As plasma levels of progesterone are very low before puberty (Elsaesser *et al.*, 1978), blocking of the progesterone receptor will have had little contribution to the attenuated hypertrophic response. Although mifepristone decreased LV hypertrophy there was a trend towards decreased ejection fraction and dP/dt_{P40}. Hence, based on our data therapeutic application of GR inhibition in post-infarct patients would appear premature.

Pigs have a clear advantage over rodent models in resembling humans more closely in terms of cardiac rates and contractility (Kass *et al.*, 1998), and autonomic control thereof (Hasenfuss, 1998; Dixon & Spinale, 2009), as well as myofilament protein composition (Hasenfuss, 1998; Dixon & Spinale, 2009) and function (Hamdani *et al.*, 2008), and calcium homeostasis (Haghighi *et al.*, 2003). Notwithstanding its translational power, an inherent drawback of the pig as a model organism is that its genome has not been fully sequenced yet. This leads to methodological challenges such as poor microarray annotation and inability to perform TFBS analysis. With the ANEXdb the annotation of the porcine microarray has been vastly improved (Couture *et al.*, 2009). The output is the human homologue of the porcine gene, which can then be used for TFBS analysis or network analysis. The fact that human instead of porcine genes had to be used for the TFBS analysis made experimental validation of the results even more important. The protein/DNA array directly measures the DNA-binding activity of TFs, but an inherent limitation of the protein/DNA array is that only a selection of TFs is analyzed. A drawback of the TFBS analysis is that it cannot distinguish between TFs that bind to similar motifs, which leads to uncertainty as to which TF actually binds to the TFBS. By combining the two data sets, we circumvented these limitations and improved the reliability of the identification of TFs. Overcoming these experimental challenges is rewarded by gaining insight into cardiac

remodeling in a large animal model with even better translational potential than murine models.

In conclusion, we showed that an unbiased '-omics' approach is feasible in a large laboratory animal. Using this approach in which we combined microarray with *in silico* TFBS analysis and protein/DNA array analysis to study post-MI LV, we identified COUP-TFII and GR as potential key mediators in post-MI remodeling. Subsequent blockade of GR *in vivo*, demonstrated, for the first time, that GR mediates the increase in LV mass after MI.

4.5 Acknowledgement

Peter van der Spek is gratefully acknowledged for providing the infrastructure for bioinformatical analysis and Justine K. Peeters for discussions on microarray analysis.
This work was supported by a grant from the Netherlands Heart Foundation (NHS2005B234).

4.6 References

Brady JP, Kantorow M, Sax CM, Donovan DM, & Piatigorsky J (1995). Murine transcription factor alpha A-crystallin binding protein I. Complete sequence, gene structure, expression, and functional inhibition via antisense RNA. *J Biol Chem* **270**, 1221-1229.

Cadepond F, Ulmann A, & Baulieu EE (1997). RU486 (mifepristone): mechanisms of action and clinical uses. *Annu Rev Med* **48**, 129-156.

Chorianopoulos E, Heger T, Lutz M, Frank D, Bea F, Katus HA, & Frey N (2010). FGF-inducible 14-kDa protein (Fn14) is regulated via the RhoA/ROCK kinase pathway in cardiomyocytes and mediates nuclear factor-kappaB activation by TWEAK. *Basic Res Cardiol* **105**, 301-313.

Colbert MC, Hall DG, Kimball TR, Witt SA, Lorenz JN, Kirby ML, Hewett TE, Klevitsky R, & Robbins J (1997). Cardiac compartment-specific overexpression of a modified retinoic acid receptor produces dilated cardiomyopathy and congestive heart failure in transgenic mice. *J Clin Invest* **100**, 1958-1968.

Conraads VM, Vrints CJ, Rodrigus IE, Hoymans VY, Van Craenenbroeck EM, Bosmans J, Claeys MJ, Van Herck P, Linke A, Schuler G, & Adams V (2010). Depressed expression of MuRF1 and MAFbx in areas remote of recent myocardial infarction: a mechanism contributing to myocardial remodeling? *Basic Res Cardiol* **105**, 219-226.

Couture O, Callenberg K, Koul N, Pandit S, Younes R, Hu ZL, Dekkers J, Reecy J, Honavar V, & Tuggle C (2009). ANEXdb: an integrated animal ANnotation and microarray EXpression database. *Mamm Genome* **20**, 768-777.

Davis FJ, Gupta M, Camoretti-Mercado B, Schwartz RJ, & Gupta MP (2003). Calcium/calmodulin-dependent protein kinase activates serum response factor transcription activity by its dissociation from histone deacetylase, HDAC4. Implications in cardiac muscle gene regulation during hypertrophy. *J Biol Chem* **278**, 20047-20058.

Davis FJ, Pillai JB, Gupta M, & Gupta MP (2005). Concurrent opposite effects of trichostatin A, an inhibitor of histone deacetylases, on expression of alpha-MHC and cardiac tubulins: implication for gain in cardiac muscle contractility. *Am J Physiol Heart Circ Physiol* **288**, H1477-H1490.

Dhakshinamoorthy S, Jain AK, Bloom DA, & Jaiswal AK (2005). Bach1 competes with Nrf2 leading to negative regulation of the antioxidant response element (ARE)-mediated NAD(P)H:quinone oxidoreductase 1 gene expression and induction in response to antioxidants. *J Biol Chem* **280**, 16891-16900.

Dixon JA & Spinale FG (2009). Large animal models of heart failure: a critical link in the translation of basic science to clinical practice. *Circ Heart Fail* **2**, 262-271.

Duncker DJ, Boontje NM, Merkus D, Versteilen A, Krysiak J, Mearini G, El Armouche A, de Beer VJ, Lamers JM, Carrier L, Walker LA, Linke WA, Stienen GJ, & van der Velden J (2009).

Prevention of myofilament dysfunction by beta-blocker therapy in postinfarct remodeling. *Circ Heart Fail* **2**, 233-242.

Elsaesser F, Parvizi N, & Ellendorff F (1978). Steroid feedback on luteinizing hormone secretion during sexual maturation in the pig. *J Endocrinol* **78**, 329-342.

Freire CM, Azevedo PS, Minicucci MF, Oliveira SJ, Martinez PF, Novo R, Chiuso-Minicucci F, Matsubara BB, Matsubara LS, Okoshi K, Novelli EL, Zornoff LA, & Paiva SA (2010). Influence of different doses of retinoic acid on cardiac remodeling. *Nutrition*.

Garlie JB, Hamid T, Gu Y, Ismahil MA, Chandrasekar B, & Prabhu SD (2011). Tumor necrosis factor receptor 2 signaling limits beta-adrenergic receptor-mediated cardiac hypertrophy in vivo. *Basic Res Cardiol* **[ePub ahead of print]**.

Gentleman RC, Carey VJ, Bates DM, Bolstad B, Dettling M, Dudoit S, Ellis B, Gautier L, Ge Y, Gentry J, Hornik K, Hothorn T, Huber W, Iacus S, Irizarry R, Leisch F, Li C, Maechler M, Rossini AJ, Sawitzki G, Smith C, Smyth G, Tierney L, Yang JY, & Zhang J (2004). Bioconductor: open software development for computational biology and bioinformatics. *Genome Biol* **5**, R80.

Georgopoulos K (2002). Haematopoietic cell-fate decisions, chromatin regulation and ikaros. *Nat Rev Immunol* **2**, 162-174.

Haghighi K, Kolokathis F, Pater L, Lynch RA, Asahi M, Gramolini AO, Fan GC, Tsiapras D, Hahn HS, Adamopoulos S, Liggett SB, Dorn GW, MacLennan DH, Kremastinos DT, & Kranias EG (2003). Human phospholamban null results in lethal dilated cardiomyopathy revealing a critical difference between mouse and human. *J Clin Invest* **111**, 869-876.

Hamdani N, de Waard MC, Messer AE, Boontje NM, Kooij V, van Dijk SJ, Versteilen A, Lamberts R, Merkus D, Dos Remedios C, Duncker DJ, Borbely A, Papp Z, Paulus W, Stienen GJ, Marston SB, & van der Velden J (2008). Myofilament dysfunction in cardiac disease from mice to men. *J Muscle Res Cell Motil* **29**, 189-201.

Hammoud L, Lu X, Lei M, & Feng Q (2011). Deficiency in TIMP-3 increases cardiac rupture and mortality post-myocardial infarction via EGFR signaling: beneficial effects of cetuximab. *Basic Res Cardiol* **106**, 459-471.

Hannenhalli S, Putt ME, Gilmore JM, Wang J, Parmacek MS, Epstein JA, Morrisey EE, Margulies KB, & Cappola TP (2006). Transcriptional genomics associates FOX transcription factors with human heart failure. *Circulation* **114**, 1269-1276.

Hasenfuss G (1998). Animal models of human cardiovascular disease, heart failure and hypertrophy. *Cardiovasc Res* **39**, 60-76.

Heineke J, Ruetten H, Willenbockel C, Gross SC, Naguib M, Schaefer A, Kempf T, Hilfiker-Kleiner D, Caroni P, Kraft T, Kaiser RA, Molkentin JD, Drexler H, & Wollert KC (2005). Attenuation of cardiac remodeling after myocardial infarction by muscle LIM protein-calcineurin signaling at the sarcomeric Z-disc. *Proc Natl Acad Sci U S A* **102**, 1655-1660.

Heusch G & Schulz R (2011). A radical view on the contractile machinery in human heart failure. *J Am Coll Cardiol* **57**, 310-312.

Ito T, Fujio Y, Takahashi K, & Azuma J (2007). Degradation of NFAT5, a transcriptional regulator of osmotic stress-related genes, is a critical event for doxorubicin-induced cytotoxicity in cardiac myocytes. *J Biol Chem* **282**, 1152-1160.

Javadov S, Rajapurohitam V, Kilic A, Hunter JC, Zeidan A, Said Faruq N, Escobales N, & Karmazyn M (2011). Expression of mitochondrial fusion-fission proteins during post-infarction remodeling: the effect of NHE-1 inhibition. *Basic Res Cardiol* **106**, 99-109.

Kass DA, Hare JM, & Georgakopoulos D (1998). Murine cardiac function: a cautionary tail. *Circ Res* **82**, 519-522.

Katz AM (2008). The "modern" view of heart failure: how did we get here? *Circ Heart Fail* **1**, 63-71.

Kawano S, Kubota T, Monden Y, Tsutsumi T, Inoue T, Kawamura N, Tsutsui H, & Sunagawa K (2006). Blockade of NF-kappaB improves cardiac function and survival after myocardial infarction. *Am J Physiol Heart Circ Physiol* **291**, H1337-H1344.

Kel A, Voss N, Jauregui R, Kel-Margoulis O, & Wingender E (2006). Beyond microarrays: find key transcription factors controlling signal transduction pathways. *BMC Bioinformatics* **7 Suppl 2:** S13.

Kel A, Voss N, Valeev T, Stegmaier P, Kel-Margoulis O, & Wingender E (2008). ExPlain: finding upstream drug targets in disease gene regulatory networks. *SAR QSAR Environ Res* **19**, 481-494.

Kleinbongard P, Heusch G, & Schulz R (2010). TNFalpha in atherosclerosis, myocardial ischemia/reperfusion and heart failure. *Pharmacol Ther* **127**, 295-314.

Krusche CA, Holthofer B, Hofe V, van de Sandt AM, Eshkind L, Bockamp E, Merx MW, Kant S, Windoffer R, & Leube RE (2011). Desmoglein 2 mutant mice develop cardiac fibrosis and dilation. *Basic Res Cardiol* **106**, 617-633.

Kuster DW, Merkus D, Jorna HJ, Dekkers DH, Duncker DJ, & Verhoeven AJ (2010). Nuclear protein extraction from frozen porcine myocardium. *J Physiol Biochem* **67**, 165-173.

McSweeney SJ, Hadoke PW, Kozak AM, Small GR, Khaled H, Walker BR, & Gray GA (2010). Improved heart function follows enhanced inflammatory cell recruitment and angiogenesis in 11betaHSD1-deficient mice post-MI. *Cardiovasc Res* **88**, 159-167.

Mito S, Ozono R, Oshima T, Yano Y, Watari Y, Yamamoto Y, Brydun A, Igarashi K, & Yoshizumi M (2008). Myocardial protection against pressure overload in mice lacking Bach1, a transcriptional repressor of heme oxygenase-1. *Hypertension* **51**, 1570-1577.

Molkentin JD, Lu JR, Antos CL, Markham B, Richardson J, Robbins J, Grant SR, & Olson EN (1998). A calcineurin-dependent transcriptional pathway for cardiac hypertrophy. *Cell* **93**, 215-228.

Morancho B, Minguillon J, Molkentin JD, Lopez-Rodriguez C, & Aramburu J (2008). Analysis of the transcriptional activity of endogenous NFAT5 in primary cells using transgenic NFAT-luciferase reporter mice. *BMC Mol Biol* **9**, 13.

Mudd JO & Kass DA (2008). Tackling heart failure in the twenty-first century. *Nature* **451**, 919-928.

Neuhold LA & Wold B (1993). HLH forced dimers: tethering MyoD to E47 generates a dominant positive myogenic factor insulated from negative regulation by Id. *Cell* **74**, 1033-1042.

Nian M, Lee P, Khaper N, & Liu P (2004). Inflammatory cytokines and postmyocardial infarction remodeling. *Circ Res* **94**, 1543-1553.

Ohno M, Zannini M, Levy O, Carrasco N, & di Lauro R (1999). The paired-domain transcription factor Pax8 binds to the upstream enhancer of the rat sodium/iodide symporter gene and participates in both thyroid-specific and cyclic-AMP-dependent transcription. *Mol Cell Biol* **19**, 2051-2060.

Ohtani T, Mano T, Hikoso S, Sakata Y, Nishio M, Takeda Y, Otsu K, Miwa T, Masuyama T, Hori M, & Yamamoto K (2009). Cardiac steroidogenesis and glucocorticoid in the development of cardiac hypertrophy during the progression to heart failure. *J Hypertens* **27**, 1074-1083.

Pereira AM, Delgado V, Romijn JA, Smit JW, Bax JJ, & Feelders RA (2010). Cardiac dysfunction is reversed upon successful treatment of Cushing's syndrome. *Eur J Endocrinol* **162**, 331-340.

Pereira FA, Tsai MJ, & Tsai SY (2000). COUP-TF orphan nuclear receptors in development and differentiation. *Cell Mol Life Sci* **57**, 1388-1398.

Ringner M (2008). What is principal component analysis? *Nat Biotechnol* **26**, 303-304.

Sack MN, Disch DL, Rockman HA, & Kelly DP (1997). A role for Sp and nuclear receptor transcription factors in a cardiac hypertrophic growth program. *Proc Natl Acad Sci U S A* **94**, 6438-6443.

Saygili E, Rana OR, Meyer C, Gemein C, Andrzejewski MG, Ludwig A, Weber C, Schotten U, Kruttgen A, Weis J, Schwinger RH, Mischke K, Rassaf T, Kelm M, & Schauerte P (2009). The angiotensin-calcineurin-NFAT pathway mediates stretch-induced up-regulation of matrix metalloproteinases-2/-9 in atrial myocytes. *Basic Res Cardiol* **104**, 435-448.

Schoenauer R, Emmert MY, Felley A, Ehler E, Brokopp C, Weber B, Nemir M, Faggian GG, Pedrazzini T, Falk V, Hoerstrup SP, & Agarkova I (2011). EH-myomesin splice isoform is a novel marker for dilated cardiomyopathy. *Basic Res Cardiol* **106**, 233-247.

Simon R, Lam A, Li MC, Ngan M, Menenzes S, & Zhao Y (2007). Analysis of gene expression data using BRB-ArrayTools. *Cancer Inform* **3**, 11-17.

Small GR, Hadoke PW, Sharif I, Dover AR, Armour D, Kenyon CJ, Gray GA, & Walker BR (2005). Preventing local regeneration of glucocorticoids by 11beta-hydroxysteroid

dehydrogenase type 1 enhances angiogenesis. *Proc Natl Acad Sci U S A* **102**, 12165-12170.

Sorop O, Merkus D, de Beer VJ, Houweling B, Pistea A, McFalls EO, Boomsma F, van Beusekom HM, van der Giessen WJ, VanBavel E, & Duncker DJ (2008). Functional and structural adaptations of coronary microvessels distal to a chronic coronary artery stenosis. *Circ Res* **102**, 795-803.

Spinale FG (2007). Myocardial matrix remodeling and the matrix metalloproteinases: influence on cardiac form and function. *Physiol Rev* **87**, 1285-1342.

Srivastava S, Chandrasekar B, Bhatnagar A, & Prabhu SD (2002). Lipid peroxidation-derived aldehydes and oxidative stress in the failing heart: role of aldose reductase. *Am J Physiol Heart Circ Physiol* **283**, H2612-H2619.

Sutton MG & Sharpe N (2000). Left ventricular remodeling after myocardial infarction: pathophysiology and therapy. *Circulation* **101**, 2981-2988.

Tapscott SJ (2005). The circuitry of a master switch: Myod and the regulation of skeletal muscle gene transcription. *Development* **132**, 2685-2695.

Thackaberry EA, Gabaldon DM, Walker MK, & Smith SM (2002). Aryl hydrocarbon receptor null mice develop cardiac hypertrophy and increased hypoxia-inducible factor-1alpha in the absence of cardiac hypoxia. *Cardiovasc Toxicol* **2**, 263-274.

van der Velden J, Merkus D, Klarenbeek BR, James AT, Boontje NM, Dekkers DH, Stienen GJ, Lamers JM, & Duncker DJ (2004). Alterations in myofilament function contribute to left ventricular dysfunction in pigs early after myocardial infarction. *Circ Res* **95**, e85-e95.

van Kats JP, Duncker DJ, Haitsma DB, Schuijt MP, Niebuur R, Stubenitsky R, Boomsma F, Schalekamp MA, Verdouw PD, & Danser AH (2000). Angiotensin-converting enzyme inhibition and angiotensin II type 1 receptor blockade prevent cardiac remodeling in pigs after myocardial infarction: role of tissue angiotensin II. *Circulation* **102**, 1556-1563.

Velagaleti RS, Pencina MJ, Murabito JM, Wang TJ, Parikh NI, D'Agostino RB, Levy D, Kannel WB, & Vasan RS (2008). Long-term trends in the incidence of heart failure after myocardial infarction. *Circulation* **118**, 2057-2062.

Venkatesan B, Valente AJ, Prabhu SD, Shanmugam P, Delafontaine P, & Chandrasekar B (2010). EMMPRIN activates multiple transcription factors in cardiomyocytes, and induces interleukin-18 expression via Rac1-dependent PI3K/Akt/IKK/NF-kappaB andMKK7/JNK/AP-1 signaling. *J Mol Cell Cardiol* **49**, 655-663.

Wei L, MacDonald TM, & Walker BR (2004). Taking glucocorticoids by prescription is associated with subsequent cardiovascular disease. *Ann Intern Med* **141**, 764-770.

Werner JC, Sicard RE, Hansen TW, Solomon E, Cowett RM, & Oh W (1992). Hypertrophic cardiomyopathy associated with dexamethasone therapy for bronchopulmonary dysplasia. *J Pediatr* **120**, 286-291.

White HD, Norris RM, Brown MA, Brandt PW, Whitlock RM, & Wild CJ (1987). Left ventricular end-systolic volume as the major determinant of survival after recovery from myocardial infarction. *Circulation* **76**, 44-51.

Wingender E, Chen X, Hehl R, Karas H, Liebich I, Matys V, Meinhardt T, Pruss M, Reuter I, & Schacherer F (2000). TRANSFAC: an integrated system for gene expression regulation. *Nucleic Acids Res* **28**, 316-319.

Wong SC, Fukuchi M, Melnyk P, Rodger I, & Giaid A (1998). Induction of cyclooxygenase-2 and activation of nuclear factor-kappaB in myocardium of patients with congestive heart failure. *Circulation* **98**, 100-103.

Zhang J, Duncker DJ, Ya X, Zhang Y, Pavek T, Wei H, Merkle H, Ugurbil K, From AH, & Bache RJ (1995). Effect of left ventricular hypertrophy secondary to chronic pressure overload on transmural myocardial 2-deoxyglucose uptake. A 31P NMR spectroscopic study. *Circulation* **92**, 1274-1283.

Zhang X, Azhar G, Chai J, Sheridan P, Nagano K, Brown T, Yang J, Khrapko K, Borras AM, Lawitts J, Misra RP, & Wei JY (2001). Cardiomyopathy in transgenic mice with cardiac-specific overexpression of serum response factor. *Am J Physiol Heart Circ Physiol* **280**, H1782-H1792.

Zhou MD, Sucov HM, Evans RM, & Chien KR (1995). Retinoid-dependent pathways suppress myocardial cell hypertrophy. *Proc Natl Acad Sci U S A* **92**, 7391-7395.

4.7 Supplemental data

Supplemental table 4.1. Genes clustering in significantly changed subgroups

Gene symbol	Gene name	Fold change[a]	FDR [b]
Cardiovascular System Development			
MMP14	matrix metalloproteinase 14	2.2	< 0.0001
PF4	platelet Factor 4	1.8	0.005
PPARG	peroxisome proliferator-activated receptor gamma	1.6	0.002
PTK2B	protein tyrosine kinase 2 beta	1.6	< 0.0001
MMP9	matrix metallopeptidase 9	1.5	0.0001
C5AR1	complement component 5a receptor 1	1.5	0.002
SELL	selectin L	1.4	0.002
AKAP5	A kinase anchor protein 5	1.4	0.0005
KIF3A	kinesin family member 3A	1.4	0.003
ODC1	ornithine decarboxylase 1	1.4	0.009
EDNRB	endothelin receptor type B	1.3	0.009
MYH10	myosin, heavy chain 10, non-muscle	−1.4	0.004
ADAM15	ADAM metallopeptidase domain 15	−1.4	0.001
FGG	fibrinogen gamma chain	−1.7	< 0.0001
ITGA2	integrin, alpha 2	−1.9	0.01
Cell mediated immune response			
MMP14	matrix metalloproteinase 14	2.2	< 0.0001
PF4	platelet Factor 4	1.8	0.005
PPARG	peroxisome proliferator-activated receptor gamma	1.6	0.002
CD14	CD14 molecule	1.6	0.0006
HAMP	hepcidin antimicrobial peptide	1.6	< 0.0001
MMP9	matrix metallopeptidase 9	1.5	0.0001
C5AR1	complement component 5a receptor 1	1.5	0.002
SELL	selectin L	1.4	0.002
MAF	v-maf musculoaponeurotic fibrosarcoma oncogene homolog	1.4	0.0004
LTBR	lymphotoxin B receptor	1.4	0.003
SMARCA4	SWI/SNF related, matrix associated, actin dependent regulator of chromatin, subfamily a, member 4	1.2	0.004
IL12RB2	interleukin 12 receptor, beta 2	−1.3	0.002
CD80	CD80 molecule	−1.3	0.0009
COTL1	coactosin-like 1	−1.3	0.005
WASL	Wiskott-Aldrich syndrome-like	−1.3	0.003
ALCAM	activated leukocyte cell adhesion molecule	−1.3	0.003
AMBP	alpha-1-microglobulin/bikunin precursor	−1.3	0.0002

IL1RN	interleukin 1 receptor antagonist	−1.3	0.001
LDLR	low density lipoprotein receptor	−1.3	0.001
ITCH	itchy E3 ubiquitin protein ligase homolog	−1.3	0.01
MYD88	myeloid differentiation primary response gene 88	−1.4	0.002

Inflammatory disease

MMP14	matrix metalloproteinase 14	2.2	< 0.0001
MYO5B	myosin VB	1.8	0.004
SSTR1	somatostatin receptor 1	1.7	< 0.0001
CAMK1D	calcium/calmodulin-dependent protein kinase ID	1.7	0.005
CD14	CD14 molecule	1.6	0.0006
PPARG	peroxisome proliferator-activated receptor gamma	1.6	0.002
TTC38	tetratricopeptide repeat domain 38	1.6	< 0.0001
MMP9	matrix metallopeptidase 9	1.5	0.0001
SLC6A3	solute carrier family 6 member 3	1.5	0.0005
C5AR1	complement component 5a receptor 1	1.5	0.002
CHSY3	chondroitin sulfate synthase 3	1.5	0.005
LSAMP	limbic system-associated membrane protein	1.5	0.002
LYST	lysosomal trafficking regulator	1.5	0.0001
RHCG	Rhesus blood group-associated C glycoprotein	1.5	< 0.0001
TRAIP	TRAF interacting protein	1.5	< 0.0001
LTBR	lymphotoxin B receptor	1.4	0.003
SSTR5	somatostatin receptor 5	1.4	< 0.0001
ANKRD27	ankyrin repeat domain 27	1.4	0.002
SERPINE2	serpin peptidase inhibitor, clade E , member 2	1.4	0.0002
GADD45A	growth arrest and DNA-damage-inducible, alpha	1.4	0.007
EDNRB	endothelin receptor type B	1.3	0.009
C1ORF21	chromosome 1 open reading frame 21	1.3	0.007
CCDC6	coiled-coil domain containing 6	1.3	0.006
MIER1	mesoderm induction early response 1 homolog	1.3	0.007
PDE4A	phosphodiesterase 4A, cAMP-specific	1.2	0.002
CTSL1	cathepsin L1	−1.2	0.003
RPS6KB1	ribosomal protein S6 kinase, 70kDa, polypeptide 1	−1.2	0.001
CD80	CD80 molecule	−1.3	0.0009
IL1RN	interleukin 1 receptor antagonist	−1.3	0.001
ALCAM	activated leukocyte cell adhesion molecule	−1.3	0.003
COTL1	coactosin-like 1	−1.3	0.005
IL12RB2	interleukin 12 receptor, beta 2	−1.3	0.002
MYD88	myeloid differentiation primary response gene 88	−1.4	0.002
CCDC38	coiled-coil domain containing 38	−1.4	0.001
IMMP2L	IMP2 inner mitochondrial membrane peptidase-like	−1.4	0.009
SOX5	SRY-box containing gene 5	−1.4	< 0.0001
ETV5	ets variant gene 5	−1.5	< 0.0001
USP1	ubiquitin specific peptidase 1	−1.5	0.002

CTNS	cystinosin, lysosomal cystine transporter	−1.5	0.003
PPFIA2	protein tyrosine phosphatase, receptor type, f polypeptide, interacting protein, alpha 2	−1.6	0.0003
ASTN2	astrotactin 2	−1.6	< 0.0001
FGG	fibrinogen gamma chain	−1.7	< 0.0001
DNAJC24	DnaJ (Hsp40) homolog, subfamily C, member 24	−1.7	0.0001
MYH3	myosin, heavy chain 3, skeletal muscle, embryonic	−1.7	0.0004
PTPN2	protein tyrosine phosphatase, non-receptor type 2	−1.7	0.001
DIRC2	disrupted in renal carcinoma 2	−1.8	< 0.0001
Respiratory disease			
SSTR1	somatostatin receptor 1	1.7	< 0.0001
PPARG	peroxisome proliferator-activated receptor gamma	1.6	0.002
CD14	CD14 molecule	1.6	0.0006
MMP9	matrix metallopeptidase 9	1.5	0.0001
SLC6A3	solute carrier family 6 member 3	1.5	0.0005
LTBR	lymphotoxin B receptor	1.4	0.003
SSTR5	somatostatin receptor 5	1.4	< 0.0001
EDNRB	endothelin receptor type B	1.3	0.009
PDE4A	phosphodiesterase 4A, cAMP-specific	1.2	0.002
FOSL1	FOS-like antigen 1	1.2	0.006
CD80	CD80 molecule	−1.3	0.0009
IL1RN	interleukin 1 receptor antagonist	−1.3	0.001
MYD88	myeloid differentiation primary response gene 88	−1.4	0.002
ERBB3	v-erb-b2 erythroblastic leukemia viral oncogene homolog 3	−2.1	0.01
Lipid metabolism			
PRKAR2B	protein kinase, cAMP-dependent, regulatory, type II, beta	1.8	0.004
CD14	CD14 molecule	1.6	0.0006
PPARG	peroxisome proliferator-activated receptor gamma	1.6	0.002
PIK3C2A	phosphoinositide-3-kinase, class 2, alpha polypeptide	1.6	0.0005
MLYCD	malonyl-CoA decarboxylase	1.6	0.0004
C5AR1	complement component 5a receptor 1	1.5	0.002
SYNJ2	synaptojanin 2	1.5	0.0007
A2M	alpha-2-macroglobulin	1.5	0.0001
STX12	syntaxin 12	1.4	0.009
SLC2A4	solute carrier family 2, member 4	1.4	0.0009
UGCG	UDP-glucose ceramide glucosyltransferase	1.4	0.0007
CYP1A2	cytochrome P450, family 1, subfamily A, polypeptide 2	1.4	0.0001
AATF	apoptosis antagonizing transcription factor	1.3	0.005
GBGT1	globoside alpha-1,3-N-acetylgalactosaminyltransferase 1	1.3	0.005
LDLR	low density lipoprotein receptor	−1.3	0.001
IL1RN	interleukin 1 receptor antagonist	−1.3	0.001

LPL	lipoprotein lipase	−1.4	0.005
MYD88	myeloid differentiation primary response gene 88	−1.4	0.002
NAGLU	N-acetylglucosaminidase, alpha	−1.4	0.005
MPDU1	mannose-P-dolichol utilization defect 1	−2.1	< 0.0001
Small molecule biochemistry			
PF4	platelet Factor 4	1.8	0.005
CD14	CD14 molecule	1.6	0.0006
PPARG	peroxisome proliferator-activated receptor gamma	1.6	0.002
PIK3C2A	phosphoinositide-3-kinase, class 2, alpha polypeptide	1.6	0.0005
MLYCD	malonyl-CoA decarboxylase	1.6	0.0004
C5AR1	complement component 5a receptor 1	1.5	0.002
SLC6A3	solute carrier family 6, member 3	1.5	0.0005
SYNJ2	synaptojanin 2	1.5	0.0007
A2M	alpha-2-macroglobulin	1.5	0.0001
GCLC	glutamate-cysteine ligase, catalytic subunit	1.4	0.003
SLC38A1	solute carrier family 38, member 1	1.4	0.001
ODC1	ornithine decarboxylase 1	1.4	0.009
SSTR5	somatostatin receptor 5	1.4	< 0.0001
PGAM1	phosphoglycerate mutase 1	1.4	0.002
STX12	syntaxin 12	1.4	0.009
SLC2A4	solute carrier family 2, member 4	1.4	0.0009
UGCG	UDP-glucose ceramide glucosyltransferase	1.4	0.0007
CYP1A2	cytochrome P450, family 1, subfamily A, polypeptide 2	1.4	0.0001
AATF	apoptosis antagonizing transcription factor	1.3	0.005
GBGT1	globoside alpha-1,3-N-acetylgalactosaminyltransferase 1	1.3	0.005
PCYOX1	prenylcysteine oxidase 1	1.3	0.01
MLLT4	myeloid/lymphoid or mixed-lineage leukemia; translocated to 4	1.3	0.004
PGLS	6-phosphogluconolactonase	1.2	0.002
LDLR	low density lipoprotein receptor	−1.3	0.001
IL1RN	interleukin 1 receptor antagonist	−1.3	0.001
LPL	lipoprotein lipase	−1.4	0.005
MYD88	myeloid differentiation primary response gene 88	−1.4	0.002
NAGLU	N-acetylglucosaminidase, alpha	−1.4	0.005
TYR	tyrosinase	−1.4	< 0.0001
TCF7L2	transcription factor 7-like 2	−1.5	0.003
FPGT	fucose-1-phosphate guanylyltransferase	−1.8	0.003
MAP1B	microtubule-associated protein 1B	−1.9	0.0004
MPDU1	mannose-P-dolichol utilization defect 1	−2.1	< 0.0001

[a]: positive when MI>sham, negative when MI<sham; [b]: False Discovery Rate adjusted p-value

Supplemental table 4.2. Transcription factors increased or decreased in DNA-binding activity in nuclear extracts from MI myocardium

Probe name	Transcription factor	Ratio MI/sham
LyF	IKZF1	∞*
AIC/CBF	COUP-TFI/II (NR2F1/2)	9.8
AF-1	COUP-TFII (NR2F2)	4.6
PEPCK PR	GR (NR3C1)	2.9
ACP BP	HIVEP1‡	2.9
XBP-1	XBP-1	2.9
MSP-1		2.9
Beta RE		2.5
PAX-6	PAX-6	2.5
PAX-8	PAX-8	2.5
RAR(DR5)	RAR	−∞†
ORE	NFAT5	−9.9
HNF-3	FOXA1/2/3	−7.4
NF-Y	NF-Y	−6.7
MEF-1	MyoD§	−6.5
TR(DR4)	THR	−5.6
CETP-CRE		−5.6
FKHR	FOXO1a	−5.3
COUP-TF	NR2F1	−5.2
ODC		−4.2
VDR(DR3)	VDR	−4.1
MyoD	MyoD1	−3.9
HSE	HSF1	−3.3
AML-1	RUNX1	−3.1
STAT-6	STAT-6	−2.8
MEF-2	MEF-2C	−2.8
C/EBP	C/EBPα	−2.7
LSF	TFCP2	−2.7
Freac-4	FOXD1	−2.5
E12/E47	TCF3	−2.2

**, signal was only detectable on post-MI array; †, signal was only detectable on sham array. ‡HIVEP1 is the most likely candidate to bind to the ACPBP binding element [1]; §MyoD is the most likely candidate to bind to the MEF-1 element [2].*

Supplemental Table 4.3. Effect of mifepristone on hemodynamical and anatomical data of MI swine

	MI	MI + mife
Anatomic data	(n = 24)	(n = 7)
Body weight (kg)	32 ± 1	31 ± 1
RVW/BW (g/kg)	1.35 ± 0.06	1.26 ± 0.07
LVW/BW (g/kg)	3.38 ± 0.06	3.05 ± 0.10*
Echocardiographic data	(n = 13)	(n = 7)
LV EDA (mm^2)	1551 ± 157	1551 ± 140
LV ESA (mm^2)	985 ± 128	1102 ± 106
2D Ejection Fraction (%)	37 ± 3	30 ± 4
Hemodynamic data	(n = 20)	(n = 6)
MAP (mm Hg)	94 ± 4	93 ± 8
Heart rate (bpm)	116 ± 7	121 ± 10
Cardiac Output (l/min)	3.3 ± 0.2	3.1 ± 0.2
Stroke Volume (ml)	30 ± 2	27 ± 3
LV dP/dt_{P40} (mm Hg/s)	1411 ± 51	1213 ± 116
Tau (ms)	43 ± 2	43 ± 2
LV EDP (mm Hg)	13.0 ± 1.4	13.0 ± 1.5

*Values are mean ± SEM. RV(W) and LV(W) indicate right and left ventricle (weight); BW, body weight; EDA, end-diastolic cross-sectional area; ESA, end-systolic cross-sectional area; MAP, mean aortic pressure; LV dP/dt_{P40}, rate of rise in LV pressure at a pressure of 40 mm Hg; EDP, end-diastolic pressure. * P<0.05 versus MI.*

Chapter 5

Transcriptional genomics of exercise-induced cardiac hypertrophy in swine; comparison with MI induced hypertrophy

Diederik W. D. Kuster, Daphne Merkus, Andreas Kremer, Wilfred F.J. van IJcken, Vincent J. de Beer, Adrie J.M. Verhoeven & Dirk J. Duncker

In preparation

Abstract

Cardiac hypertrophy is the response of the heart to an increased workload in order to maintain cardiac output. Physiological hypertrophy, as occurs after prolonged exercise-training, is associated with a reduced risk for cardiovascular disease, whereas pathological hypertrophy after stress or injury increases the risk to develop heart failure. Differences between both forms of hypertrophy may result from genetic reprogramming through differential activity of a limited set of transcription factors (TFs). The aim of this study was to identify TFs that are involved in physiological hypertrophy of the left ventricle (LV) in swine, and to compare this with the set of transcription factors involved in pathological hypertrophy.

Compared to sedentary animals, swine that underwent a 4-6 weeks exercise protocol (Ex) showed an increased LV weight (15%; p=0.03) and stroke volume (36%; p=0.02) (both normalized for body weight), without changes in other hemodynamic and anatomical parameters. Microarray analysis of LV tissue identified 339 upregulated genes and 408 downregulated genes (FDR<0.05). The promoter regions of the upregulated genes were screened for common transcription factor binding sites (TFBS). Downregulated genes were similarly analyzed. Seventeen TFBS were overrepresented >1.5-fold (p<0.01) in upregulated and 24 in downregulated genes. Nuclear protein extracts prepared from LV tissue were assayed for DNA-binding activity using a protein/DNA array. Out of 345 DNA probes, 23 showed signal intensity changes >2-fold. Of those, YY1, PAX6 and the glucocorticoid receptor (GR) showed matching results in TFBS and protein/DNA array analysis.

Similar increases in LV weight were observed in swine three weeks after a myocardial infarction. In addition, the LV showed increased end-diastolic area (68%; p=0.004) and reduced ejection fraction (40%, p<0.001) and rate of pressure development during contraction (dP/dt_{P40}) (19%, p=0.002). Gene expression profiles in both forms of hypertrophy showed little overlap. Of the 1091 affected genes, only 92 genes were similarly up- or downregulated in both models of hypertrophy, wheras 87 genes were oppositely regulated. Ten overrepresented TFBS and 3 transcription factors from the protein-DNA array were common to both forms of hypertrophy, whereas 3 TFBS and 5 transcription factors were identified for the oppositely regulated genes including PAX6, GR and GATA1-6. Notably, GR activity was found to be reduced upon exercise-training and increased after myocardial infarction.

In conclusion, using an unbiased approach, we have identified a number of transcription factors as potential mediators of physiological LV hypertrophy in a large animal. Several of these factors were also associated with pathological hypertrophy, and

thus are likely involved in the general hypertrophic response. Other factors, such as GR, discriminate between both forms of hypertrophy, and may represent potential therapeutic targets to reduce the risk for heart failure after myocardial infarction.

5.1 Introduction

Cardiac hypertrophy is the response of the heart to an increased workload, stress or injury, in an attempt to maintain cardiac output (Sutton & Sharpe, 2000; Katz, 2008). Despite its apparent appropriateness, an increased heart mass constitutes an independent risk factor for the development of heart failure (White *et al.*, 1987b; Levy *et al.*, 1990). The loss of viable myocardium following an acute myocardial infarction (MI) elicits a cascade of compensatory mechanisms, including neurohumoral activation, fluid retention and left ventricular (LV) pathological hypertrophy (Sutton & Sharpe, 2000; Katz, 2008). Conversely, physiological hypertrophy, as occurs after prolonged exercise-training, is associated with a reduced risk for cardiovascular disease (Gielen *et al.*, 2001; Maron & Pelliccia, 2006).

Pathological and physiological hypertrophy not only differ in clinical outcome but also have different cellular and molecular phenotypes (Frey & Olson, 2003; Bernardo *et al.*, 2010). While in pathological hypertrophy a number of neurohumoral pathways drive the hypertrophic response, growth factors, such as IGF-1, and phosphatidylinositol- 3-kinase/Akt signaling are involved in physiological hypertrophy (Dorn, 2007). Furthermore, the increased fibrosis and apoptosis, and decreased capillary density associated with pathological hypertrophy is not observed in exercise-induced hypertrophy (McMullen *et al.*, 2003). A number of studies have been performed comparing gene expression profiles in various rodent models of pathological and physiological hypertrophy (Kong *et al.*, 2005; Strom *et al.*, 2005; Galindo *et al.*, 2009; Beisvag *et al.*, 2009). In these models, genes involved in apoptosis and inflammation were differentially expressed in pathological hypertrophy, while expression of cell survival and fatty acid oxidation genes were altered after physiological hypertrophy. Differences between both forms of hypertrophy likely are the result from genetic reprogramming through a limited number of transcription factors.

Compared to murine models, studies into the molecular mechanisms of pathological and physiological hypertrophy in large animals are scarce. In our laboratory, we study cardiac remodeling in swine, a model that in many aspects better mimics human heart physiology and hemodynamics (Dixon & Spinale, 2009). To study the molecular pathways that underlie physiological hypertrophy and the TFs that drive these changes, we first investigated left ventricle (LV) hypertrophy caused by 4-6 weeks of exercise-training in swine. Using the changes in gene expression profiles, we searched the altered genes for common transcription factor binding sites (TFBS), and combined these data with protein/DNA array analysis of protein extracts prepared from LV nuclei. To identify transcription factors that may discriminate between both forms of hypertrophy we subsequently made a comprehensive comparison with the changes in gene expression seen after MI.

5.2 Methods

5.2.1 Experimental animals

Studies were performed in accordance with the *Guide for the Care and Use of Laboratory Animals* (NIH Publication No. 85-23, revised 1996) and with approval of the Erasmus Medical Center Animal Care Committee. Cardiac tissue was collected from 2-3 months (pre-pubescent) old male and female Yorkshire x Landrace swine. Male animals were neutered.

5.2.2 Exercise protocol

Eleven swine underwent a 4-6 week long incrementally increased exercise protocol (EX). Swine ran 5 days a week on a treadmill starting at 3 km/h for 30 minutes with an increase of 0.1 km/h and 1 minute per day to a maximum of 5 km/h for 50 minutes. Ten sedentary animals were used as the control group (SED).

5.2.3 Induction of MI

Animals were sedated with ketamine (20 mg/kg, Intramuscularly [IM]) and midazolam (0.5 mg/kg, IM), anesthetized with thiopental (10 mg/kg, intravenously [IV]), intubated and ventilated with O_2/N_2 (1/2 vol/vol) enriched with 0.1-1% (vol/vol) isoflurane (van Kats *et al.*, 2000; van der Velden *et al.*, 2004; Sorop *et al.*, 2008; Duncker *et al.*, 2009). Following a thoracotomy through the fourth left intercostal space, the heart was exposed via a small pericardial incision, the left circumflex artery (LCx) was dissected and a suture was placed around it. Subsequently, the LCx was permanently ligated in 24 swine designated to the MI group (producing a transmural infarction in the lateral wall encompassing ~25% of the left ventricle (van Kats *et al.*, 2000)), while the suture was removed in the 20 swine designated to the sham group (SHAM) (van Kats *et al.*, 2000; van der Velden *et al.*, 2004; Duncker *et al.*, 2009). Then the pericardium and the chest were closed and animals were allowed to recover, receiving analgesia (0.3 mg buprenorphine IM) for 2 days and antibiotic prophylaxis (25 mg/kg amoxicillin and 5 mg/kg gentamycin IV) for 5 days.

5.2.4 Echocardiography and hemodynamic measurements

At the end of the study period, animals were sedated with ketamine (20 mg/kg, IM) and midazolam (0.5 mg/kg, IM) and underwent echocardiography for the determination of LV end-diastolic cross-sectional area (EDA) and end-systolic cross-sectional area (ESA) (van Kats *et al.*, 2000; van der Velden *et al.*, 2004; Duncker *et al.*, 2009). 2D ejection fraction was calculated as $100 \cdot (EDA-ESA)/EDA$ %. After induction of anesthesia with pentobarbital (10-15 mg/kg per hour IV) swine were instrumented for measurement of hemodynamics (van Kats *et al.*, 2000; van der Velden *et al.*, 2004; Duncker *et al.*, 2009). After completion of all

measurements, animals underwent a sternotomy; the heart was arrested and immediately excised. The LV was divided into subendocardial and subepicardial tissue from the anterior, lateral, posterior and septal area of the left ventricle wall and cardiac tissue was snap-frozen in liquid nitrogen (i.e. within 3-5 min of excising the heart) and stored at -80 °C. For protein and RNA analysis, subendocardial tissue from the anterior wall was used, which in MI animals is the remote non-infarcted area.

5.2.5 Total RNA isolation

RNA was extracted from LV tissue from eight EX, eight SED, eight MI and eight SHAM animals (four males and four females per group). Frozen tissue samples were pulverized in liquid N_2 with a mortar and pestle and TRI Reagent (Invitrogen, Carlsbad, CA, USA) was added immediately to the powder. RNA was isolated according to manufacturer's instructions. RNA was cleaned with RNeasy clean-up kit (Qiagen, Valencia, CA, USA). Purity and quality of isolated RNA were assessed by RNA 6000 Nano assay on a 2100 Bioanalyzer (Agilent Technologies, Santa Clara, CA, USA). All samples showed a RNA integrity number >8.

5.2.6 Microarray analysis

Microarray analysis of the EX and SED animals was performed simultaneously with the MI and SHAM animals. RNA (3 µg) from each animal was used for subsequent synthesis of biotinylated cRNA. Labeled cRNA was hybridized to the GeneChip Porcine Genome Array (Affymetrix, Santa Clara, CA, USA) according to the manufacturer's instructions. The Affymetrix QC reports showed high quality of the samples and arrays, indicated by percentage of present calls, noise, background, and by a 3':5' signal ratio for glyceraldehyde-3-phosphate dehydrogenase mRNA of <1.4.

Raw intensity values of all samples were normalized in R (http://www.r-project.org). The data were corrected for variability across batches and arrays by quantile normalization according to experimental group, followed by Robust Micro-array Average normalization, using the Affy package developed by Bioconductor (Gentleman *et al.*, 2004). The normalized expression values were loaded into Partek genomic suite (Partek Inc, St. Louis, MO, USA) and multivariate principal component analysis (PCA) was performed (Ringner, 2008).

The class comparison tool of BRB-ArrayTools software (http://linus.nci.nih.gov/BRB-ArrayTools.html) was used for generation of lists of differentially expressed (DE) genes (Simon *et al.*, 2007). Genes were considered significantly different at false discovery rate (FDR) < 0.05. Because the annotation of the porcine genechip is far from complete, the annotation of ANEXdb (Couture *et al.*, 2009) was used. This open source application aligns Affymetrix porcine GeneChip target sequences to the Iowa Porcine Assembly, which is an assembly of all publicly available porcine-expressed consensus sequences. This was

subsequently aligned to the NCBI RefSeq RNA database, to give the homologous human RefSeq IDs .

5.2.7 TF binding site analysis

The genomic sequences of the human homologues of the DE genes were selected, and regions between 500 bp upstream and 100 bp downstream of the transcription start site were searched for putative TFBS using F-match implemented in the Explain Analysis System (Biobase GmbH, Wolfenbüttel, Germany) (Kel *et al.*, 2006; Kel *et al.*, 2008). The rationale for searching DE genes for common TFBS is the assumption that co-expressed genes are coordinately regulated by a limited set of TFs. Promoter regions of the DE genes were scanned for so-called positional weight matrices (Kel *et al.*, 2006), constructed from collections of known binding sites for a given TF. Promoter regions were searched using the entire vertebrate non-redundant set of transcription factors matrix from the TRANSFAC database (Wingender *et al.*, 2000). We compared upregulated versus downregulated genes to identify TFBS overrepresented in the promoter regions of upregulated genes, and downregulated versus upregulated genes to identify TFBS overrepresented in the promoters of downregulated genes (Kuster *et al.*, 2011b). Overrepresentation was determined using a one-tailed Fisher exact probability test and considered significant when more than 1.5-fold and at $p < 0.01$.

5.2.8 Protein/DNA array

With the protein/DNA array (Combo array, Panomics/Affymetrix, Milan, Italy), nuclear protein extracts were semi-quantitatively assayed by DNA binding activity for 345 TFs. Nuclear protein extracts were prepared from LV tissue as previously described (Kuster *et al.*, 2011a). Protein/DNA array analysis was performed according to the manufacturer's instructions. Briefly, nuclear protein extracts from four animals per group were pooled, and 5 µg protein of each pool was used for binding to a mix of biotin-labeled TF-specific DNA probes in solution. Subsequently, all unbound DNA probes were washed away. The TF-bound probes were denatured and then hybridized to the array membrane. After addition of streptavidin-HRP, signals were generated by enhanced chemiluminescence (ECL) and exposure to Hyperfilm ECL (Amersham Biosciences, Piscataway, NJ, USA). Various exposure times were used to obtain signals over a large dynamic range. Signal intensities were quantified using a Bio-Rad calibrated GS-800 scanner and Quantity One software (Bio-Rad, Hercules, CA, USA). Only non-saturated signals were used for further analysis. TF binding activity was considered significant when at least 2-fold signal difference between nuclear protein pools.

5.2.9 Ingenuity Pathway analysis

Ingenuity Pathway Analysis (Ingenuity Systems, Redwood City, CA, USA) was performed to explore the biological functions and molecular networks of the DE genes, using the human Refseq IDs as input. Biological groups were identified with which the DE genes were significantly associated ($p<0.001$). Interconnectivity of DE genes was visualized by construction of molecular networks. In this analysis, networks are constructed by connecting as many DE genes as possible, also allowing for genes with unaltered expression as linking hubs. The TFs from the protein/DNA array were used as input for Ingenuity Pathway Analysis, to link them to genes identified in the microarray analysis. In the 'build' function and with the 'grow' tool, DE genes were linked to the TFs if they were known from the literature to be either regulated by, or to have an experimentally validated binding site for the TFs.

5.2.10 Statistics

Data are presented as mean±SEM. Differences between two groups were analyzed by unpaired Student's *t*-test using GraphPad Prism version 5.01 (GraphPad Software, San Diego, CA, USA). $P<0.05$ was considered to be statistically significant.

5.3 Results

5.3.1 Anatomical and hemodynamical data

In swine that were exercise trained for 4-6 weeks, a 15% increase (p=0.03) in LV weight to body weight ratio was observed compared with sedentary animals (SED), indicative of LV hypertrophy (Table 5.1). This was accompanied by a trend towards a lower heart rate (12%; p=0.08). Cardiac dimensions, as determined by echocardiography in subsets of animals, were not significantly different between EX and SED animals, although end-diastolic dimensions showed a trend towards a 20% increase (p=0.26). Stroke volume index was increased by 36% compared to SED animals (p=0.02). Other hemodynamic parameters including mean aortic and pulmonary artery pressure, heart rate, cardiac output, LV dP/dt_{P40}, tau and LV end-diastolic pressure were not significantly different.

Table 5.1. Anatomic and hemodynamic data

	Sedentary	Exercise training
Anatomical data	*(n = 10)*	*(n = 11)*
BW baseline (kg)	23 ± 2	20 ± 1
BW follow-up (kg)	38 ± 2	35 ± 2
RVW/BW (g/kg)	0.83 ± 0.06	0.98 ± 0.06
LVW/BW (g/kg)	2.63 ± 0.11	3.04 ± 0.13*
Echocardiographical data	*(n = 4)*	*(n = 6)*
LV EDA (mm^2)	898 ± 178	1113 ± 76
LV ESA (mm^2)	340 ± 67	376 ± 90
2D Ejection Fraction (%)	61 ± 3	67 ± 7
Hemodynamical data	*(n = 8)*	*(n = 9)*
MAP (mm Hg)	101 ± 5	93 ± 3
Heart rate (bpm)	126 ± 5	111 ± 6
Cardiac Output (l/min)	3.9 ± 0.1	4.0 ± 0.2
Stroke Volume (ml)	31 ± 2	36 ± 2
Stroke Volume Index (ml/kg)	0.83 ± 0.04	1.12 ± 0.10*
LV dP/dt_{P40} (mm Hg/s)	1661 ± 127	1669 ± 149
Tau (ms)	43 ± 1	45 ± 4
LV EDP (mm Hg)	9.9 ± 1.8	11.2 ± 1.0
MPAP (mm Hg)	19.1 ± 1.8	17.9 ± 1.0

*Values are mean ± SEM. RV and LV, right and left ventricle, respectively; BW, RVW and LVW, body, RV and LV weight, respectively; EDA and ESA, end-diastolic and end-systolic area, respectively; MAP and MPAP, mean aortic and mean pulmonary pressure, respectively; LV dP/dt_{P40}, rate of rise of LV pressure at a pressure of 40 mm Hg. * P<0.05 versus Sedentary*

5.3.2 Microarray analysis

Global differences in LV gene expression between EX and SED swine were determined using microarray analysis. Principal component analysis showed clustering of microarrays based on experimental groups, with principal component 1 clearly separating EX from SED animals (Fig. 5.1A). The first two components together explained 33.6 % of the variability among the 16 different microarrays. There was no apparent clustering based on gender, which is likely due to the use of pre-adolescent female and neutered male pigs. Microarray

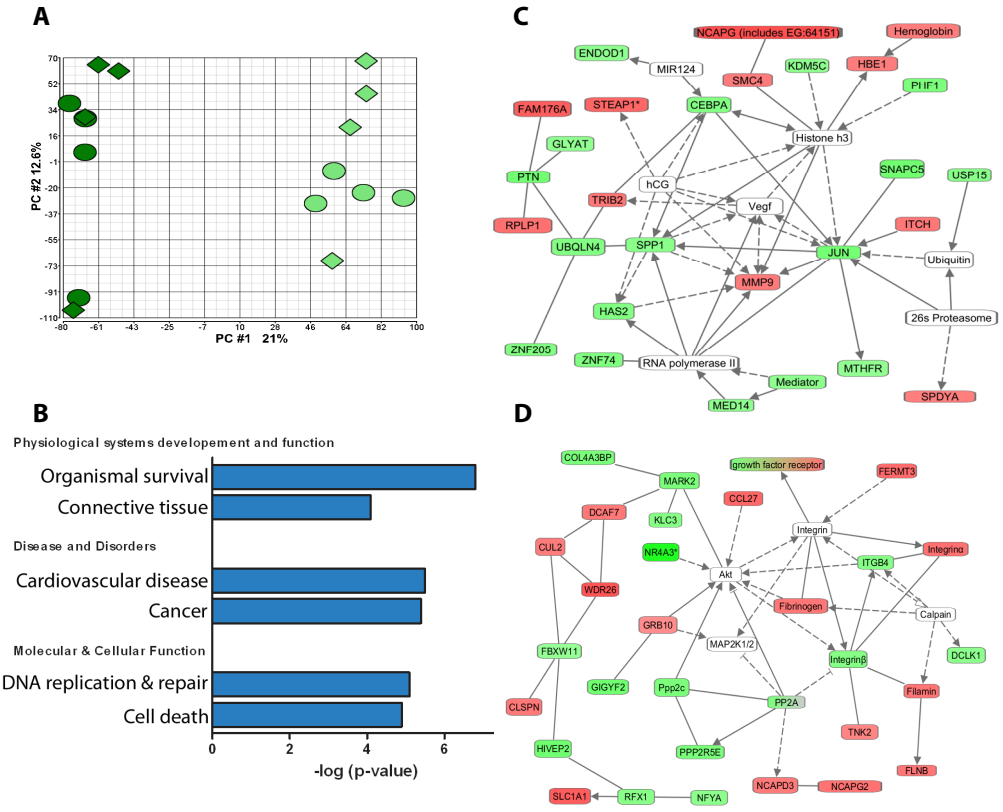

Figure 5.1. Differential gene expression in exercise-induced hypertrophy. *(A) Principal component analysis of the eight EX (dark green) and eight SED (light green) microarrays showed clear clustering according to experimental group. Females (diamonds) and males (circles) do not form separate clusters. (B) Clustering of the DE genes into functional groups; the top two groups in each category are shown. (C & D) The top two networks constructed with Ingenuity Pathway Analysis. Rectangles in green and red represent genes downregulated and upregulated after Ex compared to Sed, respectively. Dual-coloured rectangle depicts a group of genes, some of which are upregulated and some are downregulated after exercise-training. White rectangles are non-changed hub molecules that have a large number of connections with the DE genes. Uninterrupted lines indicate physical interaction between molecules, while dashed lines indicate an indirect, non- physical interaction.*

analysis revealed 339 genes of which the expression was upregulated and 408 that were downregulated in EX compared to SED animals (FDR < 0.05).

To study clustering of the differentially expressed (DE) genes in biological groups, Ingenuity Pathway Analysis was used (Fig 5.1B). Among physiological systems, genes involved in "Organismal survival" and "Connective Tissue" were most significantly overrepresented among DE genes. Related clusters were identified among Diseases and Molecular and Cellular functions. Ingenuity pathway analysis was also used to visualize relationships between the DE genes. In the first network the downregulated JUN and the unaffected angiogenic factor VEGF are central hub molecules (Fig 5.1C). In the second network the protein kinase Akt has a central role (Fig 5.1D), which is in line with the notion that Akt is an important mediator of physiological hypertrophy (DeBosch *et al.*, 2006).

5.3.3 TF binding site analysis

To identify which TFs are involved in the coordinate regulation of DE gene expression, we scanned promoter regions of the homologous human genes for overrepresentation of TF binding sites (TFBS). Seventeen TFBS were identified that were overrepresented in the promoter regions of upregulated genes, and 24 TFBS were found to be overrepresented in downregulated genes (Fold change > 1.5, $P < 0.01$, Table 5.2). The binding site for Myc was the most overrepresented TFBS among the upregulated genes, which is in accordance with the fact that mice in which c-Myc was activated showed hypertrophied hearts without contractile dysfunction (Xiao *et al.*, 2001). TFBS that are most overrepresented in the promoter regions of the downregulated genes bind TFs of the ATF family. Activation of a number of ATF family members is associated with pathological cardiac hypertrophy (Okamoto *et al.*, 2001; Lim *et al.*, 2005). Surprisingly, TFBS for the FOXO family of TFs appear in both lists, but the TFBS overrepresented in upregulated genes is distinct from the TFBS overrepresented in the downregulated genes. The FOXO family is generally associated with atrophy rather than hypertrophy (Ferdous *et al.*, 2010). The overrepresentation of FOXO TFBS in upregulated genes is therefore unexpected and warrants further study.

5.3.4 Protein/DNA array

In addition to the *in silico* analysis, protein/DNA array analysis was performed to directly compare DNA-binding activity of TFs in nuclear protein extracts from EX and SED myocardium. TF-activity was assayed by *in vitro* binding of TF-specific DNA probes to pooled nuclear protein extracts from either EX or SED myocardium. Signals above background were detected in 147 out of the 345 DNA probes in the array. Out of these 147, binding to 23 DNA probes was found to be decreased in EX compared with SED animals

Table 5.2. Transcription factor binding sites overrepresented in upregulated or downregulated genes in exercise-trained versus sedentary swine

Matrix name	Transcription Factor	Up/Down	p-value
V$CMYC_01	c-Myc, N-Myc, Max	3.4	0.002
V$FOXO1_Q5	FOXO1, FOXG1	3.0	0.001
V$FOXP1_01	FOXO4	2.6	0.0009
V$TAL1_Q6	TAL1	2.5	0.005
V$GATA1_05	GATA1-6	2.5	0.004
V$LMO2COM_01	LMO2	2.4	0.0001
V$HIF1_Q5	HIF-1A	2.3	0.0005
V$NUR77_Q5	NR4A1	2.3	0.002
V$E47_02	MRF2, MASH-1, Myf5/6, MyoD, Myogenin, HTF4γ, E47,E12,ITF1/2	2.3	0.004
V$USF_C	USF1/2b	2.2	0.005
V$NURR1_Q3	NR4A2	2.2	0.007
V$HNF1_Q6	HNF1A/B	1.8	0.01
V$EBF_Q6	EBF1/3	1.8	0.007
V$CDC5_01	CDC5L	1.6	0.007
V$CP2_02	TFCP2	1.6	0.007
V$DELTAEF1_01	ZEB1	1.6	0.0027
V$OCT1_04	POU2F1	1.6	0.00001
V$ATF_01	ATF5	−4.1	0.00001
V$CREBATF_Q6	ATF1/3/4/6/7, CREM, CREB1	−3.2	0.001
V$E4F1_Q6	E4F1	−3.2	0.0004
V$PLZF_02	PLZFB	−3.2	0.0004
V$ATF3_Q6	c-Jun, ATF2	−3.1	0.002
V$XFD2_01	P300, MEIS2, RRN3, SMAD2, TGIF1	−2.9	0.004
V$HEN1_02	HEN1	−2.6	0.005
V$YY1_Q6_02	YY1	−2.6	0.003
V$HSF1_01	HSF1/2	−2.5	0.0009
V$TATA_01	TBP	−2.4	0.009
V$FREAC4_01	FOXC1/D1/D3/F1/F2/H1/I1/J1/J2/L1/O1/O3/O4	−2.3	0.006
V$PPARG_02	PPARG	−2.3	0.005
V$PAX_Q6	PAX2-6/8	−2.2	0.0009
V$CMYB_01	MYB,MYBL2	−2.2	0.007
V$HMEF2_Q6	MEF2A/C/D	−2.1	0.006
V$RFX1_02	RFX1	−1.8	0.008
V$PR_02	PR A, PR B	−1.8	0.007
V$GRE_C	GR (NR3C1)	−1.8	0.0003
V$RFX_Q6	RFX2-5, RFXANK, RFXAP	−1.7	0.008
V$AP1_Q4	FOS, FOSB/L1/L2, JUNB/D, SMAD3	−1.7	0.007
V$CHX10_01	VSX2	−1.7	0.002
V$MEIS1AHOXA9_01	HOXA9, MEIS1	−1.7	0.004
V$IK2_01	IKZF1	−1.7	0.009

(fold change > 2, Table 5.3). A specific TF or family of TFs has been assigned to 19 of these probes. Surprisingly, no TF was identified with increased DNA-binding activity in EX compared with SED animals.

Ingenuity pathway analysis was performed to link the 19 TFs identified from the protein/DNA array to the DE genes from the microarray analysis (Fig 5.2). Eleven of these have been implicated directly or indirectly in regulation of expression of multiple DE genes, while the other 8 had no links to the DE genes based on literature information. YY1, CEBPA, GR and HNF1A all have 10 or more links to the DE genes, which might be an indication of their importance in physiological hypertrophy. Notably, CEBPA is one of the downregulated genes in the microarray analysis (fold change -1.4; FDR=0.0006), and its DNA-binding activity is also found to be reduced in the EX animals.

Five TFs were identified both in the TFBS and the protein/DNA array analysis. Two of these, TFCP2 and HNF1a, had TFBS overrepresented in the promoter regions of upregulated genes, but decreased DNA-binding activity according to the protein-DNA array. This could be explained if they were repressors of transcription, but both TFCP2 (Veljkovic & Hansen, 2004) and HNF1a (Pontoglio *et al*., 1996) are generally considered activators of gene expression. Three TFs, YY1, GR and PAX6, had decreased DNA-binding activity according to the protein-DNA array, and their TFBS were correspondingly overrepresented in promoter regions of downregulated genes.

Table 5.3: Protein/DNA array analysis

Probe name	Transcription factor	Ratio Ex/Sed
ACPBP	HIVEP1 [1]	–11.6
HOX4C	HOXD9	–11.0
MEF-3	GATA4 [2]	–10.6
Skn	POU2F3	–10.4
MBP-1	HIVEP1	–8.6
Ets	ETS1 & ETS2	–7.3
Cdx-2	CDX2	–6.3
PBGD BP	YY1	–5.8
NF-1/L	-	–5.7
LSF	TFCP2	–5.7
NF-Atp	NFATc2	–5.7
HNF-1A	HNF-1A	–5.5
MSP-1	-	–5.2
CEBP	CEBPA	–5.2
PEPCK PR	GR	–5.1
EGR-1	EGR1	–5.0
HFH-11B/11a	FOXM1	–5.0
HiNF/D3	CUX1 [3]	–4.9
PAX-6	PAX6	–4.6
PEBP-2	-	–4.2
Transferrin BP	FOXA1 [4]	–3.8
HOXD-8/9/10	HOXD8/9/10	–3.5
HFH-1	FOXQ1	–3.0

[1] HIVEP1 is the most likely candidate to bind to the ACPBP binding element (Brady et al., 1995); [2] GATA4 is the most likely candidate to bind to the MEF-3 element (Ip et al., 1994); - no candidate TF identified; [3] CUX1 most likely candidate to bind to the HiNF/D3 element (van Wijnen et al., 1996); [4] FOXA1 is the most likely candidate to bind to the Transferrin BP element (Auge-Gouillou et al., 1993)

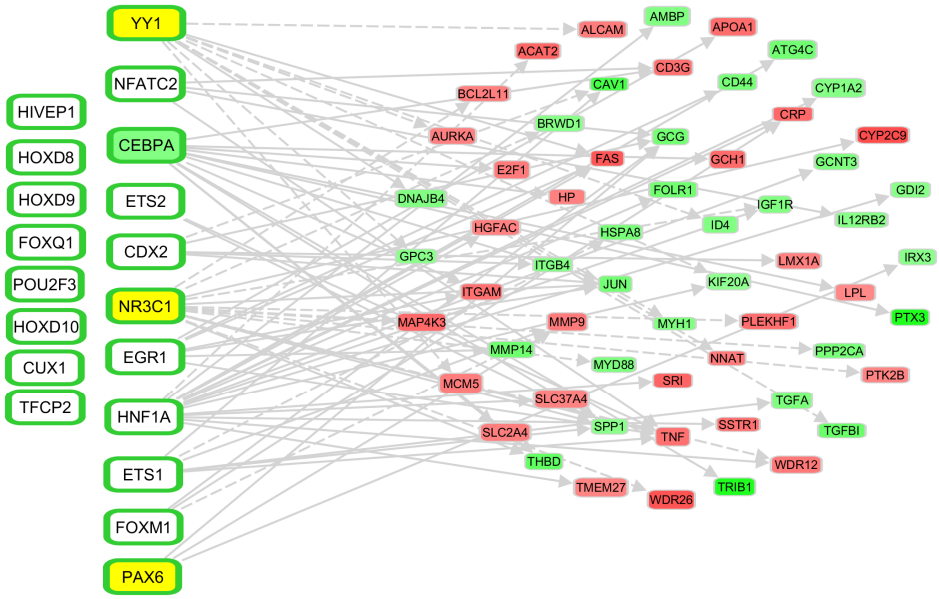

Figure 5.2. Linking of TFs identified by protein/DNA array to DE genes. TFs that show less (green outline) DNA-binding activity in Ex LV tissue are depicted at the left and are connected by IPA with upregulated (red) and downregulated (green) genes depicted on the right. TFs in yellow were identified in both protein/DNA array and TFBS analysis. CEBPA is green, because its expression at the mRNA level was downregulated in Ex compared with Sham. A line was drawn between a TF and a gene if it was known from the literature that the TF can cause the expression of the gene. Uninterrupted and dashed lines indicate physical and indirect interactions between TF and target gene.

5.3.5 Anatomical and functional differences between physiological and pathological hypertrophy

Subsequently, we compared the changes observed in physiological hypertrophy with changes observed in pathological hypertrophy in swine following MI (Kuster *et al.*, 2011). While the LV to body weight ratio was similarly increased after EX and MI by 15% and 18% compared to their respective control groups (Fig 5.3A), there were striking differences in other structural and functional parameters. In contrast to EX, MI led to marked LV dilation, as illustrated by an increased end-diastolic area (Fig 5.3B), to a decrease in the 2D ejection fraction (Fig 5.3C) and a decrease in LV dP/dt_{P40} (Fig 5.3D). Conversely, an increase in stroke volume index was only apparent in physiological hypertrophy (Fig 5.3E).

5.3.6 Gene expression in physiological versus pathological hypertrophy

Principal component analysis of the variability among the 32 microarrays showed that the four groups of eight animals (SED, EX, MI, SHAM) each had clearly distinct gene expression

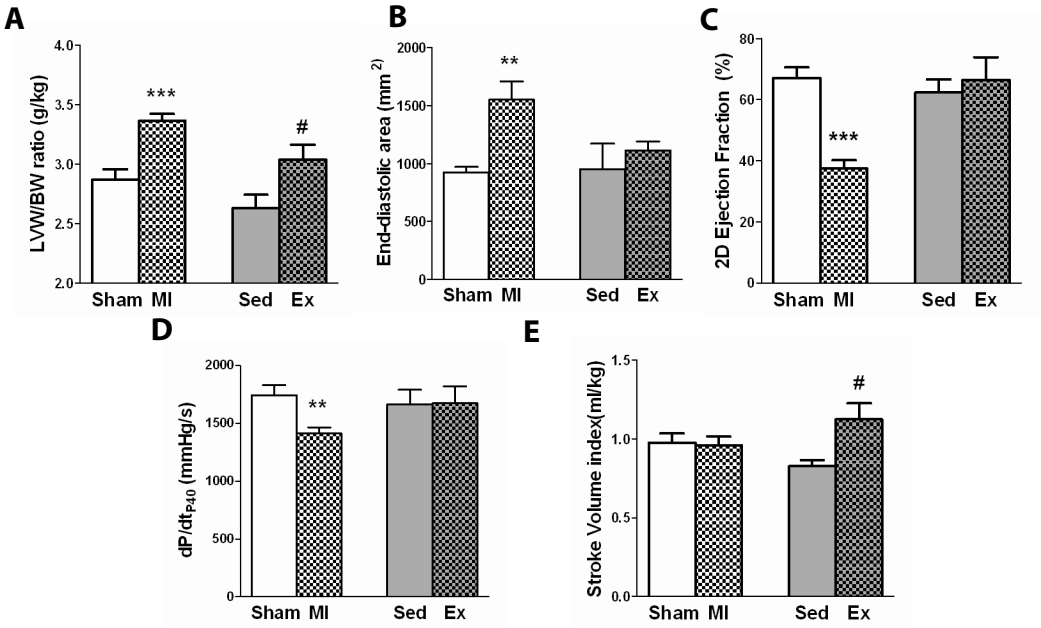

***Figure 5.3*. Comparison of the effects of a pathological and physiological stimulus on cardiac remodeling and function.** *Sham (n=20), MI (n=23), Sed (n=10) and Ex (n=11) animals were studied. (A) LVW/BW ratios. (B) LV end-diastolic area. (C) LV 2D-Ejection Fraction. (D) LV dP/dt_{P40} and (E) Stroke volume index. *P<0.05, **P<0.01; ***P<0.001 MI vs.sham; #P<0.05 EX vs SED. Data are mean ±SEM.*

patterns (Fig 5.4A). The first three components explained 30.2% of the variability among microarrays. Of the four groups, MI and EX animals clustered most closely together. SHAM and SED groups clustered quite far apart, stressing the necessity to compare expression patterns of MI with SHAM animals, and EX with SED animals. The differences and overlap in gene expression following exercise-training or MI are illustrated in Figure 5.4B. Of the 1091 affected genes, 912 (84%) had only changed either in MI or Ex animals. Only 46 genes were upregulated both in MI and EX animals, and 46 genes were downregulated in both groups compared to their respective controls. These may be considered to represent general hypertrophic genes. In the network that was constructed based on the 92 overlapping genes, these were mainly coupled through NF-κB and MAPKs such as JNK and p38 (Fig 5.4C).

The expression of 87 genes was oppositely regulated after MI or EX. Forty-four genes were found to be upregulated after MI, but downregulated after exercise-training, and 43 genes *vice versa* (Fig 5.4B). These genes potentially discriminate between pathological and physiological hypertrophy. They include MMP14 (also known as MT1-MMP), which is upregulated after MI, but downregulated in EX animals. MMP-14 has been

associated with adverse cardiac remodeling in a murine post-MI model (Spinale *et al.*, 2010). In the network that was constructed based on these 87 genes, the main hubs again proved to be NF-κB and MAPKs, but now ERK1/2, rather than JNK or p38 (Fig 5.4D).

Networks were also constructed for genes upregulated or downregulated exclusively in either the physiological or pathophysiological hypertrophy model. Similar to figure 5.1C, the network built from DE genes specific for physiological hypertrophy had Akt as a hub molecule, but now also the pro-apoptotic cytochrome c and caspases became prominent (Fig 5.5A). Similar to our previous report on post-MI remodeling of swine heart (Kuster *et al.*, 2011b), the network built from exclusively pathological hypertrophy genes had the inflammatory mediator NF-κB and the pro-hypertrophic phosphatase calcineurin as central hub molecules (Fig 5.5B).

5.3.7 Overlap and differences in TFs involved in both forms of hypertrophy

Five TFBS were overrepresented in genes upregulated in both MI and Ex animals compared to their respective controls, and five TFBS were found to be overrepresented in genes downregulated both in MI and in Ex animals (Table 5.4). Three TFs were found to be decreased in DNA binding activity in nuclear extracts from both MI and Ex. If the TFs that bind to the overrepresented TFBS, and TFs identified from the protein-DNA array play a role in cardiac remodeling, they are presumably activated or inactivated as part of a general hypertrophic response.

There were also a number of TFs that were activated after EX but inactivated after MI, or *vice versa*. Only one TFBS, i.e. GATA1-6, was overrepresented in genes upregulated in EX animals and downregulated post-MI. Two TFBS, i.e. GRE and AP1, were overrepresented in genes downregulated in EX and upregulated after MI. Five TFs, among which the glucocorticoid receptor (GR) and PAX6, showed reduced DNA-binding activity in EX hearts but increased activity post-MI.

5.4 Discussion

To our knowledge this is the first time changes in gene expression upon physiological hypertrophy of the left ventricle have been studied in a large animal model in an unbiased and integrative fashion. We carried out gene expression profiling in EX swine, and compared that with SED animals. Subsequently, we assessed the TFs that are responsible for the differential expression of these genes, by TFBS as well as protein/DNA array analysis. A number of interesting candidate TFs were identified whose activities in nuclear protein extracts were downregulated, i.e. YY1, GR and PAX6. The genetic reprogramming and the TFs involved during this form of hypertrophy were then compared to the changes that

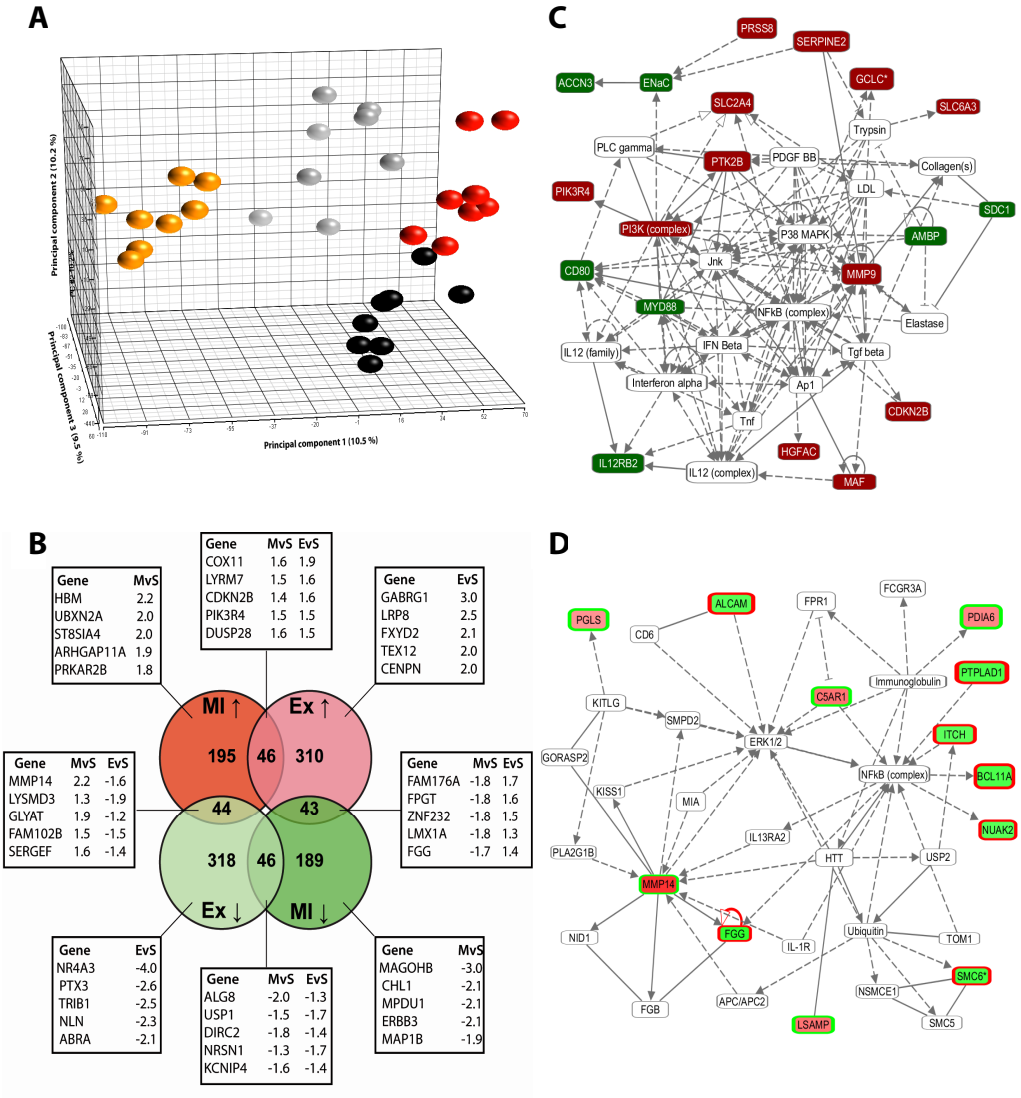

Figure 5.4. Differences and overlap in gene expression after a physiological and pathological hypertrophic stimulus. *(A) Principal component analysis clearly separated the microarrays of the four experimental groups. Principal component 1 separates Exercise (red) from Sedentary (yellow) while principal component 3 separates MI (black) from Sham (grey). (B) Changes in gene expression in MI vs Sham (MvS) and Ex vs Sed (EvS), with fold changes given for the top 5 genes of each subgroup. (C) Network constructed from the genes that were regulated in parallel in EX and MI (dark red, upregulated; dark green, downregulated genes) relative to the respective controls. (D) Network constructed from the genes that were oppositely regulated in EX and MI (green with red outline, up in EX and down in MI; red with green outline, down in EX and up in MI).*

occur in the remote area of the left ventricle after MI, a well-established cause of pathological hypertrophy. LV hypertrophy, as deduced from the increase in LV weight to body weight ratio was similar in both types of hypertrophy. Other indices of LV remodeling, such as LV dilation, ejection fraction, and cardiac contractility and stroke volume index, were strikingly different, in accordance with the expected differences between physiological and pathological hypertrophy. There was little overlap in differentially expressed genes between both forms of hypertrophy. A number of TFs were similarly activated or inactivated in both forms of hypertrophy and were assumed to be part of a general hypertrophic pathway. Another group of TFs was differentially regulated following EX or MI, with GR and PAX6 as the most striking examples.

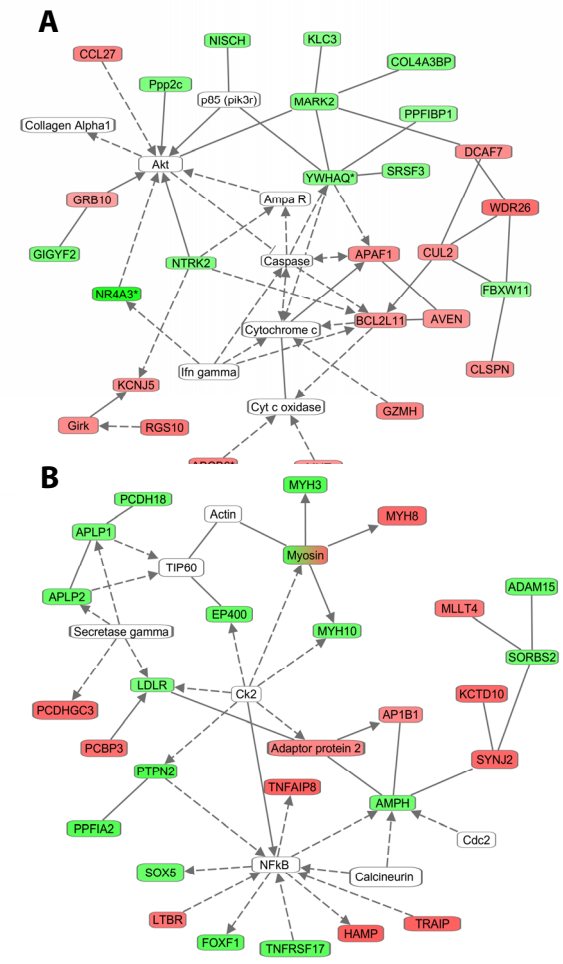

Fig 5.5. Networks constructed of exclusive physiological or pathological hypertrophy genes. *Networks were constructed of genes of which expression is affected exclusively in either physiological (A) or pathological (B) hypertrophy relative to respective controls. Rectangles in green and red represent genes downregulated and upregulated after exercise-training versus sedentary (A), or after MI compared with sham (B). The dual-coloured rectangle depicts a group of genes, some of which are upregulated and some are downregulated after MI. White rectangles are hub molecules, of which the expression is not altered, but that generally have a large number of connections with the DE genes. Uninterrupted and dashed lines indicate physical and indirect interactions between molecules.*

5.4.1 Physiological hypertrophy

To study the molecular and physiological mechanisms

underlying physiological hypertrophy, various animal models and hypertrophy stimuli are used (Wang *et al.*, 2010). The majority of studies involve mice and treadmill running, voluntary wheel running or swim training. The amount of hypertrophy is generally limited, with the biggest effect seen with chronic swim training (Wang *et al.*, 2010). Larger animal

Table 5.4: Comparison of TFs involved in exercise-training and MI-induced hypertrophy

	Matrix/probe	**Transcription factor**
Up in Ex & MI		
TFBS	V$CMYC_01	c-Myc, N-Myc, Max
	V$FOXP1_01	FOXO4
	V$LMO2COM_01	LMO2
	V$USF_C	USF1/2b
	V$E47_02	MRF2, MASH-1, Myf5/6, MyoD, Myogenin, HTF4γ, E47,E12,ITF1/2
PD array	-	-
Down in Ex & MI		
TFBS	V$ATF_01	ATF5
	V$CREBATF_Q6	ATF1/3/4/6/7, CREM, CREB1
	V$YY1_Q6_02	YY1
	V$FREAC4_01	FOXC1/D1/D3/F1/F2/H1/I1/J1/J2FOXL1/O1/O3/O4
	V$CMYB_01	MYB,MYBL2
PD array	MEF-3	GATA4 [1]
	LSF	TFCP2
	CEBP	CEBPA
Down in Ex, up in MI		
TFBS	V$GRE_C	**GR (NR3C1)**
	V$AP1_Q4	FOS, FOSB/L1/L2, JUNB/D, SMAD3
PD array	ACPBP	HIVEP1 [2]
	HNF-1A	HNF-1A
	MSP-1	
	PEPCK PR	**GR (NR3C1)**
	PAX-6	PAX6
Up in Ex, down in MI		
TFBS	V$GATA1_05	GATA1-6
PD array	-	-

[1] GATA4 is the most likely candidate to bind to the MEF-3 element (Ip et al., 1994); [2] HIVEP1 is the most likely candidate to bind to the ACPBP binding element (Brady et al., 1995)

models, which more closely emulate human cardiovascular physiology, have also been used to study physiological hypertrophy, most notably dogs and swine exercise-trained on treadmills. An extended period of exercise training in swine results in cardiac hypertrophy (White *et al.*, 1987a; Laughlin *et al.*, 1991), as well as increased coronary blood flow capacity (Duncker & Bache, 2008), decreased heart rate (Laughlin *et al.*, 1991) and increased stroke volume (White *et al.*, 1987a). In the present study , a protocol of 4-6 weeks exercise-training in adolescent and neutered pigs resulted in a 16% increase in LV weight to body weight ratio and a 35% increase in stroke volume index, whereas heart rate showed a trend towards lower values, respectively.

To date, gene expression profiling studies of heart tissue after exercise training have only been performed in rodents (Diffee *et al.*, 2003; Kong *et al.*, 2005; Strom *et al.*, 2005; Iemitsu *et al.*, 2005; Galindo *et al.*, 2009; Beisvag *et al.*, 2009). Changes in gene expression mainly occurred in genes associated with fatty acid or glucose metabolism (Kong *et al.*, 2005; Strom *et al.*, 2005), or in genes associated with cellular growth and organismal survival (Kong *et al.*, 2005; Galindo *et al.*, 2009). In our analysis, organismal survival was the top biological function in which the differentially expressed genes clustered. Galindo *et al.* compared a number of studies in which gene expression profiling was performed in several mouse and rat models of physiological hypertrophy, and identified a set of 57 genes as common to physiological hypertrophy (Galindo *et al.*, 2009). Of this set of common genes, only three genes are also present in our dataset from swine, i.e. protein phosphatase 2 regulatory subunit (PP2R), c-reactive protein (CRP) and a disintegrin and metalloprotease domain 19 (ADAM19). Similar to the murine models, CRP was upregulated and PP2R and ADAM19 were downregulated in LV tissue after exercise-training. The role of ADAM19 in hypertrophy is not clear, but PP2R is a negative regulator of Akt (Beaulieu *et al.*, 2005), a kinase that is central to physiological hypertrophy signaling (McMullen *et al.*, 2003; DeBosch *et al.*, 2006). CRP is also associated with physiological hypertrophy, as the serum CRP level is correlated with increased LV growth after exercise-training in humans (Mann *et al.*, 2010).

5.4.2 TFs in physiological hypertrophy

To identify TFs that drive the changes in gene expression in physiological hypertrophy, we combined *in silico* scanning of the promoters of the DE genes for common TFBS with protein/DNA array analysis. This yielded three TFs that had matching results in both datasets, i.e. YY1, GR and PAX6. The binding sites for all three TFs were overrepresented in genes that were downregulated in EX swine, and all three had lower DNA-binding activity in the LV nuclei of EX swine compared to SED controls. YY1 levels and DNA-binding activity have been shown to be increased in failing human hearts (Sucharov *et al.*, 2003), although this might be a protective mechanism as YY1 is also reported to protect against pathological hypertrophy (Sucharov *et al.*, 2008). PAX6 has mainly been described in eye

development, while its role in the heart remains unclear. The decreased DNA-binding activity of GR and overrepresentation of GR binding sites in downregulated genes observed in physiological hypertrophy in swine is interesting, as opposite changes occur in swine heart after a myocardial infarction (Kuster *et al.*, 2011b). The role of GR in physiological hypertrophy is incompletely understood. In a high intensity exercise training model, rats were found to have reduced serum cortisol levels and an increased cytosolic GR expression as measured by [^{3}H]-dexamethasone binding (Hickson *et al.*, 1984). Blockade of this receptor in hypertrophy post-MI with mifepristone led to an attenuated hypertrophic response (Kuster *et al.*, 2011b).

5.4.3 Physiological versus pathological hypertrophy

Differential gene expression between physiological and pathological hypertrophy has been studied in mice (Galindo *et al.*, 2009) and rats (Kong *et al.*, 2005; Strom *et al.*, 2005; Beisvag *et al.*, 2009). As in swine, overlap in gene expression profiles between the pathological and physiological hypertrophy was relatively small (Kong *et al.*, 2005; Galindo *et al.*, 2009; Beisvag *et al.*, 2009). Comparison of exercise-training with high-salt diet-induced pathological hypertrophy showed that insulin signaling and protein synthesis-related genes were overrepresented in the former, and apoptosis-related genes were overrepresented in the latter form of hypertrophy (Kong *et al.*, 2005). While insulin signaling was not significantly overrepresented in EX swine, phosphoinositide-3-kinase regulatory subunit 4 (PIK3R4) and PI3K were indeed overrepresented. Immune-response genes were identified as an overrepresented category in isoprotenerenol-induced pathological but not in swimming-exercise induced physiological hypertrophy in mice (Galindo *et al.*, 2009). We also observed genes associated with the immune response in post-MI swine (Kuster *et al.*, 2011b). Beisvag *et al.* compared gene expression in rats following coronary artery ligation with treadmill exercise and observed reduced expression of genes involved in fatty acid oxidation in pathological hypertrophy (Beisvag *et al.*, 2009). In our EX swine, changes in lipid metabolism genes were not evident, whereas in our post-MI swine, lipid metabolism was one of the important clusters of differentially expressed genes (Kuster *et al.* 2011b). Hence, many but not all differences in gene expression between physiological and pathological cardiac hypertrophy reported in rodent models could also be observed in swine.

Surprisingly, NF-κB was found as hub molecule in both networks constructed of the genes regulated in parallel (Fig 5.4C) and oppositely in Ex and MI animals (Fig 5.4D). This might be due suboptimal network building due to the relatively low number of selected genes, or to publication bias, as NF-κB is an intensively studied protein with consequently many possible links to other proteins. Hence, networks built from few genes should be interpreted with caution. Although MAPKs were also prominent hubs in both networks, p38 and Jnk dominate in the former, and ERK1/2 in the latter network.

5.4.4 Methodological considerations

Pigs have a clear advantage over rodent models for studying cardiovascular physiology as they resemble humans more closely in terms of heart rate and cardiac contractility and autonomic control thereof (Hasenfuss, 1998; Dixon & Spinale, 2009), as well as myofilament protein composition and function (Hamdani *et al.*, 2008), and calcium homeostasis (Haghighi *et al.*, 2003). A drawback of using pigs to study transcriptional genomics is that its genome has not yet been fully sequenced, which leads to methodological challenges such as poor microarray annotation and inability to perform TFBS analysis. With the ANEXdb the annotation of the porcine microarray has been vastly improved (Couture *et al.*, 2009). The output is the human homologue of the porcine gene, which can then be used for TFBS analysis or network analysis. Not every TFBS is unique for a single TF. Hence, experimental validation of the TFs is important. The protein/DNA array directly measured the DNA-binding activity of TFs, but an inherent limitation of the protein/DNA array is that only a selection of TFs is analyzed. By combining the two data sets, we circumvented these limitations and improved the reliability of the identification of TFs. Overcoming these experimental challenges is rewarded by gaining insight into cardiac remodeling in a large animal model with even better translational potential than murine models.

In this study we chose 4-6 weeks of exercise training as a model for physiological cardiac remodeling, to compare with post-MI, pathological remodeling, as both models gave a similar degree of LV hypertrophy as based on the increase in LV weight to body weight ratio. It should be noted however that in contrast to the EX hearts, approximately 20% of cardiac tissue in the post-MI hearts is lost due to the MI and has been replaced by scar tissue. Hence, the relative LV weight slightly underestimates the degree of hypertrophy of remote surviving myocardium in the post-MI heart. Nevertheless, the number of differentially expressed genes was higher in the model for physiological than for pathological cardiac remodeling.

5.5.5 Conclusions

In the present study, we used an unbiased approach to identify TFs that may mediate genetic reprogramming in physiological LV hypertrophy. We combined *in silico* TFBS analysis of microarray data with protein/DNA array analysis of nuclear protein extracts from LV tissue of EX swine. The results were then compared with the changes occurring in a post-MI model of pathological hypertrophy. Besides TFs and genes that were similarly affected in both forms of cardiac remodeling, and likely represent a common hypertrophic response, we observed 5 TFs and 87 genes that were oppositely regulated in physiological versus pathological hypertrophy. These TFs and genes may therefore discriminate physiological

from pathological forms of LV hypertrophy. In particular, the activity of the glucocorticoid receptor was increased in post-MI and decreased in exercise-induced cardiac remodeling. In a previous study (Kuster *et al.*, 2011b) we have shown that treatment of swine with a glucocorticoid receptor agonist partially reversed post-MI induced LV hypertrophy. There is clinical evidence that MI patients benefit from EX. The results of our study could be interpreted to suggest that EX after MI might partially reverse genetic programming in the remote, non-infarcted area of the heart. The TFs that are oppositely regulated during post-MI and exercise-induced cardiac remodeling may be potential pharmacologic targets to improve recovery after MI and prevent progression towards heart failure. These targets should be the subject of future studies.

5.6 References

Auge-Gouillou C, Petropoulos I, & Zakin MM (1993). Liver-enriched HNF-3 alpha and ubiquitous factors interact with the human transferrin gene enhancer. *FEBS Lett* **323**, 4-10.

Beaulieu JM, Sotnikova TD, Marion S, Lefkowitz RJ, Gainetdinov RR, & Caron MG (2005). An Akt/beta-arrestin 2/PP2A signaling complex mediates dopaminergic neurotransmission and behavior. *Cell* **122**, 261-273.

Beisvag V, Kemi OJ, Arbo I, Loennechen JP, Wisloff U, Langaas M, Sandvik AK, & Ellingsen O (2009). Pathological and physiological hypertrophies are regulated by distinct gene programs. *Eur J Cardiovasc Prev Rehabil* **16**, 690-697.

Bernardo BC, Weeks KL, Pretorius L, & McMullen JR (2010). Molecular distinction between physiological and pathological cardiac hypertrophy: experimental findings and therapeutic strategies. *Pharmacol Ther* **128**, 191-227.

Brady JP, Kantorow M, Sax CM, Donovan DM, & Piatigorsky J (1995). Murine transcription factor alpha A-crystallin binding protein I. Complete sequence, gene structure, expression, and functional inhibition via antisense RNA. *J Biol Chem* **270**, 1221-1229.

Couture O, Callenberg K, Koul N, Pandit S, Younes R, Hu ZL, Dekkers J, Reecy J, Honavar V, & Tuggle C (2009). ANEXdb: an integrated animal ANnotation and microarray EXpression database. *Mamm Genome* **20**, 768-777.

DeBosch B, Treskov I, Lupu TS, Weinheimer C, Kovacs A, Courtois M, & Muslin AJ (2006). Akt1 is required for physiological cardiac growth. *Circulation* **113**, 2097-2104.

Diffee GM, Seversen EA, Stein TD, & Johnson JA (2003). Microarray expression analysis of effects of exercise training: increase in atrial MLC-1 in rat ventricles. *Am J Physiol Heart Circ Physiol* **284**, H830-H837.

Dixon JA & Spinale FG (2009). Large animal models of heart failure: a critical link in the translation of basic science to clinical practice. *Circ Heart Fail* **2**, 262-271.

Dorn GW (2007). The fuzzy logic of physiological cardiac hypertrophy. *Hypertension* **49**, 962-970.

Duncker DJ & Bache RJ (2008). Regulation of coronary blood flow during exercise. *Physiol Rev* **88**, 1009-1086.

Duncker DJ, Boontje NM, Merkus D, Versteilen A, Krysiak J, Mearini G, El Armouche A, de Beer VJ, Lamers JM, Carrier L, Walker LA, Linke WA, Stienen GJ, & van der Velden J (2009). Prevention of myofilament dysfunction by beta-blocker therapy in postinfarct remodeling. *Circ Heart Fail* **2**, 233-242.

Ferdous A, Battiprolu PK, Ni YG, Rothermel BA, & Hill JA (2010). FoxO, autophagy, and cardiac remodeling. *J Cardiovasc Transl Res* **3**, 355-364.

Frey N & Olson EN (2003). Cardiac hypertrophy: the good, the bad, and the ugly. *Annu Rev Physiol* **65**, 45-79.

Galindo CL, Skinner MA, Errami M, Olson LD, Watson DA, Li J, McCormick JF, McIver LJ, Kumar NM, Pham TQ, & Garner HR (2009). Transcriptional profile of isoproterenol-induced cardiomyopathy and comparison to exercise-induced cardiac hypertrophy and human cardiac failure. *BMC Physiol* **9**, 23.

Gentleman RC, Carey VJ, Bates DM, Bolstad B, Dettling M, Dudoit S, Ellis B, Gautier L, Ge Y, Gentry J, Hornik K, Hothorn T, Huber W, Iacus S, Irizarry R, Leisch F, Li C, Maechler M, Rossini AJ, Sawitzki G, Smith C, Smyth G, Tierney L, Yang JY, & Zhang J (2004). Bioconductor: open software development for computational biology and bioinformatics. *Genome Biol* **5**, R80.

Gielen S, Schuler G, & Hambrecht R (2001). Exercise training in coronary artery disease and coronary vasomotion. *Circulation* **103**, E1-E6.

Haghighi K, Kolokathis F, Pater L, Lynch RA, Asahi M, Gramolini AO, Fan GC, Tsiapras D, Hahn HS, Adamopoulos S, Liggett SB, Dorn GW, MacLennan DH, Kremastinos DT, & Kranias EG (2003). Human phospholamban null results in lethal dilated cardiomyopathy revealing a critical difference between mouse and human. *J Clin Invest* **111**, 869-876.

Hamdani N, de Waard MC, Messer AE, Boontje NM, Kooij V, van Dijk SJ, Versteilen A, Lamberts R, Merkus D, Dos Remedios C, Duncker DJ, Borbely A, Papp Z, Paulus W, Stienen GJ, Marston SB, & van der Velden J (2008). Myofilament dysfunction in cardiac disease from mice to men. *J Muscle Res Cell Motil* **29**, 189-201.

Hasenfuss G (1998). Animal models of human cardiovascular disease, heart failure and hypertrophy. *Cardiovasc Res* **39**, 60-76.

Hickson RC, Galassi TM, Kurowski TT, Daniels DG, & Chatterton RT, Jr. (1984). Androgen and glucocorticoid mechanisms in exercise-induced cardiac hypertrophy. *Am J Physiol* **246**, H761-H767.

Iemitsu M, Maeda S, Miyauchi T, Matsuda M, & Tanaka H (2005). Gene expression profiling of exercise-induced cardiac hypertrophy in rats. *Acta Physiol Scand* **185**, 259-270.

Ip HS, Wilson DB, Heikinheimo M, Tang Z, Ting CN, Simon MC, Leiden JM, & Parmacek MS (1994). The GATA-4 transcription factor transactivates the cardiac muscle-specific troponin C promoter-enhancer in nonmuscle cells. *Mol Cell Biol* **14**, 7517-7526.

Katz AM (2008). The "modern" view of heart failure: how did we get here? *Circ Heart Fail* **1**, 63-71.

Kel A, Voss N, Jauregui R, Kel-Margoulis O, & Wingender E (2006). Beyond microarrays: find key transcription factors controlling signal transduction pathways. *BMC Bioinformatics* **7 Suppl 2:** S13.

Kel A, Voss N, Valeev T, Stegmaier P, Kel-Margoulis O, & Wingender E (2008). ExPlain: finding upstream drug targets in disease gene regulatory networks. *SAR QSAR Environ Res* **19**, 481-494.

Kong SW, Bodyak N, Yue P, Liu Z, Brown J, Izumo S, & Kang PM (2005). Genetic expression profiles during physiological and pathological cardiac hypertrophy and heart failure in rats. *Physiol Genomics* **21**, 34-42.

Kuster DW, Merkus D, Jorna HJ, Dekkers DH, Duncker DJ, & Verhoeven AJ (2011a). Nuclear protein extraction from frozen porcine myocardium. *J Physiol Biochem* **67**, 165-173.

Kuster DW, Merkus D, Kremer A, van IJcken WF, de Beer VJ, Verhoeven AJ, & Duncker DJ (2011b). Left ventricular remodeling in swine after myocardial infarction: a transcriptional genomics approach. *Basic Res Cardiol* ***In press***.

Laughlin MH, Hale CC, Novela L, Gute D, Hamilton N, & Ianuzzo CD (1991). Biochemical characterization of exercise-trained porcine myocardium. *J Appl Physiol* **71**, 229-235.

Levy D, Garrison RJ, Savage DD, Kannel WB, & Castelli WP (1990). Prognostic implications of echocardiographically determined left ventricular mass in the Framingham Heart Study. *N Engl J Med* **322**, 1561-1566.

Lim JY, Park SJ, Hwang HY, Park EJ, Nam JH, Kim J, & Park SI (2005). TGF-beta1 induces cardiac hypertrophic responses via PKC-dependent ATF-2 activation. *J Mol Cell Cardiol* **39**, 627-636.

Mann JJ, Payne JR, Shah T, Pennell DJ, Humphries SE, & Montgomery HE (2010). C-reactive protein gene variant and the human left ventricular growth response to exercise: data from The LARGE Heart Study. *J Cardiovasc Pharmacol* **55**, 26-29.

Maron BJ & Pelliccia A (2006). The heart of trained athletes: cardiac remodeling and the risks of sports, including sudden death. *Circulation* **114**, 1633-1644.

McMullen JR, Shioi T, Zhang L, Tarnavski O, Sherwood MC, Kang PM, & Izumo S (2003). Phosphoinositide 3-kinase(p110alpha) plays a critical role for the induction of physiological, but not pathological, cardiac hypertrophy. *Proc Natl Acad Sci U S A* **100**, 12355-12360.

Okamoto Y, Chaves A, Chen J, Kelley R, Jones K, Weed HG, Gardner KL, Gangi L, Yamaguchi M, Klomkleaw W, Nakayama T, Hamlin RL, Carnes C, Altschuld R, Bauer J, & Hai T (2001). Transgenic mice with cardiac-specific expression of activating transcription factor 3, a stress-inducible gene, have conduction abnormalities and contractile dysfunction. *Am J Pathol* **159**, 639-650.

Pontoglio M, Barra J, Hadchouel M, Doyen A, Kress C, Bach JP, Babinet C, & Yaniv M (1996). Hepatocyte nuclear factor 1 inactivation results in hepatic dysfunction, phenylketonuria, and renal Fanconi syndrome. *Cell* **84**, 575-585.

Ringner M (2008). What is principal component analysis? *Nat Biotechnol* **26**, 303-304.

Simon R, Lam A, Li MC, Ngan M, Menenzes S, & Zhao Y (2007). Analysis of gene expression data using BRB-ArrayTools. *Cancer Inform* **3**, 11-17.

Sorop O, Merkus D, de Beer VJ, Houweling B, Pistea A, McFalls EO, Boomsma F, van Beusekom HM, van der Giessen WJ, VanBavel E, & Duncker DJ (2008). Functional and structural adaptations of coronary microvessels distal to a chronic coronary artery stenosis. *Circ Res* **102**, 795-803.

Spinale FG, Mukherjee R, Zavadzkas JA, Koval CN, Bouges S, Stroud RE, Dobrucki LW, & Sinusas AJ (2010). Cardiac restricted overexpression of membrane type-1 matrix metalloproteinase causes adverse myocardial remodeling following myocardial infarction. *J Biol Chem* **285**, 30316-30327.

Strom CC, Aplin M, Ploug T, Christoffersen TE, Langfort J, Viese M, Galbo H, Haunso S, & Sheikh SP (2005). Expression profiling reveals differences in metabolic gene expression between exercise-induced cardiac effects and maladaptive cardiac hypertrophy. *FEBS J* **272**, 2684-2695.

Sucharov CC, Dockstader K, & McKinsey TA (2008). YY1 protects cardiac myocytes from pathologic hypertrophy by interacting with HDAC5. *Mol Biol Cell* **19**, 4141-4153.

Sucharov CC, Mariner P, Long C, Bristow M, & Leinwand L (2003). Yin Yang 1 is increased in human heart failure and represses the activity of the human alpha-myosin heavy chain promoter. *J Biol Chem* **278**, 31233-31239.

Sutton MG & Sharpe N (2000). Left ventricular remodeling after myocardial infarction: pathophysiology and therapy. *Circulation* **101**, 2981-2988.

van der Velden J, Merkus D, Klarenbeek BR, James AT, Boontje NM, Dekkers DH, Stienen GJ, Lamers JM, & Duncker DJ (2004). Alterations in myofilament function contribute to left ventricular dysfunction in pigs early after myocardial infarction. *Circ Res* **95**, e85-e95.

van Kats JP, Duncker DJ, Haitsma DB, Schuijt MP, Niebuur R, Stubenitsky R, Boomsma F, Schalekamp MA, Verdouw PD, & Danser AH (2000). Angiotensin-converting enzyme inhibition and angiotensin II type 1 receptor blockade prevent cardiac remodeling in pigs after myocardial infarction: role of tissue angiotensin II. *Circulation* **102**, 1556-1563.

van Wijnen AJ, van Gurp MF, de Ridder MC, Tufarelli C, Last TJ, Birnbaum M, Vaughan PS, Giordano A, Krek W, Neufeld EJ, Stein JL, & Stein GS (1996). CDP/cut is the DNA-binding subunit of histone gene transcription factor HiNF-D: a mechanism for gene regulation at the G1/S phase cell cycle transition point independent of transcription factor E2F. *Proc Natl Acad Sci U S A* **93**, 11516-11521.

Veljkovic J & Hansen U (2004). Lineage-specific and ubiquitous biological roles of the mammalian transcription factor LSF. *Gene* **343**, 23-40.

Wang Y, Wisloff U, & Kemi OJ (2010). Animal models in the study of exercise-induced cardiac hypertrophy. *Physiol Res* **59**, 633-644.

White FC, McKirnan MD, Breisch EA, Guth BD, Liu YM, & Bloor CM (1987a). Adaptation of the left ventricle to exercise-induced hypertrophy. *J Appl Physiol* **62**, 1097-1110.

White HD, Norris RM, Brown MA, Brandt PW, Whitlock RM, & Wild CJ (1987b). Left ventricular end-systolic volume as the major determinant of survival after recovery from myocardial infarction. *Circulation* **76**, 44-51.

Wingender E, Chen X, Hehl R, Karas H, Liebich I, Matys V, Meinhardt T, Pruss M, Reuter I, & Schacherer F (2000). TRANSFAC: an integrated system for gene expression regulation. *Nucleic Acids Res* **28**, 316-319.

Xiao G, Mao S, Baumgarten G, Serrano J, Jordan MC, Roos KP, Fishbein MC, & MacLellan WR (2001). Inducible activation of c-Myc in adult myocardium in vivo provokes cardiac myocyte hypertrophy and reactivation of DNA synthesis. *Circ Res* **89**, 1122-1129.

Chapter 6

General discussion & future perspectives

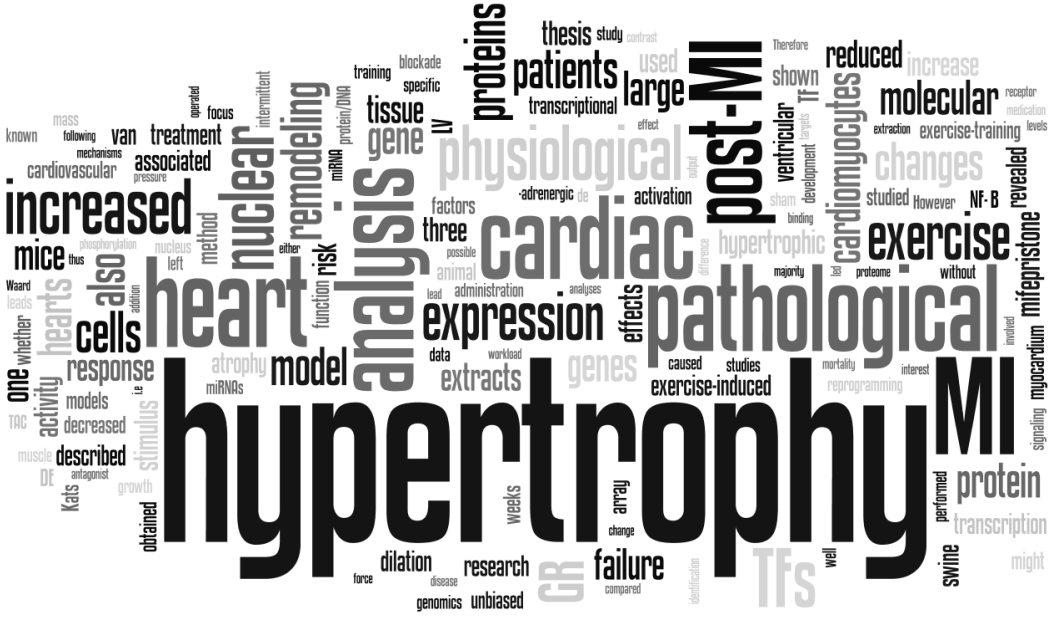

6.1 Summary and general discussion

Adaptation of the heart to increased loading conditions was the subject of this thesis. These changes in loading conditions were either caused by a pathological stimulus (myocardial infarction (MI)) or by a physiological one (aerobic exercise training). Both stimuli predominantly lead to eccentric hypertrophy of the heart (see Fig 1.2). Despite its appropriateness in increasing cardiac output, cardiac remodeling post MI –consisting of hypertrophy and dilation- is an independent risk factor for the development of heart failure (White *et al.*, 1987). On the other hand, exercise-induced hypertrophy is not associated with an increased risk of cardiovascular disease (Pelliccia *et al.*, 2010). These differences between pathological and physiological hypertrophy are likely caused by genetic reprogramming early after the hypertrophic stimulus, leading to differences in gene expression. Identifying the transcription factors (TFs) responsible for this reprogramming was the main focus of this thesis.

The loss of muscle mass caused by MI increases the workload of the non-infarcted myocardium, as it attempts to pump the same amount of blood with less muscle. Immediately after MI, the cardiac output drops and the body responds by neurohumoral activation, which leads to an increase in heart rate as well as force of contraction. Prolonged exposure to an increased wall tension leads to structural adaptations of the heart. This process is called remodeling, in which hypertrophy (growth of individual cardiomyocytes) and dilation (increase in ventricular diameter) takes place. In light of the increased risk of heart failure, growth of cardiomyocytes in response to stimuli, such as MI or hypertension, is called pathological hypertrophy.

The progression from post-MI remodeling to the severely dilated and dysfunctioning heart seen in heart failure is associated with a host of detrimental changes in the heart, such as increased fibrosis (Jugdutt, 2003; de Waard *et al.*, 2007), apoptosis (Narula *et al.*, 2006; Dorn, 2009), infiltration of inflammatory mediators (Nian *et al.*, 2004), contractile dysfunction of surviving cardiomyocytes (van der Velden *et al.*, 2004) and reduced capillary density (Haitsma *et al.*, 2001).

In recent years, much has been learned about the molecular mechanisms underlying pathological hypertrophy (Frey & Olson, 2003; Heineke & Molkentin, 2006; Kehat & Molkentin, 2010). However, the vast majority of these data have been obtained from studies in transgenic mouse models, while molecular data from large animal models has been scarce. Furthermore, most studies have been reductionistic in nature, focusing on the function of single genes or pathways, whilst unbiased, global analyses have mostly been lacking. To fully understand complex processes such as the heart's response to MI, it should be studied at multiple levels, from the organism to the molecular level and subsequently

these levels should be integrated. Therefore in **Chapter 2** we argued for using unbiased molecular analysis techniques in conjunction with integrative physiology to gain more insight into cardiac remodeling. Swine three weeks after an MI showed a blunted exercise-induced increase in cardiac contractility and relaxation despite exaggerated serum catecholamine levels, indicating that the β-adrenergic response is blunted. In cardiomyocytes isolated from post-MI hearts, an increased Ca^{2+}-sensitivity of force development was observed compared with sham-operated hearts. The increased force development at lower Ca^{2+} concentrations could contribute to the impaired relaxation, and thus filling, of the heart. The difference in Ca^{2+} sensitivity between post-MI and sham hearts was abolished upon *in vitro* incubation with protein kinase A (PKA), a key downstream kinase of the β-adrenergic receptor (β-AR). That β-adrenergic signaling was truly disturbed was shown by administration of the β-AR agonist dobutamine. In sham operated animals dobutamine administration led to an increased phosphorylation of the PKA target protein troponin I. In post-MI remodeled myocardium, this increase in troponin I phosphorylation was significantly attenuated. Global gene expression analysis revealed specific disturbances in the expression of genes encoding for components of the β-adrenergic/PKA signaling pathway in post-MI hearts, corresponding with reduced activation of PKA.

The main focus of this thesis was the changes in transcriptional control of pathological and physiological hypertrophy. For the analysis of transcription factors (TFs), nuclear protein extracts are needed. Nuclear protein extraction protocols are typically optimized for either fresh tissue or cultured cells, while readily available frozen tissue samples stored in biobanks are much less suited for these methods. In **Chapter 3** we presented an optimized method to easily and reproducibly isolate nuclear proteins from frozen heart tissue. Enrichment of nuclear proteins achieved with this method was similar to that for fresh tissue. The nuclear extracts were essentially devoid of cytosolic and myofilament proteins. This nuclear extraction method was used to show the translocation of the phosphorylated TF signal transducer and activator of transcription 3 (STAT3) to the nucleus upon β-adrenergic stimulation. This simple and reproducible protocol was subsequently used for the analysis of TFs in physiological and pathological hypertrophy.

A drawback of working with tissue as opposed to cultured cells is that in heart tissue the majority of cells are not cardiomyocytes. While 75% of the volume of the myocardium is occupied by cardiomyocytes, they constitute only one third of the cells of the heart (Opie & Hasenfuss, 2011), with other cells types such as fibroblasts, endothelial cells and vascular smooth muscle cells constituting the majority of cells. Thus, when performing nuclear extracts on cardiac tissue there will be a large number of mRNA's as well as proteins that do not originate from cardiomyocytes. On the other hand, human (Schneider & Pfitzer, 1973) and porcine (Grabner & Pfitzer, 1974) cardiomyocytes can have two or more (up to 16) nuclei per cell in contrast to the other cells. However, one should take into account that the hearts hypertrophic response is not limited to the

cardiomyocytes but also includes fibrosis, angiogenesis and arteriogenesis involving fibroblasts, endothelial cells and smooth muscle cells. Isolation of cellular RNA and nuclear protein extracts from whole heart tissue may therefore allow us to analyze genetic reprogramming simultaneously in all relevant cells, and thus may turn out superior over analysis of separate cell types.

In **Chapter 4**, microarray analysis was used to study changes in gene expression between post-MI hearts and hearts from sham operated swine. Genes involved in 'Cell-Mediated Immune Response' and 'Inflammatory Disease' were significantly overrepresented among differentially expressed (DE) genes. Network analysis of the DE genes revealed key roles for the pro-hypertrophic molecules calcineurin and nuclear factor κB (NF-κB). To study the TFs underlying these changes in gene expression, the microarray data were used as a read-out of TF activity. With bioinformatical analysis, the promoter regions of DE genes were scanned for overrepresented TF binding sites. This *in silico* approach was complemented by protein/DNA array analysis of nuclear protein extracts. Protein/DNA array analysis semi-quantitatively assays the activity of 345 TFs in nuclear protein extracts obtained according to the method described in **Chapter 3**. Combining TFBS analysis with protein/DNA array analysis revealed matching results for two TFs, i.e. the glucocorticoid receptor (GR) and chicken ovalbumin upstream promoter TF II (COUP-TFII). To validate our transcriptional genomics approach, we treated post-MI pigs with the GR antagonist mifepristone. GR blockade led to an attenuation of the hypertrophic response three weeks post-MI.

As post-MI hypertrophy is considered a risk factor for the development of heart failure (White *et al.*, 1987), the question can be asked whether hypertrophy after MI is necessary or that we should develop therapies that prevent hypertrophy. Data from transgenic or knockout mice subjected to pressure-overload suggested that it is possible to curb hypertrophy without subsequent ventricular dilation or decompensation (Esposito *et al.*, 2002). Therefore therapies that aim to reduce hypertrophy are thought to be of great clinical relevance. In a large cohort of patients with hypertension that were treated with antihypertensive drugs, the reduction of left ventricular mass was strongly associated with decreased mortality (Devereux *et al.*, 2004). Drugs that interfere with the renin-angiotensin system (RAS) where originally developed for the treatment of hypertension, but later they were also shown to reduce cardiac remodeling. For instance, administration of the angiotensin II receptor blocker losartan to hypertensive patients caused regression of LV mass associated with decreased mortality, that could not be explained by the reduction in blood pressure alone (Dahlof *et al.*, 2002). That interfering with the RAS system is also functional in reducing post-MI remodeling, was shown by angiotensin converting enzyme (ACE) inhibitor treatment of MI patients. In these patients, it decreased left ventricular dilation and reduced mortality (Pfeffer *et al.*, 1992). In our model of post-MI remodeling, blockade of GR with the antagonist mifepristone resulted in an attenuated hypertrophic

response to MI. In contrast to the salutary effects of blockers of RAS in our model (van Kats *et al.*, 2000), the reduced hypertrophy with mifepristone was not associated with improvement of cardiac function or attenuation of LV dilation, at least in the short-term. This finding could be interpreted to suggest that solely striving for a reduction of hypertrophy in the treatment of patients following MI may not be sufficient.

The lack of functional improvement upon GR blockade post-MI might be due to its pro-inflammatory effects. In the absence of mifepristone, GR translocates to the nucleus upon cortisol binding. In the nucleus it mediates its anti-inflammatory effect by interacting with, and thereby blocking, the pro-inflammatory NF-κB (McKay & Cidlowski, 1999). NF-κB is known to be activated in post-MI hypertrophy (Tillmanns *et al.*, 2006) and that blocking NF-κB activation leads to reduced infarct size (Morishita *et al.*, 1997; Brown *et al.*, 2005). Mifepristone treatment prevents activation and thus nuclear translocation of GR, thereby impairing GRs ability to block NF-κB. Unfortunately, we did not measure infarct size in our MI model, as it would give more insight if mifepristone treatment increased infarct size. In addition, more research into the timing of GR blockade after MI, and the effect of GR antagonists other than mifepristone, is warranted.

That growth of the heart can also be a beneficial adaptation, is illustrated by exercise-induced hypertrophy. Athletes participating in endurance exercise have hypertrophy and increased ventricular diameter (Morganroth *et al.*, 1975; Pelliccia *et al.*, 1999), without an increased risk of heart failure (Pelliccia *et al.*, 2010). Cardiac growth without an increased risk of cardiovascular disease is termed physiological hypertrophy as opposed to pathological hypertrophy. In **Chapter 5** we studied the transcriptional genomics of exercise-induced hypertrophy in swine. Microarray analysis revealed DE genes that were involved in organismal survival. Network analysis of the DE genes demonstrated an important role for Akt, a known mediator of physiological hypertrophy in mice (DeBosch *et al.*, 2006). TFBS analysis and protein/DNA array analysis yielded matching results for three TFs, i.e. yin-yang 1 (YY1), paired box 6 (PAX6) and GR. The activity of all three TFs was less in hearts from exercise-trained swine compared to sedentary animals. The finding that the activity of GR is reduced in exercise-trained myocardium is particularly intriguing, given the increased activity seen in post-MI hearts.

Both exercise-training and MI induced a similar increase in the left ventricular (LV) weight normalized to body weight. A deterioration of cardiac function was observed in post-MI remodeling, as illustrated by the decreased ejection fraction and cardiac contractility, which was absent in exercise-induced hypertrophy. The gene expression profiles of both forms of hypertrophy showed remarkably little overlap. A comprehensive analysis of the differences in gene expression between pathological and physiological hypertrophy was performed in **Chapter 5**. This allowed us to discriminate genes and TFs that are specific for either pathological or physiological hypertrophy from genes and TFs that are part of a general hypertrophic response.

Exercise-training and MI both result in increased workload of the heart, so why do they cause such different types of hypertrophy? A difference between pathological and physiological hypertrophy is that the stimulus of pathological hypertrophy is sustained (as in MI) while the physiological hypertrophy stimulus is usually intermittent (e.g. daily exercise). In an elegant study by Perrino *et al.* gave mice an intermittent pathological stimulus (in this case pressure overload in the form of transverse aortic constriction (TAC)) for the same time-period as a swimming exercise protocol (Perrino *et al.*, 2006). They showed that the intermittent TAC mice had hypertrophy without a change in fractional shortening similar to swimming exercise trained mice, while chronic TAC mice had a higher degree of hypertrophy and decreased fractional shortening. However, further analysis revealed that intermittent TAC mice had reduced cellular contractility, increased fibrosis and reduced capillary density, all pathological features that were not present in the exercise trained mice (Perrino *et al.*, 2006). It seems therefore that the nature of the stimulus rather than chronicity determines pathogenicity. Another argument for this hypothesis is that during pregnancy the heart experiences volume overload over a prolonged period which results in hypertrophy with increased stroke volume that is reversed postpartum (Schannwell *et al.*, 2002). It could be speculated that the heart is primed for the changes in cardiovascular workload that occur during exercise as discussed in **Chapter 2**, while the heart is unable to cope with the sudden fall in cardiac output occurring after a large MI, leading to a so-called "surrender" phenotype (Tardiff, 2006).

Taken together, the research described in this thesis shows that at the present time large scale unbiased molecular analyses can be performed in a large animal model. We show that pathological and physiological hypertrophy each have distinct gene expression patterns and that the transcription factors that drive these changes are also different. GR is a particularly interesting TF, as it is activated in pathological hypertrophy, while it is becomes less active in physiological hypertrophy.

6.2 Future perspectives

The studies on pathological and physiological hypertrophy were performed on myocardium obtained three weeks after MI and after 4-5 weeks of exercise training. This implies that the molecular changes at only one time-point were studied. It has been shown that an increase in cardiac mass is already evident one week following MI (van Kats *et al.*, 2000), so it might also be interesting to study the changes that occur at earlier time-points. On the other hand, it might be difficult to distinguish the effects of surgery from true effects of cardiac remodeling (van Kats *et al.*, 2000).

Future research should also focus on improving the model for pathological hypertrophy so that the findings can be more easily translated to the clinic. Swine more closely resemble humans in cardiovascular physiology and anatomy than the often studied mice and rats. However, there is still a lot of ground to cover before data obtained from young healthy swine can be translated to the typical MI patient, i.e. a person of older age who is overweight and has various co-morbidities. An additional difference is that in our model the left circumflex coronary artery is permanently ligated, while in patients therapy is specifically aimed at removing the occlusion and restoring myocardial perfusion as soon as possible. Another possible caveat in translating our findings to humans is that in our post-MI model, no medication was given except for the experimental mifepristone, while almost all patients receive β-blockers, ACE inhibitors, anti-coagulation treatment and lipid lowering medication following MI. It has already been shown that administration of ACE-inhibitors (van Kats *et al.*, 2000) and β-blockers starting from day one after the MI, resulted in, respectively, attenuated LV hypertrophy and dilation (van Kats et al., 2000) and normalization of β-adrenergic/PKA signaling and cardiac function (Duncker *et al.*, 2009; Boontje *et al.*, 2010) three weeks post-MI. Adding the standard medication to the animal model together with an ischemia-reperfusion model of adult swine fed on Western diet will further increase the translational potential of the current model.

In this thesis post-MI remodeling was contrasted with exercise-induced cardiac hypertrophy. In addition, it would also be important to evaluate whether exercise-training after MI could lead to a (partial) reversal of the pathological hypertrophy. In small animal models, the beneficial effects of exercise-training post-MI have been well described (de Waard *et al.*, 2007) (de Waard *et al.*, 2010). A large meta-analysis of the effects of exercise-training on LV remodeling in patients after MI revealed that exercise started early after MI had the most beneficial effect (Haykowsky *et al.*, 2011). Guidelines from the European Society of Cardiology (Van de Werf *et al.*, 2008) and American Heart Association (Antman *et al.*, 2004) recommend 30 minutes of moderate intensity aerobic exercise three to five times a week in patients recovering from MI. The mechanisms by which exercise improves cardiac function after MI are not fully understood. Therefore it would be of considerable interest to investigate whether exercising swine after a MI leads to a molecular signature that is more physiological than pathological, and the pathological signature can be reversed by exercise-training. Specifically, it would be of interest to look whether the activation of GR is abolished by exercise training. Identifying the proteins that are responsible for mediating the salutary effects of exercise training on post-MI remodeling might also result in the identification of potential targets for therapy, the so-called "exercise in a pill".

The transcriptional genomics approaches described in **Chapter 4 & 5** use unbiased microarray analysis with bioinformatical TF binding site analysis, combined with protein/DNA array measuring the activity of 345 TFs. A more complete picture of the molecular changes occurring in cardiac hypertrophy could be obtained if we included

proteomic analysis of nuclear extracts. A change in mRNA is only one way in which a protein can change its activity level. In addition, proteins can translocate from one subcellular location to the other, or proteins can be post-translationally modified (PTM), e.g. by phosphorylation. Proteomics, which quantitatively measures protein expression as well as PTM of proteins is increasingly being applied in cardiovascular research (Van Eyk, 2011). The ubiquitous presence of myofilament proteins in the cardiomyocytes can mask low abundant proteins such as TFs. Subcellular fractionation can overcome this problem (Huber *et al.*, 2003; Agnetti *et al.*, 2011). As illustrated in this thesis, the nuclear proteome can be used for the analysis of TFs, and comparing the nuclear proteome of sham operated and post-MI allows the identification of TFs that become more abundant in the nucleus upon a pathological hypertrophy stimulus. Another advantage of proteomics in studying TFs is that PTMs can be studied, as a large proportion of TFs appears to be activated by PTM. The nuclear protein extraction method described in **Chapter 3** provides a good method for obtaining relatively pure nuclear extracts for proteome analysis.

Recently, a new class of small non-coding RNAs has been discovered that modulate gene expression, known as microRNAs (miRNA). miRNAs are ~22 nucleotide single stranded RNAs that inhibit the expression of specific target mRNAs (Small & Olson, 2011), and are thought to be involved also in heart failure (Naga Prasad *et al.*, 2009). MicroRNAs could possibly be used as biomarkers for disease progression or risk stratification (Tijsen *et al.*, 2010). In a recent article, miRNA 199b was found to be upregulated in mouse models of pathological hypertrophy, and its expression was higher in biopsies from human heart failure patients compared to healthy donor hearts (da Costa Martins *et al.*, 2010). Administration of a miRNA antagonist to specifically silence miRNA 199b led to an almost complete abrogation of the cardiac hypertrophic response to pressure overload. Studying which miRNAs are differentially expressed in our models of pathological and physiological hypertrophy, might lead to the identification of new miRNAs that mediate cardiac hypertrophy. Furthermore, our transcriptional genomics approach could be employed to identify which TFs activate or repress the expression of the differentially expressed miRNAs.

In contrast to cardiac hypertrophy, cardiac atrophy, has until recently received relatively little attention. Atrophy of the heart occurs in a state of cardiac unloading, such as during a prolonged period of bed rest or weightlessness (Perhonen *et al.*, 2001). Since the use of LV assist devices (LVADs), cardiac atrophy has become the focus of more research (Drakos *et al.*, 2011). Despite the renewed interest, still little is known about the molecular mechanisms underlying cardiac atrophy. Molecular signaling in atrophy is not simply a reversal of hypertrophic gene reprogramming or deactivation of pro-hypertrophic proteins, as hypertrophy and atrophy both are associated with the re-induction of some fetal genes (Depre *et al.*, 1998). If specific atrophy proteins could be identified, they could prove to be therapeutic targets for reducing hypertrophy in heart failure patients.

Conclusions

The research described in this thesis shows that at the present time large scale unbiased molecular analyses can be performed in a large animal model. We have shown that pathological and physiological hypertrophy each have distinct patterns of gene expression and that the transcription factors that drive these changes are also different. Future studies should be aimed at assessing the relative importance of the transcription factors in both forms of hypertrophy and whether to can be used as therapeutic targets to prevent the progression from pathological hypertrophy to heart failure.

6.3 References

Agnetti G, Husberg C, & Van Eyk JE (2011). Divide and conquer: the application of organelle proteomics to heart failure. *Circ Res* **108**, 512-526.

Antman EM, Anbe DT, Armstrong PW, Bates ER, Green LA, Hand M, Hochman JS, Krumholz HM, Kushner FG, Lamas GA, Mullany CJ, Ornato JP, Pearle DL, Sloan MA, Smith SC, Jr., Alpert JS, Anderson JL, Faxon DP, Fuster V, Gibbons RJ, Gregoratos G, Halperin JL, Hiratzka LF, Hunt SA, & Jacobs AK (2004). ACC/AHA guidelines for the management of patients with ST-elevation myocardial infarction: a report of the American College of Cardiology/American Heart Association Task Force on Practice Guidelines (Committee to Revise the 1999 Guidelines for the Management of Patients with Acute Myocardial Infarction). *Circulation* **110**, e82-292.

Boontje NM, Merkus D, Zaremba R, Versteilen A, de Waard MC, Mearini G, de Beer VJ, Carrier L, Walker LA, Niessen HW, Dobrev D, Stienen GJ, Duncker DJ, & van der Velden J (2010). Enhanced myofilament responsiveness upon beta-adrenergic stimulation in post-infarct remodeled myocardium. *J Mol Cell Cardiol*.

Brown M, McGuinness M, Wright T, Ren X, Wang Y, Boivin GP, Hahn H, Feldman AM, & Jones WK (2005). Cardiac-specific blockade of NF-kappaB in cardiac pathophysiology: differences between acute and chronic stimuli in vivo. *Am J Physiol Heart Circ Physiol* **289**, H466-H476.

da Costa Martins PA, Salic K, Gladka MM, Armand AS, Leptidis S, el Azzouzi H, Hansen A, Coenen-de Roo CJ, Bierhuizen MF, van der Nagel R, van Kuik J, de Weger R, de Bruin A, Condorelli G, Arbones ML, Eschenhagen T, & De Windt LJ (2010). MicroRNA-199b targets the nuclear kinase Dyrk1a in an auto-amplification loop promoting calcineurin/NFAT signalling. *Nat Cell Biol* **12**, 1220-1227.

Dahlof B, Devereux RB, Kjeldsen SE, Julius S, Beevers G, de Faire U, Fyhrquist F, Ibsen H, Kristiansson K, Lederballe-Pedersen O, Lindholm LH, Nieminen MS, Omvik P, Oparil S, & Wedel H (2002). Cardiovascular morbidity and mortality in the Losartan Intervention For Endpoint reduction in hypertension study (LIFE): a randomised trial against atenolol. *Lancet* **359**, 995-1003.

de Waard MC, van der Velden J, Bito V, Ozdemir S, Biesmans L, Boontje NM, Dekkers DH, Schoonderwoerd K, Schuurbiers HC, de Crom R., Stienen GJ, Sipido KR, Lamers JM, & Duncker DJ (2007). Early exercise training normalizes myofilament function and attenuates left ventricular pump dysfunction in mice with a large myocardial infarction. *Circ Res* **100**, 1079-1088.

DeBosch B, Treskov I, Lupu TS, Weinheimer C, Kovacs A, Courtois M, & Muslin AJ (2006). Akt1 is required for physiological cardiac growth. *Circulation* **113**, 2097-2104.

Depre C, Shipley GL, Chen W, Han Q, Doenst T, Moore ML, Stepkowski S, Davies PJ, & Taegtmeyer H (1998). Unloaded heart in vivo replicates fetal gene expression of cardiac hypertrophy. *Nat Med* **4**, 1269-1275.

Devereux RB, Wachtell K, Gerdts E, Boman K, Nieminen MS, Papademetriou V, Rokkedal J, Harris K, Aurup P, & Dahlof B (2004). Prognostic significance of left ventricular mass change during treatment of hypertension. *JAMA* **292**, 2350-2356.

Dorn GW (2009). Apoptotic and non-apoptotic programmed cardiomyocyte death in ventricular remodelling. *Cardiovasc Res* **81**, 465-473.

Drakos SG, Kfoury AG, Selzman CH, Verma DR, Nanas JN, Li DY, & Stehlik J (2011). Left ventricular assist device unloading effects on myocardial structure and function: current status of the field and call for action. *Curr Opin Cardiol* **26**, 245-255.

Duncker DJ, Boontje NM, Merkus D, Versteilen A, Krysiak J, Mearini G, El Armouche A, de Beer VJ, Lamers JM, Carrier L, Walker LA, Linke WA, Stienen GJ, & van der Velden J (2009). Prevention of myofilament dysfunction by beta-blocker therapy in postinfarct remodeling. *Circ Heart Fail* **2**, 233-242.

Esposito G, Rapacciuolo A, Naga Prasad SV, Takaoka H, Thomas SA, Koch WJ, & Rockman HA (2002). Genetic alterations that inhibit in vivo pressure-overload hypertrophy prevent cardiac dysfunction despite increased wall stress. *Circulation* **105**, 85-92.

Frey N & Olson EN (2003). Cardiac hypertrophy: the good, the bad, and the ugly. *Annu Rev Physiol* **65**, 45-79.

Grabner W & Pfitzer P (1974). Number of nuclei in isolated myocardial cells of pigs. *Virchows Arch B Cell Pathol* **15**, 279-294.

Haitsma DB, Bac D, Raja N, Boomsma F, Verdouw PD, & Duncker DJ (2001). Minimal impairment of myocardial blood flow responses to exercise in the remodeled left ventricle early after myocardial infarction, despite significant hemodynamic and neurohumoral alterations. *Cardiovasc Res* **52**, 417-428.

Haykowsky M, Scott J, Esch B, Schopflocher D, Myers J, Paterson I, Warburton D, Jones L, & Clark AM (2011). A meta-analysis of the effects of exercise training on left ventricular remodeling following myocardial infarction: start early and go longer for greatest exercise benefits on remodeling. *Trials* **12**, 92.

Heineke J & Molkentin JD (2006). Regulation of cardiac hypertrophy by intracellular signalling pathways. *Nat Rev Mol Cell Biol* **7**, 589-600.

Huber LA, Pfaller K, & Vietor I (2003). Organelle proteomics: implications for subcellular fractionation in proteomics. *Circ Res* **92**, 962-968.

Jugdutt BI (2003). Ventricular remodeling after infarction and the extracellular collagen matrix: when is enough enough? *Circulation* **108**, 1395-1403.

Kehat I & Molkentin JD (2010). Molecular pathways underlying cardiac remodeling during pathophysiological stimulation. *Circulation* **122**, 2727-2735.

McKay LI & Cidlowski JA (1999). Molecular control of immune/inflammatory responses: interactions between nuclear factor-kappa B and steroid receptor-signaling pathways. *Endocr Rev* **20**, 435-459.

Morganroth J, Maron BJ, Henry WL, & Epstein SE (1975). Comparative left ventricular dimensions in trained athletes. *Ann Intern Med* **82**, 521-524.

Morishita R, Sugimoto T, Aoki M, Kida I, Tomita N, Moriguchi A, Maeda K, Sawa Y, Kaneda Y, Higaki J, & Ogihara T (1997). In vivo transfection of cis element "decoy" against nuclear factor-kappaB binding site prevents myocardial infarction. *Nat Med* **3**, 894-899.

Naga Prasad SV, Duan ZH, Gupta MK, Surampudi VS, Volinia S, Calin GA, Liu CG, Kotwal A, Moravec CS, Starling RC, Perez DM, Sen S, Wu Q, Plow EF, Croce CM, & Karnik S (2009). Unique microRNA profile in end-stage heart failure indicates alterations in specific cardiovascular signaling networks. *J Biol Chem* **284**, 27487-27499.

Narula J, Haider N, Arbustini E, & Chandrashekhar Y (2006). Mechanisms of disease: apoptosis in heart failure--seeing hope in death. *Nat Clin Pract Cardiovasc Med* **3**, 681-688.

Nian M, Lee P, Khaper N, & Liu P (2004). Inflammatory cytokines and postmyocardial infarction remodeling. *Circ Res* **94**, 1543-1553.

Opie LH & Hasenfuss G (2011). Mechanisms of cardiac contraction and relaxation. In *Braunwald's Heart Disease*, eds. Bonow RO, Mann DL, Zipes DP, & Libby P, pp. 459-486. Elsevier Saunders, Philadelphia.

Pelliccia A, Culasso F, Di Paolo FM, & Maron BJ (1999). Physiologic left ventricular cavity dilatation in elite athletes. *Ann Intern Med* **130**, 23-31.

Pelliccia A, Kinoshita N, Pisicchio C, Quattrini F, Dipaolo FM, Ciardo R, Di GB, Guerra E, De BE, Casasco M, Culasso F, & Maron BJ (2010). Long-term clinical consequences of intense, uninterrupted endurance training in olympic athletes. *J Am Coll Cardiol* **55**, 1619-1625.

Perhonen MA, Franco F, Lane LD, Buckey JC, Blomqvist CG, Zerwekh JE, Peshock RM, Weatherall PT, & Levine BD (2001). Cardiac atrophy after bed rest and spaceflight. *J Appl Physiol* **91**, 645-653.

Perrino C, Naga Prasad SV, Mao L, Noma T, Yan Z, Kim HS, Smithies O, & Rockman HA (2006). Intermittent pressure overload triggers hypertrophy-independent cardiac dysfunction and vascular rarefaction. *J Clin Invest* **116**, 1547-1560.

Pfeffer MA, Braunwald E, Moye LA, Basta L, Brown EJ, Jr., Cuddy TE, Davis BR, Geltman EM, Goldman S, Flaker GC, & . (1992). Effect of captopril on mortality and morbidity in patients with left ventricular dysfunction after myocardial infarction. Results of the survival and ventricular enlargement trial. The SAVE Investigators. *N Engl J Med* **327**, 669-677.

Schannwell CM, Zimmermann T, Schneppenheim M, Plehn G, Marx R, & Strauer BE (2002). Left ventricular hypertrophy and diastolic dysfunction in healthy pregnant women. *Cardiology* **97**, 73-78.

Schneider R & Pfitzer P (1973). Die Zahl der Kerne in isolierten Zellen des menschlichen Myokards. *Virchows Arch B Cell Pathol* **12**, 238-258.

Small EM & Olson EN (2011). Pervasive roles of microRNAs in cardiovascular biology. *Nature* **469**, 336-342.

Tardiff JC (2006). Cardiac hypertrophy: stressing out the heart. *J Clin Invest* **116**, 1467-1470.

Tijsen AJ, Creemers EE, Moerland PD, De Windt LJ, van der Wal AC, Kok WE, & Pinto YM (2010). MiR423-5p as a circulating biomarker for heart failure. *Circ Res* **106**, 1035-1039.

Tillmanns J, Carlsen H, Blomhoff R, Valen G, Calvillo L, Ertl G, Bauersachs J, & Frantz S (2006). Caught in the act: in vivo molecular imaging of the transcription factor NF-kappaB after myocardial infarction. *Biochem Biophys Res Commun* **342**, 773-774.

Van de Werf F, Bax J, Betriu A, Blomstrom-Lundqvist C, Crea F, Falk V, Filippatos G, Fox K, Huber K, Kastrati A, Rosengren A, Steg PG, Tubaro M, Verheugt F, Weidinger F, & Weis M (2008). Management of acute myocardial infarction in patients presenting with persistent ST-segment elevation: the Task Force on the Management of ST-Segment Elevation Acute Myocardial Infarction of the European Society of Cardiology. *Eur Heart J* **29**, 2909-2945.

van der Velden J, Merkus D, Klarenbeek BR, James AT, Boontje NM, Dekkers DH, Stienen GJ, Lamers JM, & Duncker DJ (2004). Alterations in myofilament function contribute to left ventricular dysfunction in pigs early after myocardial infarction. *Circ Res* **95**, e85-e95.

Van Eyk JE (2011). Overview: the maturing of proteomics in cardiovascular research. *Circ Res* **108**, 490-498.

van Kats JP, Duncker DJ, Haitsma DB, Schuijt MP, Niebuur R, Stubenitsky R, Boomsma F, Schalekamp MA, Verdouw PD, & Danser AH (2000). Angiotensin-converting enzyme inhibition and angiotensin II type 1 receptor blockade prevent cardiac remodeling in pigs after myocardial infarction: role of tissue angiotensin II. *Circulation* **102**, 1556-1563.

White HD, Norris RM, Brown MA, Brandt PW, Whitlock RM, & Wild CJ (1987). Left ventricular end-systolic volume as the major determinant of survival after recovery from myocardial infarction. *Circulation* **76**, 44-51.

List of publications
Ph D Portfolio
Acknowledgements
Curriculum Vitae

List of publications

Full papers

- **Kuster DW**, Cholid Bawazeer A, Zaremba R, Goebel M, Boontje NM & van der Velden J (2011). Cardiac Myosin binding protein C phosphorylation in cardiac disease.: *J Muscle Res Cell Motil* **[In press]**

- **Kuster DW**, Merkus D, Kremer A, van IJcken WF, de Beer VJ, Verhoeven AJ & Duncker DJ (2011) Post-infarct left ventricular remodeling in swine: a transcriptional genomics approach. *Basic Res Cardiol* **[ePub ahead of print]**

- Welvaart WN, Paul MN, **Kuster DW**, van Wieringen WN, Rustenburg F, Stienen GJM, Vonk-Noordegraaf A & Ottenheijm CAC (2011). Gene expression profile in the diaphragm following contractile inactivity during thoracic surgery. *Int J Physiol Pathophysiol Pharmacol* **3**, 167-175

- de Beer VJ, Taverne YJ, **Kuster DW**, Najafi A, Duncker DJ & Merkus D (2011). Prostanoids suppress the coronary vasoconstrictor influence of endothelin after myocardial infarction. *Am J Physiol Heart Circ Physiol* **301**, H1080-1089

- van Deel ED, de Boer M, **Kuster DW**, Boontje NM, Holemans P, Sipido KR, van der Velden J & Duncker DJ (2011). Exercise training does not improve cardiac function in compensated or decompensated left ventricular hypertrophy induced by aortic stenosis. *J Mol Cell Card* **50,**1017-25

- **Kuster DW**, Merkus D, van der Velden J, Verhoeven AJ & Duncker DJ (2011). "Integrative Physiology 2.0": integration of systems biology into physiology and its application to cardiovascular homeostasis. *J Physiol* **589,**1037-1045

- **Kuster DW**, Merkus D, Jorna HJ, Dekkers DH, Duncker DJ & Verhoeven AJ. (2011). Nuclear protein extraction from frozen porcine myocardium. *J Physiol Biochem* **67**:165-173

- Dekkers DHW, Bezstarosti K, **Kuster DW**, Adrie J.M. Verhoeven & Dipak K. Das (2010). Application of proteomics in cardiovascular research. Curr Proteomics **7**, 108-115

- de Waard MC, van der Velden J, Boontje NM, Dekkers DH, van Haperen R, **Kuster DW**, Lamers JM, de Crom R & Duncker DJ.(2009). Detrimental effect of combined exercise training and eNOS overexpression on cardiac function after myocardial infarction. *Am J Physiol Heart Circ Physiol* **296,**H1513-1523

- Kol MA, **Kuster DW**, Boumann HA, de Cock JJ, Heck AJ, de Kruijff B & de Kroon AI (2004) Uptake and remodeling of exogenous phosphatidylethanolamine in E. Coli. *Biochim Biophys Acta* **1636**: 205-212

Book Chapters

- **Kuster DW**, Dekkers DH., Bezstrarosti K & Verhoeven AJ (2010). Methods in cardiovascular proteomics: In: Methods in Redox Signaling, ed. D.K. Das. *Mary Ann Liebert, Inc.*.

Abstracts

- **Kuster DW**, Verhoeven AJ, Merkus D, van der Velden J & Duncker DJ (2011). Integrative approach reveals specific disturbances in beta-adrenergic/cAMP signaling in post-myocardial infarction remodeling in swine. *FASEB J* **25**, 863.8

- **Kuster DW**, Verhoeven AJ, Merkus D & Duncker DJ (2010). Integrative approach to study the molecular basis of post-myocardial infarction remodeling in porcine hearts. *FASEB J* **24**, 100.8

- **Kuster DW**, Merkus D, Dekkers D, Duncker DJ & Verhoeven AJ.(2009). Nuclear protein extraction from frozen porcine myocardium. *FASEB J* **23**,LB246

Ph D portfolio

Name PhD student: Diederik Kuster	PhD period: 2006-2011
Erasmus MC Department: Experimental Cardiology/Biochemistry	Promotor(s): Prof.Dr. DJ Duncker;Prof Dr. JMJ Lamers
Research School: COEUR	Supervisor: Dr. AJM Verhoeven

1. PhD training

	Year	ECTS
General academic skills		
- Biomedical English Writing and Communication	2009	2
- Research Integrity	2007	2
Research skills		
- Statistics	2008	6
In-depth courses (e.g. Research school, Medical Training)		
- NHS course Cardiac Function and Adaptation	2006	1.5
- COEUR Courses (6 courses)	2006-2007	9
- Reading and discussing literature (MGC)	2006	6
- Experimental approach to Molecular and Cell Biology (MGC)	2007	6
- Analysis of microarray gene expression (MGC)	2007	1.5
Presentations		
- Experimental Biology	2010/2011	0.5
International conferences		
- Experimental Biology	2009/2010/2011	3
- European Society of Cardiology	2009	1
- European Society of Cardiology Summer School	2011	1
Seminars and workshops		
- COEUR seminars	2006-2010	1

2. Teaching activities

	Year	Workload (Hours/ECTS)
Supervising practicals and excursions		
- MGC PhD student workshop Heidelberg	2008	2
Supervising Bachelor/Master theses		
- Higher laboratory education (Y. Karssen)	2008	3
- Cardiovascular Research master (A. Cholid Bawazeer)	2011	4
Other		
-		

Dankwoord

Het is er dan toch van gekomen. Het laatste hoofdstuk dat nog geschreven moet worden, voordat het boekje naar de drukker kan! Alhoewel je soms het gevoel hebt dat je er alleen voor staat tijdens je onderzoek, heb je toch begeleiders, collega's, vrienden en familie nodig om je te helpen. Voor hen is dit schrijven.

Allereerst mijn promotores. Prof Dr JMJ Lamers en Prof Dr DJGM Duncker. Jos, jij was degene die mij een kans gaf om als promovendus aan de slag te gaan. Jouw enthousiasme en positivisme waren erg prettig voor een beginnende wetenschapper. Helaas kon je door een ongeluk mij slechts een aantal maanden begeleiden. Je hebt mij in die korte tijd veel geleerd en ik ben blij dat je weer hersteld bent en van het leven kan genieten.

Dirk, jij hebt de begeleiding vervolgens overgenomen. Het zal niet altijd gemakkelijk geweest zijn om als fysioloog een chemicus met een vrij moleculair project te superviseren. Toch ging het goed samen. Vooral door jouw niet-aflatend enthousiasme voor de wetenschap, wat enorm inspirerend was. Toen we samen de presentatie hebben gemaakt voor het European Society of Cardiology congres in Barcelona, had ik het gevoel dat we door onze verschillende achtergronden veel van elkaar konden leren. Het was vooral prettig om na iedere werkbespreking weer vol energie naar buiten te komen. Ook de buitenlandse congressen samen waren altijd zeer geslaagd, ook in de avonduren. Nu rest de uitdaging om het gezinsleven met het runnen van een afdeling te blijven combineren.

Mijn copromotor Dr AJM Verhoeven verdient ook speciale dank. Beste Adrie, jij was van het begin bij het project betrokken en heb mij het meeste begeleid van iedereen. Het was erg prettig om met je samen te werken. Je was/bent een man met een kritische blik zowel op experimentele data, als op manuscripten. Je probeerde mijn moreel niet te knakken door aan het einde van een lange verbetersessie te zeggen, "maar het is ook een kwestie van smaak". Gelukkig konden we ook op sociaal gebied goed met elkaar overweg en was het prettig om iemand in Rotterdam over Ajax te kunnen praten. Ik hoop dat je nog veel plezier gaat beleven op de Interne Geneeskunde.

Mijn huidige begeleider Dr J van der Velden wil ik ook hartelijk bedanken. Jolanda, jij hebt mij de kans gegeven om tijdens mijn derde jaar al te beginnen met een nieuw onderzoek in het VU medische centrum. Je hebt mij altijd op het hart gedrukt om toch vooral ook niet te vergeten mijn proefschrift af te ronden. Desondanks bleek het nieuwe onderzoek toch meer te trekken dan het afronden van die laatste experimenten en het opschrijven van de data. Gelukkig heb je me genoeg gesteund en het resultaat is daar. Qua enthousiasme zijn Dirk en jij twee handen op één buik, dat is erg prettig! Bedankt voor het vertrouwen en we gaan hopelijk de komende jaren nog genoeg met elkaar samen werken. Ook bedankt voor het kritisch bekijken van mijn proefschrift.

Prof.Dr. Danser en prof.dr. Philipsen, hartelijk dank voor het beoordelen van mijn proefschrift.

Prof. Dr. D.N. Meijer, Dr. H.J. Duckers en Prof. Dr. C.P. Verrijzer dank voor het opponeren tijdens mijn promotie. Peter ook bedankt voor jouw eerlijkheid en medewerking in mijn overgang van Biochemie naar Experimentele Cardiologie.

Mijn paranimfen Huub en Vincent verdienen natuurlijk ook dank. Huub, jij was samen met Boet en Ruud mijn vaste lunchpartner in het Sofia. Het was goed om lekker over niet wetenschappelijke dingen te kunnen praten. Als stereotype Brabander zorgde jij altijd voor een goede sfeer tijdens het werk, lunch of bij borrels. Even tussen experimenten door een bakkie doen was een goed ontspanmoment! Vin, toen ik van de zesde naar de 23ste verhuisde, kwam ik bij jou op de kamer. Het klikte al vrij snel, en het scheelde dat we dezelfde soort humor hadden (mooi dankwoord cliché). Vooral op het jaarlijkse EB congres in de VS was het goed toeven (don't stop believing!). Het was bovendien zeer nuttig om iemand te hebben die in de zelfde fase van zijn AIO-schap zat, voor vragen en klagen.

Mijn eerste periode heb ik doorgebracht op de afdeling Biochemie. Mijn kamergenoten Nellie, Christina en Diederik wil ik bedanken voor het inwerken en de prettige werksfeer. Dick, bedankt voor jouw expertise! Ik heb veel van je geleerd en je was nooit te beroerd om het mij uit te leggen. Andere mensen van de zesde verdieping die ik wil bedanken: Aryandi, Karel en Jeroen, Wilfred, Berrina, Tommy, Wim en Elly, Koos, Marcin en waarschijnlijk nog andere mensen die ik vergeten ben (sorry).

Ashok, thanks for the great times. I enjoyed our conversations very much (and still like your quote "if your antibody is working, you're happy"). Also enjoyed the beers and the Indian food together with Dev.

Mijn vaste lunchgenoten in het Sofia, Ruud en Boet. Het was altijd gezellig om even een half uurtje (soms meer) stoom af te blazen of gewoon onzin te ouwehoeren. Ruud, ik hoop dat je promotieonderzoek soepel gaat en dat je binnenkort zelf aan de beurt bent.

Mijn tweede gedeelte is gereserveerd voor de mensen op de 23ste verdieping. Mijn kamergenoten, Daphne, Liz, Zichao, Shanti, Maaike, Annemarie en wisselende groepen studenten bedankt. Daphne, bedankt voor jouw input op artikelen. Je begon je altijd te verontschuldigen, met "ik weet hier niet zoveel vanaf" om vervolgens een hele scherpe opmerking te maken. Ook heel erg bedankt voor de experimenten met de varkens!

Maaike, Inge, Annemarie en alle studenten, bedankt voor het dierexperimenteel werk. Het enige wat ik kon doen, was toekijken en af en toe een klem aangeven.

Martine en Elza bedankt voor de gezellige borrels en stoom-afblaassessies! Martine bedankt voor alle leuke gesprekken over welke nieuwe bandjes we nog moeten luisteren. Jouw positivisme is een zegen voor een promovendus in zijn terminale fase. Geniet nog van je vele reizen en voor je het weet ga je zelf promoveren. Elza, je was altijd in voor een borrel (goed begin). Jouw directe manier van communiceren bevalt mij altijd wel. Je bent zelf bijna aan de beurt dus alvast succes!
Andere mensen van de Experimentele Cardio die ik wil bedanken zijn: Marc (altijd gezellig op congressen), Rob (voor de digitale ondersteuning en de borrels!), Mieke, Andre, Monique (voor al het regelwerk en de dropjes) en de rest van de groep.
Studenten brengen vaak leven in de brouwerij en daarom wil ik een aantal studenten bedanken. Han en Yannick, jullie waren beide zeer gedreven, maar ook zeer sociaal. Borrels en feestjes waren altijd gezellig. Aref, ik moest laatst een praatje geven bij jouw afstudeerceremonie. Daarin zei ik al dat wij elkaar lijken te achtervolgen. Op de Erasmus 2x, in het VUMC tijdens je master en nu weer als AIO. Je bent een harde werker en enthousiast persoon, ik weet zeker dat je een goed promotieonderzoek gaat doen.

Mijn laatste periode ben ik werkzaam geweest op de afdeling Fysioloie van het VUMC. Aangezien dit werk vooral gericht was op mijn postdoc project zal ik slechts kort de mensen bedanken. Kamergenoten Viola, Josine, Loek, Pleuni en Ahmet bedankt voor de kopjes koffie en gezelligheid. Leden van de groep Stienen/van der Velden, Paul (mijn look-a-like), Vasco (future Nobel price winner), Max, Rosalie, Silvia, Emmy, Nicky, Amira (thanks!), Coen, Ruud, Sabine, Nazha en Robert (not a member of the cardio group, but thanks for the lunches and drinks).

Er schijnt ook een wereld buiten de wetenschap te zijn. Een aantal mensen moet hier ook bedankt worden. Mijn voetbalteam bijvoorbeeld, RCH zondag 4. Het was altijd heerlijk om op woensdag te trainen en zondag een wedstrijd te spelen. Een goede manier om wat frustraties weg te spelen.

Ook zijn er genoeg vrienden geweest die mij (al dan niet onderbewust) geholpen hebben deze periode door te komen (klinkt heel dramatisch), met vakanties, pizza's en potje, kroegbezoek, zaterdag loempia's halen en voetbal kijken. Dus bedankt Jacques, Rik, Friso, Maarten, Jaap, Alphons, Andre, Jur en Maurits.

Steef, wij hebben de begin periode van mijn promotieonderzoek samen in Haarlem op de Drapenierstraat gewoond. Bedankt voor je kookkunsten (kom binnenkort weer curry

eten) en ook bedankt voor het ontwerp van de omslag van dit proefschrift! Het voelt goed aan om iemand te hebben om op terug te kunnen vallen.

Pap en mam, jullie hebben mij altijd gesteund in alles wat ik wilde doen. Dank jullie wel voor alles!! Jullie hebben altijd voor mij klaargestaan en dat ik weet dat jullie trots zijn dat er toch nog een Kuster gaat promoveren. Ik houd van jullie.

Als laatste uiteraard, Kady. Het is er eindelijk van gekomen. Het is af. Het was heerlijk om bij je thuis te komen na een lange dag werken. Ik weet dat soms van mijn werk baalde (vooral van de werktijden), maar je hebt me altijd gesteund. Ik houd van je! Verken met mij de wereld!!

Curriculum Vitae

Diederik Wouter Dimitri Kuster is geboren op 22 mei 1980 te Haarlem. In 1998 haalde hij zijn VWO diploma aan het Sancta Maria in Haarlem. In dat zelfde jaar startte hij de studie Scheikunde aan de Universiteit van Utrecht. In het laatste jaar deed hij onderzoek op de afdeling Biochemie van Membranen onder leiding van Prof Dr de Kruijff en Dr de Kroon. In 2003 behaalde hij zijn doctoraaldiploma Scheikunde met genoegen. Vervolgens heeft hij in 2004 negen maanden gewerkt op de afdeling Imaging van het farmaceutisch bedrijf Merck in West Point, Pennsylvania in de Verenigde Staten. Vervolgens begon hij in 2006 als promovendus op de afdelingen Biochemie en Experimentele Cardiologie in het Erasmus Medische Centrum te Rotterdam onder begeleiding van Prof.dr. Lamers, Prof.dr Duncker en Dr. Verhoeven. De resultaten die uit dit onderzoek zijn voortgekomen zijn beschreven in dit proefschrift. In 2010 is hij begonnen als parttime postdoc op de afdeling Fysiologie van het VU Medisch Centrum onder begeleiding van Dr van der Velden. Per januari 2011 werd dit voltijds. Per 1 januari 2012 gaat hij aan de slag als postdoc op de afdeling Cell and Molecular Physiology van de Loyola University of Chicago onder leiding van Dr Sadayappan

Chapter 7

Nederlandse samenvatting

7.1 Samenvatting en algemene discussie

Adaptatie van het hart aan een toegenomen belasting was het onderwerp van dit proefschrift. De veranderingen in belasting werden veroorzaakt door een pathologische stimulus (hartinfarct) of door een fysiologische stimulus (aerobische inspanningstraining). Beide stimuli leiden hoofdzakelijk tot eccentrische hypertrofie van het hart (zie figuur 1.2). Alhoewel remodelering (bestaande uit hypertrofie en dilatatie) na een hartinfarct de cardiale output van het hart verhoogt, is dit proces een risicofactor voor de ontwikkeling van hartfalen. Aan de ander kant, hypertrofie na een hartinfarct is niet geassocieerd met een toegenomen kans op hart- en vaatziekten. Deze verschillen tussen pathologische en fysiologische hypertrofie worden hoogstwaarschijnlijk veroorzaakt door genetische herprogrammering vroeg na de hypertrofie stimulus. Het identificeren van de transcriptie factoren die verantwoordelijk zijn voor deze herprogrammering was het belangrijkste doel van dit proefschrift.

Het verlies van spierweefsel veroorzaakt door het hartinfarct leidt tot een toename van de arbeid die het resterende deel van het hart moet leveren, omdat het hart dezelfde hoeveelheid bloed moet rondpompen met minder spierweefsel. Onmiddellijk na het hartinfarct, daalt het hartminuutvolume en het lichaam reageert door middel van neurohumorale activatie, wat leidt tot een toename van de hartslag en contractiliteit. Op de lange termijn leidt de toegenomen wandspanning tot structurele aanpassingen van het hart. Dit proces wordt remodellering genoemd, waar hypertrofie (groei van hartspiercellen) en dilatatie (toename in de diameter van het ventrikel) plaatsvinden. Aangezien deze vorm van hypertrofie geassocieerd is met een verhoogde kans op hartfalen, wordt de groei van hartspiercellen na een hartinfarct of na hypertensie, pathologische hypertrofie genoemd.

De progressie van het geremodelleerde hart na een hartinfarct tot het zeer gedilateerde en slecht functionerende hart in hartfalen, vindt plaats door middel van een verzameling van veranderingen die plaats hebben in het hart. Onder andere een toename van fibrose, apoptose, infiltratie van inflammatoire mediatoren, contractiele dysfunctie van de overlevende hartspiercellen en verminderde dichtheid van de capillairen. De laatste jaren zijn we veel te weten gekomen over de moleculaire mechanismes die pathologische hypertrofie veroorzaken. Echter, deze informatie is grotendeels verkregen uit studies die gebruik maken van transgene muismodellen, terwijl moleculaire data over grote diermodellen schaars zijn. Tevens zijn de meerderheid van de uitgevoerde studies reductionistisch, waarbij de focus ligt op een enkel gen of signaaltransductieketen. Globale analyses die kijken naar de veranderingen in een groot aantal genen, niet gehinderd door een van te voren vastgestelde hypothese, zijn nog niet veel uitgevoerd. Om een complex proces zoals de reactie van het hart op een hartinfarct te begrijpen, moet dit op

verschillende niveaus bestudeerd worden. Van het organisme tot het moleculaire niveau en deze verschillende niveaus moeten vervolgens geïntegreerd worden.

Daarom beargumenteren wij in Hoofdstuk 2 dat hypothese-vrije moleculaire analyse technieken met integratieve fysiologie gecombineerd dienen te worden om zo meer inzicht te krijgen in remodelering van het hart. Varkens, drie weken na een hartinfarct hebben een verminderde inspanningstraining geïnduceerde stijging van de contractiliteit en relaxatatie van het hart, ondanks verhoogde catecholamines in het serum. Dit is een indicatie dat de β-adernerge response vermindert is. In hartspiercellen geïsoleerd uit harten na een hartinfarct, wordt een toegenomen calcium gevoeligheid van de kracht ontwikkeling gemeten, vergeleken met controle varkens. De toegenomen krachtontwikkeling bij lage calciumconcentraties kan bijdragen aan de verstoorde relaxatie en dus het vullen van het hart. De verschillen in calcium gevoeligheid tussen controle harten en harten na een hartinfarct was verdwenen na in vitro incubaties met protein kinase A (PKA), een belangrijk onderdeel van de β-adrenerge receptor (β-AR) signaaltransductieketen. Dat beta-adrenerge signaaltransductie daadwerkelijk verstoord was, werd aangetoond door behandeling met de β-AR agonist dobutamine. In controle varkens leidde dobutamine infusie tot een toename van de fosoforylatie van het PKA doelwit troponine I. In het myocard na een hartinfarct was deze toename van troponine I fosforylatie significant minder groot. Globale genexpressie analyse onthulde specifieke verstoringen in de expressie van genen coderend voor componenten van het β-adrenerge/PKA signaaltransductieketen in harten na een hartinfarct, leidend tot een verminderde activatie van PKA.

Het belangrijkste onderwerp van dit proefschrift waren de veranderingen in transcriptionele regulation van pathologische en fysiologische hypertrofie. Voor de analyse van transcriptie factoren (TFs) zijn nucleaire eiwit extracten nodig. Protocollen voor nucleaire eiwit extracties zijn meesttijds geoptimaliseerd voor niet bevroren weefsel of cellen gekweekt in celcultuur, terwijl bevroren weefsel wat opgeslagen ligt in weefselbanken veel minder geschikt is voor deze methodes. In hoofdstuk 3 presenteren wij een geoptimaliseerde methode om eenvoudig en reproduceerbaar kerneiwitten te isoleren uit bevroren hartweefsel. In het verkregen nucleaire extract waren vrijwel geen cytosol of myofilament eiwitten meer aanwezig. Onze nucleaire extractie methode werd vervolgens gebruikt om de translocatie van de gefosoforyleerde TF STAT3 van het cytosol naar de kern na β-adrenerge receptor stimulatie aan te tonen. Het protocol werd vervolgens toegepast voor de analyse van TFs in fysiologische en pathologische hypertrofie.

Een nadeel van het werken met weefsel ten opzichte van gekweekte cellen is dat in hartweefsel de meerderheid van de cellen geen hartspiercellen zijn. Alhoewel 75% van het volume van het myocard wordt ingenomen door hartspiercellen, vormen ze slecht 1/3^{e} van de totale celpopulatie in het hart. Andere celtypes zoals fibroblasten, endotheelcellen en gladde spiercellen vormen de rest van de hartcellen. Dit houdt in dat wanneer er nucleaire

eiwit extracties gedaan worden op hartweefsel, een groot deel van de eiwitten niet uit hartspiercellen komen. Aan de andere kant kunnen menselijke en varkens hartspiercellen 2 tot 16 kernen per cel hebben. Men moet ook in ogenschouw nemen dat de hypertrofe respons van het hart niet beperkt is tot hartspiercellen, maar onder andere ook fibrose, angio- en arteriogenese omvat, waarbij fibroblasten, endotheelcellen en gladde spiercellen betrokken zijn. Isolatie van RNA en nucleaire eiwitten uit hartweefsel maakt het dus mogelijk om genetische herprogrammering te bestuderen in alle relevante hartcellen en is dus mogelijk beter dan analyse van één enkel celtype.

In hoofdstuk 4 werd microarray analyse gebruikt om de veranderingen in genexpressie tussen harten van controle varkens en harten na een hartinfarct te bekijken. Genen betrokken bij "Cell gemedieerde Immuunrespons" en "Inflammatoire Ziektes" waren oververtegenwoordigd in de genen die veranderd waren in expressie (DE genen). Network analyse van de DE genen liet een belangrijke rol zijn voor de pro-hypertrofe eiwitten calcineurin en NF-κB. Om de TFs te bestuderen die de verandering in genexpressie teweeg brengen, werden de promotorregio's van de DE genen gescand voor oververtegenwoordigde transcriptie factor bindingsplaatsen (TFBPs) Deze in silico methode werd gecomplementeerd met eiwit/DNA array analyse van nucleaire eiwit extracten, verkregen met de methode beschreven in Hoofdstuk 3. Eiwit/DNA array analyse meet semi-quantitatief de activiteit van 345 TFs . Het combineren van de data van de TFBP analyse met de eiwit/DNA array analyse leverde overeenkomstige resultaten voor twee TFs, namelijk de glucocorticoid receptor (GR) en COUP-TFII. Om onze transcriptionale genomics aanpak te valideren, behandelden wij varkens met een hartinfarct met de GR antagonist mifepristone. Blokkade van GR resulteerde in een verminderde hypertrofe respons drie weken na een hartinfarct.

Aangezien hypertrofie na een hartinfarct een risicofactor is voor het ontstaan van hartfalen, kan de vraag gesteld worden of hypertrofie na een hartinfarct wel nodig is of dat therapie gericht moet zijn om hypertrofie te beperken. Data verkregen uit transgene muismodellen toont aan dat het mogelijk is om hypertrofie te beperken zonder daaropvolgende ventriculaire dilatatie of decompensatie. Dit suggereert dat therapieën die hypertrofie verminderen van grote klinische relevantie zijn. In a groot cohort van patiënten met hypertensie dat werd behandeld met bloeddruk verlagende medicijnen, werd een sterke associatie gevonden tussen de reductie van linker ventrikel massa en verlaagde mortaliteit. Medicijnen die ingrijpen in het renine-angiotensine system (RAS) waren oorspronkelijk ontwikkeld voor de behandeling van hypertensie, maar later bleken ze ook de remodelering van het hart te reduceren. Bijvoorbeeld, toediening van de angiotensine II receptor blokker losartan bij hypertensie patiënten, resulteerde in regressie van linker ventrikel massa die geassocieerd was met verminderde mortaliteit. Deze verminderde mortaliteit was voor een groot deel onafhankelijk van de verlaging in de bloeddruk in de

patiënten. Dat ingrijpen in het renine angiotensine systeem ook leidt tot vermindering van remodelering van het hart na een hartinfarct, werd aangetoond in patiënten na een hartinfarct werden behandeld met een angiotensin converting enzyme (ACE) inhibitor . In deze patiënten leidde dit tot verminderde linker ventrikel dilatatie en verminderde mortaliteit. In ons model van remodelering na een hartinfarct, resulteerde blokkade van GR met mifepristone tot een verminderde hypertrofe respons. In tegenstelling tot de positieve effecten van RAS blokkers, resulteerde de verminderde hypertrofie na mifepristone behandeling niet, in ieder geval niet op de korte termijn, in verbetering van de hartfunctie of vermindering van de ventriculaire diameter. Deze vinding zou kunnen worden geïnterpreteerd dat alleen mikken op vermindering van hypertrofie in de behandeling van patiënten met een hartinfarct niet genoeg zou zijn.

Het ontbreken van functionele verbetering door GR blokkade na een hartinfarct zou veroorzaakt kunnen worden door de pro-inflammatoire effecten van mifepristone. In de afwezigheid van mifepristone, transloceert GR na cortisol binding naar de kern. In de kern medieert GR zijn anti-inflammatoire effecten mede door een interactie aan te gaan met NF-κB. Op deze manier blokkeert GR de pro-inflammatoire TF NF-κB. Uit de literatuur is bekend dat NF-κB is geactiveerd in hypertrofie na een hartinfarct en dat het blokkeren van NF-κB activatie leidt tot een verminderde infarctgrootte. Mifepristone voorkomt activatie en dus translocatie naar de kern van GR en voorkomt dus ook de mogelijkheid dat GR NF-κB blokkeert. Helaas hebben wij niet de infarctgrootte gemeten in ons diermodel, aangezien dat antwoord zou geven op de vraag of mifepristone behandeling infarctgrootte beïnvloed. Tevens zou er meer onderzoek moeten plaatsvinden om vast te stellen wat de ideale timing is van GR blokkade na een hartinfarct. Ook get het gebruik van andere GR antagonisten verdient aanbeveling.

Dat hartgroei ook een gunstige aanpassing kan zijn blijkt uit inspanningstraining geïnduceerde hypertrofie. Atleten die participeren in evenementen met inspanningstraining ontwikkelen hypertrofie met een toegenomen ventriculaire diameter, zonder dat zij een hoger risico lopen op hartfalen. Groei van het hart in de afwezigheid van een verhoogd risico op hart- en vaatziekten wordt fysiologsiche hypertrofie genoemd. In Hoofdstuk 5 hebben wij de transcriptionele genomics van inspanningstraining geïnduceerde hypertrofie in varkens bestudeerd. Microarray analyse liet zien dat de genen die veranderde van expressie betrokken waren bij “Overleving van het Organisme”. Netwerk analyse van de DE genen onthulde een belangrijke rol voor Akt, een mediator van fysiologische hypertrofie in muizen. TFBS analyse en eiwit/DNA array analyse leverde overeenkomstige resultaten voor drie TFs, namelijk YY1, PAX6 en de glucocorticoid receptor. Alle drie de TFs zijn vermindert in activiteit in de harten van getrainde varkens, ten opzichte van sedentaire dieren. De vinding dat de activiteit van GR verminderd is in harten na inspanningstraining is intrigerend aangezien de GR juist geactiveerd is in harten na een hartinfarct.

Zowel inspanningstraining als een hartinfarct leidde tot een vergelijkbare toename van het linker ventrikel gewicht. Verslechtering van de hartfunctie vindt alleen plaats in hypertrofie na een hartinfarct. De genexpressie patronen in beide vormen van hypertrofie vertonen opmerkelijk weinig overlap. Een uitvoerig overzicht van de verschillen en overeenkomsten in genexpressie tussen pathologische en fysiologische hypertrofie is beschreven in Hoofdstuk 5. Deze vergelijking stelde ons in staat om onderscheid te maken tussen genen en TFs die specifiek zijn voor pathologische of fysiologische hypertrofie en genen en TFs die onderdeel zijn van een algemene hypertrofie respons.

Inspanningstraining en een hartaanval vragen beide om toegenomen inspanning van het hart. Waarom veroorzaken zij dan zulke uiteenlopende types hypertrofie? Een verschil tussen pathologische en fysiologische hypertrofie is dat de pathologische stimulus continue is (zoals bij een hartinfarct) en dat de fysiologische stimulus slechts een gedeelte van de dag aanwezig is (zoals bij inspanningstraining). Dat dit niet het verschil verklaart, werd aangetoond in een elegante studie, waarin de pathologische stimulus (in dit geval drukoverbelasting door middel van aorta constrictie (TAC)) voor dezelfde tijdsduur werd toegepast als de fysiologische stimulus (zwemtraining). De niet-continue TAC muizen ontwikkelden hypertrofie zonder verschillen in fractionele verkorting, vergelijkbaar met de hypertrofie die ontstond na zwemtraining. Muizen die werden blootgesteld aan continue TAC hadden meer hypertrofie en een verminderde fractionele verkorting. Verder analyse liet echter zien dat de niet-continue TAC muizen verminderde contractiliteit hadden, toegenomen fibrose en een verminderde capillaire dichtheid, allemaal kenmerken van pathologische hypertrofie die niet werden teruggevonden bij de muizen die zwemtraining ondergingen. Dit wijst erop dat de aard van de stimulus en niet de chroniciteit bepalen of de stimulus pathogeen is. Een ander argument voor deze hypothese is de hypertrofie plaatsvindt tijdens zwangerschap. Het hart van een zwangere vrouw ondergaat aan langdurige volume-overbelasting, dit resulteert in hypertrofie met een toegenomen slagvolume, die normaliseert na de bevalling. Het zou kunnen dat het hart ingesteld is om de veranderingen in belasting op het hart tijdens inspanningstraining op te vangen, zoals is bediscussieerd in Hoofdstuk 2. Terwijl het hart de plotseling daling in het hartminuutvolume niet aankan en dit leidt tot een zogenaamde “overgave” fenotype.

Samenvattend, het onderzoek beschreven in dit proefschrift laat zien dat grootschalige hypothese-vrije moleculaire analyses uitgevoerd kunnen worden in een groot diermodel. Wij hebben laten zien dat pathologische en fysiologische hypertrofie een kenmerkend genexpressie profiel hebben, die weinig overlap vertonen. De transcriptie factoren die deze genexpressie profielen aansturen zijn ook verschillend in beide vormen van hypertrofie. De glucocorticoid receptor is een interessante transcriptiefactor omdat GR geactiveerd wordt in pathologische hypertrofie, terwijl hij juist minder actief wordt in fysiologische hypertrofie.